PHOTOIONIZATION OF ATOMIZED AND MOLECULAR GASES

A THESIS

SUBMITTED FOR THE DEGREE OF

DOCTOR OF PHILOSOPHY

OF THE

GUJARAT UNIVERSITY

BY

E. KRISHNAKUMAR

JULY 1981

043



B11490

PHYSICAL RESEARCH LABORATORY

AHMEDABAD 380 009

INDIA

THE LIBRARY
PHYSICAL RESEARCH LABORATORY
NAVRANGPURA AHMEDABAD-380009
INDIA

T O M Y P A R E N T S

C E R T I F I C A T E

I hereby declare that the work presented in this thesis is original and has not formed the basis for the award of any degree or diploma by any University or Institution.

E. Krishnakumar

E. Krishnakumar

Certified by:

Vijay Kumar

Vijay Kumar
Ahmedabad.
July, 1981

CONTENTS

		Certificate	
		Statement	
		Acknowledgements	
CHAPTER I		Introduction	1
	I	Photoionization	1
	I.1	Processes in Photoionization	1
	I.2	Photoionization and Photoelectron Spectra	5
	I.3	The Photoionization Continuum	8
	I.4	Autoionization	10
	I.4.1	Selection Rules	14
	I.5	Photoelectron Spectroscopy	15
	I.6	Present Status of Photoionization Studies	22
	I.6.1	Atoms	22
	I.6.2	Molecules	23
	I.7	Electron Scattering Studies using Photoelectron Spectroscopy	27
CHAPTER II		Photoelectron Spectrometer	30
	II.1	Introduction	30
	II.2	Electron Energy Analyzer	31
	II.2.1	Choice of the Analyzer	32
	II.2.2	Cylindrical Mirror Analyzer-Design Aspects	36
	II.2.3	Analyzer Details	38
	II.3	Beam Splitter, Vacuum System and other details	40
	II.4	Electron Detector	42

	II.5	VUV Monochromator	43
	II.6	Light Source	44
	II.7	Data Acquisition System	45
	II.8	Operation of the Spectrometer	48
	II.9	Performance of the Spectrometer	49
	II.9.1	Effect of the Earth's Magnetic Field	50
	II.9.2	Effect of Contact Potential	51
	II.9.3	Effect of Draw-out Voltage	54
	II.9.4	Effect of Electron Scattering	54
	II.9.5	Collecting Efficiency Calibration	55
	II.9.6	Energy Calibration	56
	II.9.7	Resolution	57
CHAPTER	III	Photoelectron Spectroscopy and Autoionization of O_2, H_2 and CO_2	59
	III.1	Introduction	59
	III.2	Molecular Oxygen	60
	III.3	Molecular Hydrogen	70
	III.4	Carbon Dioxide	73
	III.4.1	(ν_1,0,0) levels	77
	III.4.2	(0,0, ν_3) and (ν_1 ,0, ν_3) levels	78
	III.4.3	(0,1,0) level	79
	III.4.4	Vibrational Intensities and Autoionization	82
CHAPTER	IV	Photoelectron Spectroscopy of Atomized Species	84
	IV.1	Introduction	84
	IV.2	Experimental Details	85

CHAPTER	IV.2.1	The Phase Sensitive Detection Technique	85
	IV.2.2	Instrumental Details	88
	IV.2.3	Operation and Performance	90
	IV.3	$O_2(a\,^1\Delta_g)$ Photoelectron Spectra	91
CHAPTER	V	Total Electron Scattering Cross-section for Molecular Hydrogen at low energies by Photoelectron Spectroscopy	94
	V.1	Introduction	94
	V.2	Experimental Details	96
	V.3	Measurement of the Cross-section	97
	V.4	Results and Discussions	101
	V.5	Major Sources of Errors	102
	V.6	Conclusion	103
CHAPTER	VI	Scope for Further Work	105

LIST OF PUBLICATIONS

REFERENCES

STATEMENT

The basic aim of the work presented in this thesis is to study the photoionization of atomized and molecular gases as a function of the incident energy of the ionizing radiation. The powerful technique of photoelectron spectroscopy was used for this purpose. A photoelectron spectrometer set up with ultraviolet light source, VUV monochromator and a cylindrical mirror analyzer was built. This set up successfully provided accurate data on electronic and vibrational intensities of molecular ions independent of the angular distribution of the electrons.

High resolution photoelectron spectra of O_2, H_2 and CO_2 were obtained at a number of ionizing wavelengths with a view to study the effects of possible autoionization at some wavelengths. Accurate vibrational intensities independent of electron angular distribution for the $X^2\Pi_g$ and $a^4\Pi_u$ states of O_2^+ were measured from the photoelectron spectrum of O_2 at 736 Å. The contribution of autoionization to the vibrational intensities of O_2^+ states at 736 Å was obtained by a comparison of the O_2 spectra at 736 Å and 744 Å. This result along with the photoionization efficiency curve given by Dehmer and Chupka (1975) was used to obtain a qualitative picture of the nature of the autoionizing state at 736 Å for which no satisfactory picture is available so far. The autoionizing state seems to be a repulsive state of the neutral molecule with very short

autoionizing time such that it forms a stable ion in the $X^2\Pi_g$ or a $^4\Pi_u$ state before it dissociates. This autoionizing mechanism could be used to explain similar broad humps seen in high resolution photoionization efficiency curves of other molecules also.

In the case of H_2 no effect of autoionization could be seen at 736 Å as reported earlier by Samson (1976). The photoelectron spectra of CO_2 were studied at 584, 736, 744 and 876 Å. The spectra at 736 and 876 Å showed strong departure due to autoionization from the direct ionization spectra at 584 and 744 Å. A number of additional vibrational levels which have not been observed so far in the photoelectron spectra were observed at 736 Å. Because of the presence of the larger number of vibrational levels, the vibrational constants of the symmetric and antisymmetric stretching modes could be measured with better accuracy than in the previous measurements using photoelectron spectroscopy. Also the vibrational populations of (0,0,0), (1,0,0) and (2,0,0) levels at 584, 736 and 744 Å spectra were measured and a detailed comparison was made. The 876 Å spectrum of CO_2 showed the presence of the (0,1,0) level showing autoionization through a bent excited state. From this state the vibrational constant of the bending mode also was derived.

The phase sensitive detection technique employed to obtain the spectra of the atomized species did not succeed because of the low count rate of the energy analyzed electrons. This could

be attributed to low intensity of the ultraviolet light after monochromatization. However photoelectron spectra of $O_2(a^1\Delta_g)$ were obtained with weak intensity at 584 and 736 Å without the use of phase sensitive detection.

A method was developed to obtain the total electron scattering cross section using photoelectron spectroscopy. This was the first time the electron scattering cross section was measured in this manner. The relative total cross section for $e^- - H_2$ scattering in the energy range 0.02 to 1.14 eV was measured by this technique.

ACKNOWLEDGEMENTS

I take this opportunity to thank Dr.Vijay Kumar under whose guidance this thesis work was carried out. I am sincerely grateful to him for his enthusiasm, encouragement and affection.

I thank sincerely Dr.V.B.Sheorey for his help and encouragement through many useful discussions during the course of this work. The advice and suggestions of Professor Satya Prakash especially in the early stages of the work is gratefully acknowledged.

I am extremely thankful to Messrs.A.P.Gohil, I.T.Kriplani and J.K.Dave for helping with the data acquisition system and other relevant instruments and Messrs.A.K.Dutta, R.S.Patel and I.A.Prajapati for their invaluable help and enthusiasm throughout this work. I have had unlimited cooperation from the staff of the workshop and the glass blowing section for which I am very grateful.

I sincerely thank all my friends and well wishers who have directly and indirectly helped in completing this work successfully.

I thank Mr.M.Arvindnath for the neat and fast typing of the thesis and Mr.Bhupendra for the speedy duplicating work.

E. Krishnakumar

(E. Krishnakumar)

Ahmedabad 380 009
July, 1981

CHAPTER II

INTRODUCTION

I Photoionization

Photoionization is one of the important phenomena occuring in nature when electromagnetic radiation interacts with matter. Photoionization takes place when the interacting electromagnetic radiation is energetic enough to effect the emission of an electron from the atom or molecule leaving it in the ionic state. This is a major phenomenon in stellar and planetary atmospheres and in laboratory as well as space plasmas. Hence the data on photoionization are important in determining the dynamics of the above systems. The photoionization data provide various details of the atomic and molecular structure and are important in developing and testing various theoretical models on atoms and molecules.

I.1 Processes in Photoionization

When electromagnetic radiation interacts with atoms or molecules it can get scattered or absorbed. The scattering

process is a function of the energy of the photons and is classified into Rayleigh scattering, Thomson scattering and Compton scattering. In the energy range where Rayleigh scattering is dominant, Raman scattering is also possible. All these scattering processes and the electron positron pair production which takes place at photon energies greater than about 1 MeV, are second order processes. The absorption of radiation by atoms or molecules is a first order process and hence is much more dominant than the various scattering processes. At energies below the onset of dissociation or ionization, the absorption occurs only at discrete energies which are characteristic of the atom or molecule concerned. Above the ionization or dissociation threshold, the absorption of photons leads to final products with a continuous set of energy values and hence the absorption cross section is continuously variable with respect to the photon energy. Above the ionization threshold, various primary processes can happen and these are listed below for the case of molecules.

Direct ionization: The molecule AB forms a stable ion, the cross section for this process being σ_k

$$AB + h\nu \xrightarrow{\sigma_k} AB^+ + e^- \qquad \text{I.1}$$

Ion fragmentation:

$$AB + h\nu \xrightarrow{\sigma_g} A^+ + B + e^- \qquad \text{I.2}$$

Ion pair production:

$$AB + h\nu \xrightarrow{\sigma_p} A^+ + B^- \qquad \text{I.3}$$

Formation of superexcited neutral state:

$$AB + h\nu \xrightarrow{\sigma_t} AB^* \qquad \text{I.4}$$

The above superexcited state may decay by autoionization with rates k_1, k_2, and k_3 for the three following processes.

$$AB^* \xrightarrow{k_1} AB^+ + e^- \qquad \text{I.5}$$

$$AB^* \xrightarrow{k_2} A^+ + B + e^- \qquad \text{I.6}$$

$$AB^* \xrightarrow{k_3} A^+ + B^- \qquad \text{I.7}$$

Non ionic decay of the superexcited state is also possible (assuming only first order process) with a total probability k_n.

Dissociation:

$$AB^* \rightsquigarrow A + B \qquad \text{I.8}$$

Predissociation:

$$AB^* \rightsquigarrow AB^{**} \rightsquigarrow A + B \qquad \text{I.9}$$

Fluorescence:

$$AB^* \longrightarrow AB + h\nu \qquad \text{I.10}$$

Internal conversion:

$$AB^* \rightsquigarrow AB \qquad \text{I.11}$$

The total photoabsorption cross section σ_a is the sum of the cross-sections for all these processes. The total absorption cross-section

$$\sigma_a = \sigma_k + \sigma_g + \sigma_p + \sigma_t \qquad \text{I.12}$$

and the total photoionization cross-section

$$\sigma_i = \sigma_k + \sigma_g + \sigma_p + \sigma_t\left(\frac{k_1 + k_2 + k_3}{k_1 + k_2 + k_3 + k_m}\right) \qquad \text{I.13}$$

For conditions where the ion pair production processes (I.3) and (I.7) may be neglected (i.e., assuming $\sigma_p = 0$ and $k_3 = 0$), the photoionization efficiency γ_i which is the number of ions produced per photon absorbed is given by

$$\gamma_i = \frac{\sigma_i}{\sigma_a} = \frac{\sigma_k + \sigma_g + \sigma_t\left(\frac{k_1 + k_2}{k_1 + k_2 + k_3}\right)}{\sigma_k + \sigma_g + \sigma_t} \qquad \text{I.14}$$

and in this case γ_i is equal to the photoelectron yield. However, if ion pair production processes (I.3) and (I.7) are significant, the photoionization efficiency as defined above would no longer be given by σ_i/σ_a. For atoms, γ_i will be generally equal to unity at wavelengths shorter than the first ionization threshold but could conceivably be less than unity in regions where the ionization continuum interacts with superexcited neutral states, and the superexcited neutral state goes through non ionic decay similar to the processes (I.10) and (I.11). In the case of most of the molecules, γ_i is less than unity at shorter wavelengths near the ionization threshold. This again is due to the decay channels of superexcited states other than by autoionization represented by the non ionic decay processes (I.8) to (I.11). For very short wavelength γ_i tends to reach unity.

Apart from the processes listed above, another primary process can occur at higher photon energies. This is multiple ionization. Some secondary processes may also occur when the ion formed is in its excited states. These are fluorescence due to deexcitation of the ion, predissociation, and multiple ionization through Auger processes.

Of these processes listed above the processes of direct ionization and autoionization have been studied by the author. These studies have been confined to the photon wavelengths where there is ionization from the outer shells only. The powerful technique of photoelectron spectroscopy has been used for this purpose.

I.2 Photoionization and Photoelectron Spectra

In the single particle approximation, the electronic structure of an atom or molecule is characterized by an electron configuration $S(j)$ based on a set of atomic or molecular orbitals j_1, j_2, j_3 ... having definite energies. Ionization corresponds to removal of a bound electron, with simultaneous reorganization of the orbitals and energies of the remaining electrons, leaving the newly formed ion in the reorganized configuration $S'(j)$. The ionization potential I is the energy expended in removing the expelled electron to infinity. According to the Born - Oppenheimer approximation, the initial

state ψ_n corresponding to the electron configuration S ($\underline{j}$) can be separated into a product of electronic e, vibrational v, and rotational r wavefunctions as

$$\psi_n = \Theta_e \, \Theta_v \, \Theta_r \qquad \text{I.15}$$

and the internal energy E_n into a sum of electronic, vibrational and rotational energies as

$$E_n = E_e + E_v + E_r \qquad \text{I.16}$$

The final wave function $\psi_{\underline{j}}$ after ionization is

$$\psi_{\underline{j}} = \psi_k \, \psi_e \qquad \text{I.17}$$

where ψ_k is the total wavefunction of the ion formed in the k^{th} discrete state and ψ_e is the wavefunction corresponding to the continuum state of the electron removed from the j^{th} orbital of the neutral species.

Interaction between the electrons in a particular electronic configuration can often give rise to several electronic states having different energies. The ionization potential will therefore be characteristic of the formation of the ion in a particular electronic state e'. For a molecular species, the ion will be formed not only in a particular electronic state but also in well defined vibrational v' and rotational r' levels, so that we can characterize the ionization potential as

$$I = E[S'(j); e', v', r'] - E[S(j), e, v, r] \qquad \text{I.18}$$

If the molecule M, initially in the energy state $E\left[S(j);\ e,v,r\right]$ suffers a collision with a photon energy $h\nu \geq I$, photoionization will occur with a cross-section σ_i leading to ejection of an electron:

$$h\nu + M\left[S(j);\ e,v,r\right] \longrightarrow M^{+}\left[S'(j);\ e',v',r'\right] + e^{-} \qquad \text{I.19}$$

In practice the recoil energy of the ion is negligible so that the kinetic energy of the photoelectron is given by

$$\frac{1}{2} m V^2 = h\nu - I \qquad \text{I.20}$$

where m is the mass of the electron and V its velocity. The photoelectron spectrum is a record of the number of electrons emitted at each energy and a peak is found in the spectrum at each energy, $h\nu - I_j$, corresponding to the binding energy, I_j, of an electron in the atom or molecule. In the case of molecules the photoelectron spectra contain peaks corresponding to vibrational and rotational states also.

The vibrational intensity distribution of the ion is determined by the Franck-Condon principle. According to this principle, the electronic transitions takes place so rapidly that the nuclei do not change their internuclear distance or momentum during the transition. As a result, those vibrational levels of the ions will be populated during ionization for which the internuclear distance is the same as that of the initial neutral state. Thus the vibrational intensity distribution of the various ionic states depends

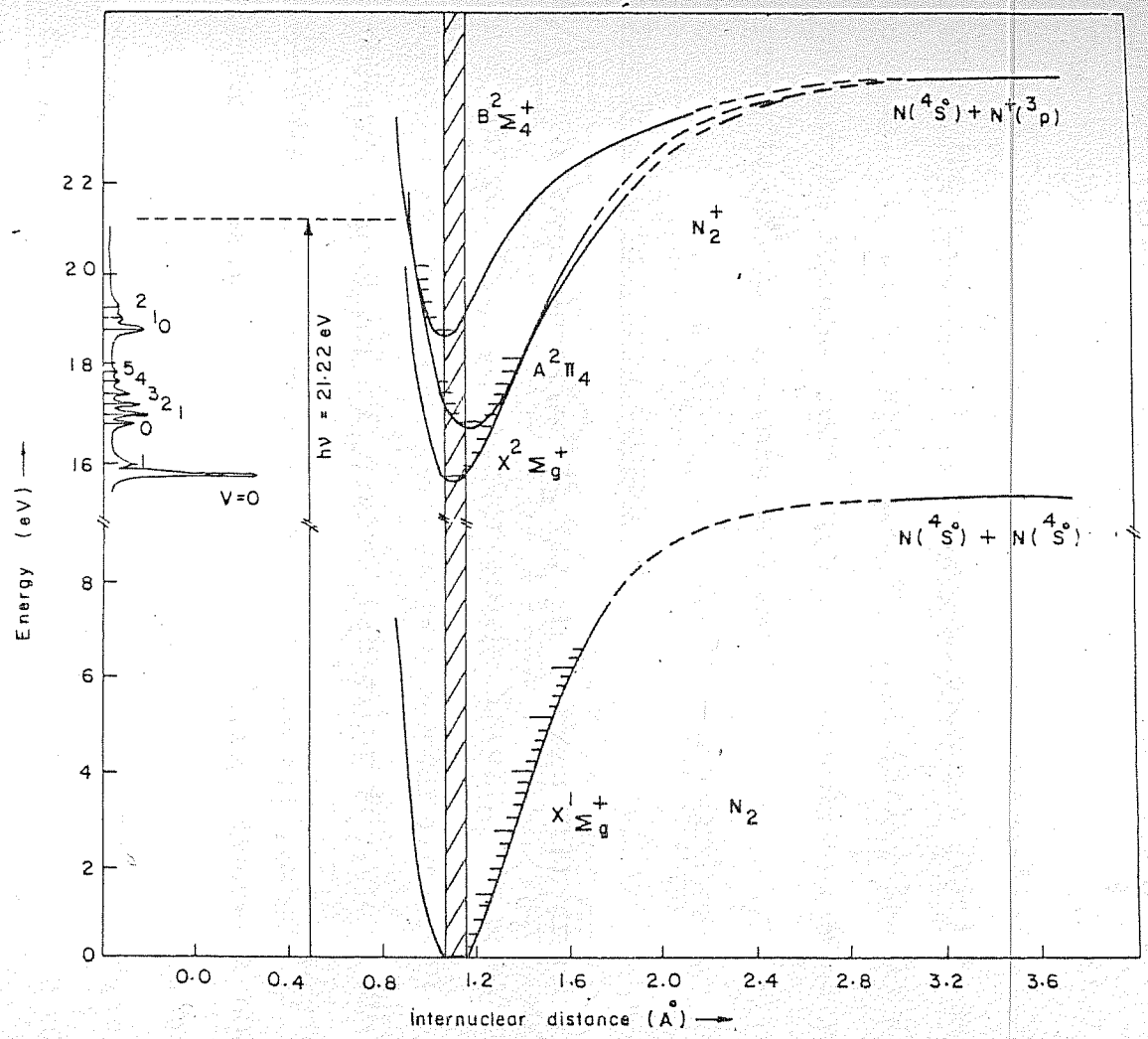


Fig. I. I Photoionization of N_2 by He I 21.22 eV radiation

on thd internuclear distances of the electronic states and hence the respective Franck-Condon factors. This is clearly seen from Fig I.1 where the photoionization of molecular nitrogen with HeI 21.22 eV radiation is shown. The Franck-Condon region for the transition from the $v = 0$ level of $N_2, X\,{}^1\Sigma_g^+$ state is the vertical shaded portion. On the left is given the vibrational population obtained for the three ionic states. It can be seen that the vibrational levels falling within the Franck-Condon region are populated, with intensities proportional to the amount of overlap.

I.3 The Photoionization Continuum

The cross-section σ_k for photoionization producing a singly charged ion in a particular energy level E_k is ideally a step function of the incident radiation energy $h\nu$. For atoms, one observes two kinds of general behaviour for the variation of σ_k with $h\nu$. The first type based on the data of Lowry et al (1965) is shown in Fig I.2 a. The figure shows a sharp rise of σ_k for helium at the threshold followed by a slow regular decrease at higher photon energies. The photoionization data for neon (Ederer and Tomboulian, 1964) in Fig.I.2 b shows the second type of behaviour. The threshold for production of the ${}^2P_{3/2}$ and ${}^2P_{1/2}$ states of $2s^22p^5$ Ne II is in the neighbourhood of 575 Å, with a cross-section of 6.3 Mb. As photon energy increases, the cross section first increases to a maximum of

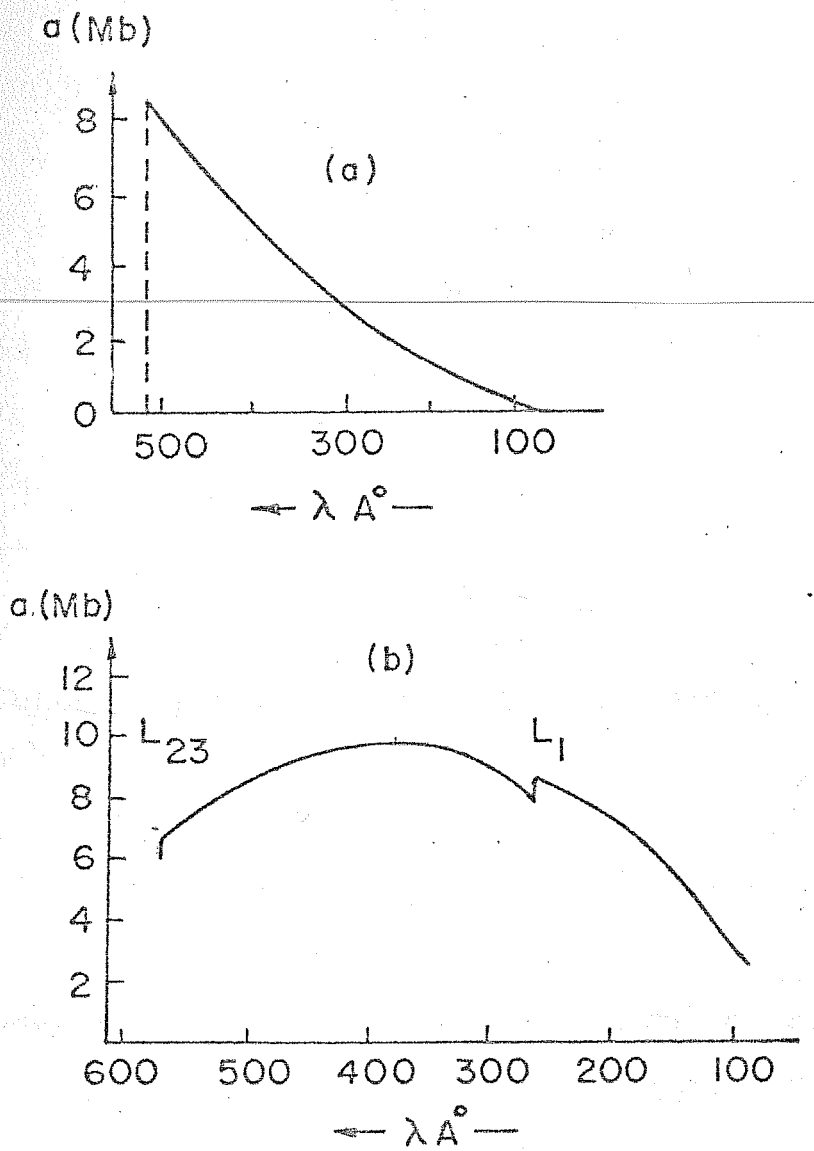


Fig. I. 2. Photoionization cross section function for (a) Helium and (b) Neon.

10 Mb at 375 Å and then decreases to a value of 7.8 Mb at about 260 Å, the threshold wavelength for the production of the excited $2s2p^6\ ^2S_{\frac{1}{2}}$ state of Ne II. The two types of photoionization functions are related to the presence or absence of a node in the bound state radial wavefunction of the ejected electron (Hasted 1964). When a new ionization level $E_{k'}$ is reached with increasing photon energy, there should be a new threshold step in the σ vs $h\nu$ curve. Above this new threshold the $\sigma_{k'}$ function will be superimposed on the σ_k function. This is clearly seen in Fig I.2b where the jump at the $2s2p^6\ ^2S_{\frac{1}{2}}$ level of Ne II is of the order of 0.7 Mb.

Discontinuities at the photoionization threshold above the lowest ionization potential are not always observed. Samson (1966) found no evidence for a discontinuity at 260 Å for neon. Fano and Cooper (1965) have shown that interference effects related to autoionization processes can make the photoionization cross-section function increase, decrease, or remain virtually unchanged at thresholds corresponding to higher ionization potentials.

For molecular systems the ionization cross-section curve shows large amount of discrete structure near the first ionization threshold. In addition to the effect of autoionization phenomenon, there will be variation of ionization probabilities with vibrational state, electronic transition moments which are a function of internuclear distance,

molecular rotation, and dissociation. The abrupt rise at the threshold is not always apparent for molecules. In the simplest molecules like H_2, O_2 and N_2, the behaviour of the continuum is largely obscured by very strong autoionization features.

I.4 Autoionization

It has been mentioned previously that the photoionization cross-section curves for atoms and molecules exhibit discrete structure at definite energies. These discrete structures are due to the existence of superexcited states of the neutral atoms or molecules above their first ionization threshold. These states have very short life times and decay into the ionic state emitting an electron. This process is called autoionization.

The autoionization process is schematically shown in Fig I.3. The absorption of the photon $h\nu$ by the ground state X of the neutral molecule M gives rise to a superexcited neutral state i which is located above the ground electronic state k of the ion M^+. This is followed by a radiationless transition without any energy change to form an ion and an electron. The electron kinetic energy is the energy difference between f and k as shown in the figure. The true wave function of the state reached on photoabsorption is a linear combination of the wavefunction of the excited bound state i and the wavefunction of the continuum state k. The energy halfwidth of the

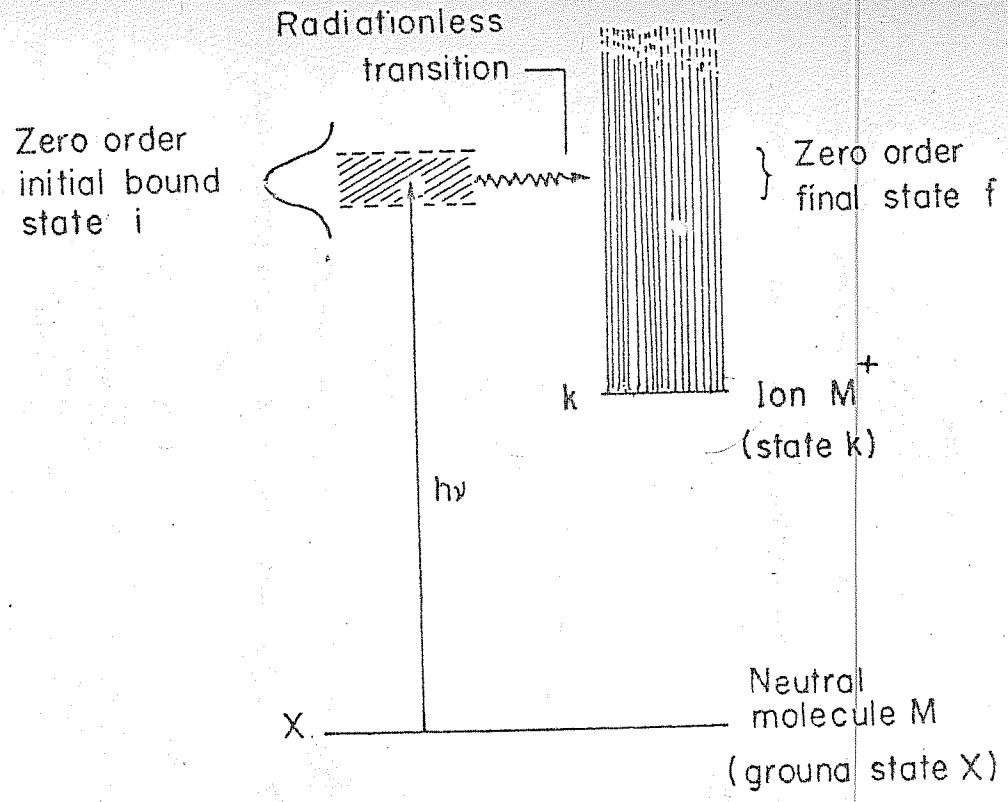


FIG. I.3 The Autoionization Process

autoionizing level will depend on various processes that depopulate the autoionizing state i and is given by $h/2\pi\tau$ where τ is the life time and can be written as

$$\tau = \frac{1}{\left(P_{if} + \sum_q k_q\right)} \qquad \text{I.21}$$

where P_{if} is the probability of autoionization and $\sum_q k_q$ represents the sum of the rates of all radiative or nonradiative relaxation processes which depopulate i besides autoionization. For free atoms the magnitude of the second term is of the order of 10^9-10^{10} sec^{-1}. Since the energy width of a single ground state level is normally much less than $h/2\pi\tau$ the line width for the absorption process $i \leftarrow X$ is proportional to $1/\tau$, the energy width of the autoionizing level. For a single excited neutral state, the autoionization process may be considered to be essentially an optical resonance phenomenon since the absorption line shape determines the photoexcitation function.

In an atomic system, the superexcited states occur because of two electron excitation or inner shell excitation. When electron spin is taken into account, then even the excitation of an outermost shell electron into Rydberg levels can lead to excitation of the neutral atom above the first ionization threshold. An example of such a case is shown in Fig I.4 for xenon. For xenon, the outermost orbital is completely filled with p electrons. The electric dipole selection rules permit ns and nd states to be reached for transitions emanating from this orbital. As n approaches infinity, the residual ionic

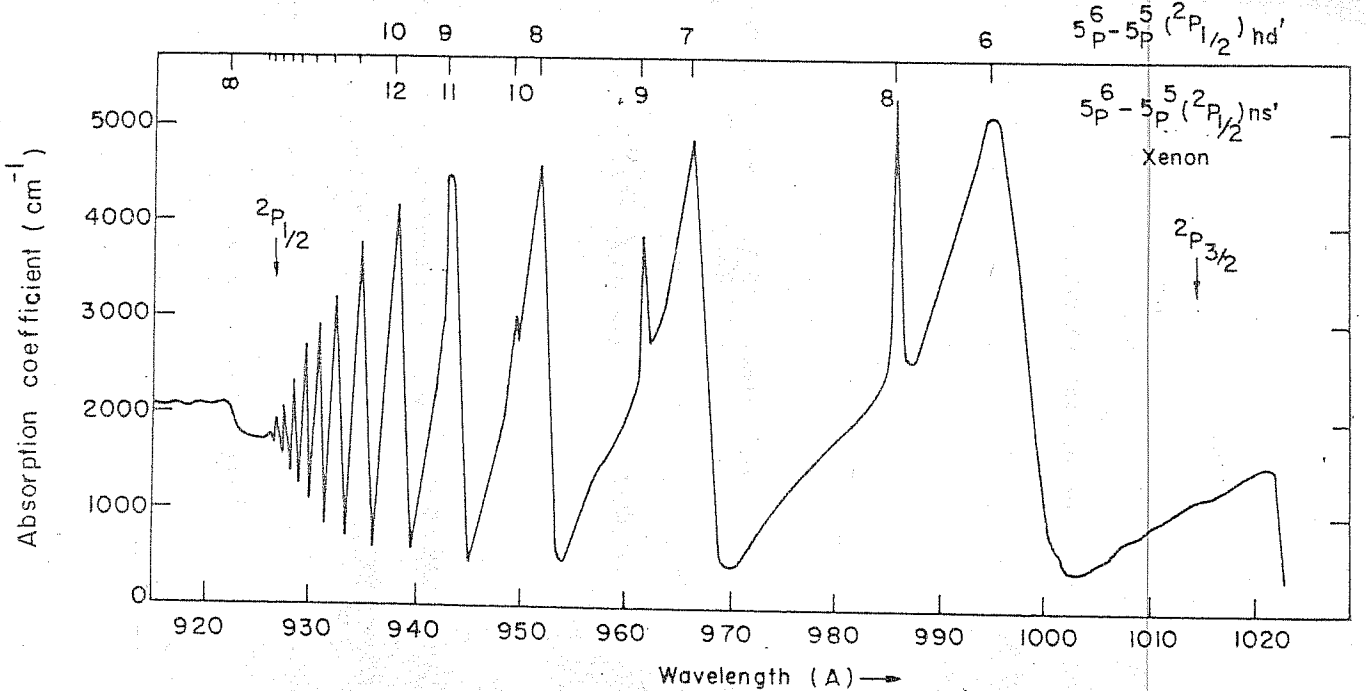


Fig. I.4. Photoabsorption coefficients of Xe as a function of wavelength in the autoionizing region between the $2P_{1/2}$ and $2P_{3/2}$ levels
Huffman et al (1963)

system is left with l = 1 (due to the missing p electron) and s = $\pm \frac{1}{2}$ which corresponds to the states of $Xe^+, {}^2P_{3/2}$ and $^2P_{1/2}$ separated in energy by 1.306 eV. The peaks in the figure are the ns and nd Rydberg states which converge to the $^2P_{1/2}$ limit of Xe^+.

In molecules two types of autoionization processes can be seen, depending on whether the molecular ion produced by autoionization is in the same or a different state from that of the ion core of the autoionizing state. In the former case, the ejected electron is the one excited in the resonance absorption process. The excited state has a Rydberg character with an outer electron revolving about an inner core and may be vibrationally and/or rotationally excited, in such a way that the total energy of the system lies above the ionization limit. The autoionization then results from the vibrational-electronic or rotational - electronic interaction and energy relaxation into electronic energy, so that the Rydberg electron is removed. This is called vibrational or rotational autoionization. It has been studied theoretically by Berry (1966), who deduced a 'propensity rule' predicting that the autoionization rate should decrease rapidly for a transition involving a variation of more than one vibrational quantum.

$$\tau_{\Delta V=1} \ll \tau_{\Delta V=2} \ll \tau_{\Delta V=3} \qquad \text{I.22}$$

where τ represents the life time of the autoionizing state. When the molecular ion produced by autoionization is in a

different electronic state from that of the ion core of the autoionizing state, the process is called electronic autoionization and is similar to the case of atomic autoionization as discussed above.

The first experimental evidence of autoionization process was observed in the Auger effect discovered (Auger, 1925) when irradiating atoms with X-rays or high energy electrons producing very highly excited states due to inner shell excitation or ionization. Experimental observation of electronic autoionization was first reported by Beulter (1935). In the absorption spectra of argon, krypton, and xenon, numerous absorption lines near the first ionization threshold were observed. These lines due to autoionization were found to be broad and asymmetrical in shape, tailing off towards shorter wavelengths. The broad nature of the peaks showed the short life time of the states involved. The asymmetric shape of the lines was explained by Fano (1935). He suggested that the asymmetry arises from the sharp variation in the coefficients of the various configurations as the energy value of the excited state passes through the stationary state. This qualitative explanation was extended in the form of a comprehensive analysis of the profiles of the autoionized absorption lines by Fano and Cooper (Fano, 1961; Fano and Cooper, 1965). The configuration interaction between a discrete state and an overlapping continuum was considered

and it was found that the profiles of the autoionization lines may be represented by

$$\sigma(\epsilon) = \sigma_a \left[\frac{(q+\epsilon)^2}{1+\epsilon^2}\right] + \sigma_b \qquad \text{I.23}$$

where ϵ is the difference between the photon energy and the unperturbed energy of the discrete states divided by the mean life time of the level with respect to autoionization, σ_b is the absorption cross-section due to direct ionization, σ_a is the absorption cross-section due to autoionization and q is a numerical index characterising the line profile.

I.4.1 Selection Rules

The autoionization process is the result of the interaction between the superexcited discrete state and the low lying continuum state. If the mixing of the wavefunctions of these two states does not take place, the superexcited state cannot autoionize. This implies certain selection rules for this process.

The selection rules for this process to be allowed are as given by Kronig (1928). They are,

(1) $\Delta J = 0$ i.e., both the states must have the same total angular momentum.

(2) $\Delta S = 0$ i.e., both the states must have the same multiplicity

(3) $\Delta A = 0$ or ± 1 i.e., orbital angular momentum should change by 0 or ± 1.

(4) $+ \nleftrightarrow -$; $+ \longleftrightarrow +$; $- \longleftrightarrow -$ i.e., both states

must be positive or both must be negative.
(5) for homonuclear molecules, u $\nleftrightarrow$ g; u $\longleftrightarrow$ u; g $\longleftrightarrow$ g i.e., both states must have the same molecular symmetry. While (1), (4), and (5) are rigorous, (2) and (3) hold only approximately, especially as (3) is only appropriate when Λ is well defined. While applying the selection rules, care has to be taken to include in the final state both the ion as well as the emitted electron.

I.5 Photoelectron Spectroscopy

The experimental studies on photoionization are carried out by determining the characteristics and spatial distribution of the products of ionization. As described earlier, there are various processes in photoionization and each of these can be understood by a proper study of the ions, ion fragments, electrons, and the fluorescent photons. The total photoionization cross-section as defined in section I.1 is one of the most important parameters measured in an ionization study. This involves the measurement of the number of primary ions produced for a given number of photons and the neutral particles. This measurement of the total photoionization cross-section is accurately done using the double ion chamber developed by Samson (Samson, 1964, '66). The processes of dissociative and multiple ionizations are studied by photon mass spectrometry.

The threshold for the photoionization process, i.e., the ionization potential, is an important quantity measured in a photoionization process. The ionization potentials of atomic gases are usually measured from the Rydberg series which converge to the edge of the ionization continuum. For molecules, this method is difficult since only a few Rydberg series are found in these spectra. From a measurement of the total photoionization cross-section as a function of the photon energy, it should be possible to determine the various ionization thresholds. But observations of these thresholds as the photon energy varies are prone to difficulties caused by Franck-Condon distribution effects. There is often considerable difficulty in relating the measurement to a particular vibrational transition in the molecule, since the maximum in the related Franck-Condon distribution may occur at a high vibrational level of the upper state. Thus if the equilibrium internuclear distances of the two electronic states are very different, there will be a difference between the "vertical" and "adiabatic" ionization potentials. Therefore in using the total cross-section method for finding the ionization potential, the shape of the curve near the threshold is of great importance.

The most accurate method to determine the ionization potentials in the absence of a Rydberg series analysis is that of photoelectron spectroscopy, where for a given incident

photon energy, the energies of the ejected photoelectrons are measured. The technique of photoelectron spectroscopy was initiated in the early 1960s independently by two groups, one led by Turner in London (Aljobeury and Turner, 1962,63) and the other by Vilxasov in Leningrad (Vilesov et al, 1961). Siegbahn and his group at Uppsala had evolved a similar technique a little earlier (Siegbahn et al., 1967), but they used X-rays instead of ultraviolet light and at first concentrated more on the study of solids than on free atoms or molecules. It can be seen from eqn I.20 that corresponding to each ionization potential, there is a definite kinetic energy for the electrons. Therefore the distribution of the kinetic energy of the electrons in the photoelectron spectra given the ionization potentials.

The photoelectron spectra directly represents the various states of the ion formed during photoionization. The intensities of the peaks in the spectra represents the probabilities for formation of the corresponding states. These probabilities when multiplied by the total ionization cross section give partial photoionization cross section. The ionic fluorescence spectroscopy initiated by Judge et al (1963) has also been found to give the partial photoionization cross-sections. But this technique suffers from the low intensity of the fluorescent radiation and the presence of metastable states. This further emphasizes the importance of photoelectron spectroscopy in the

study of photoionization phenomena.

Photoelectron spectroscopy is also useful in determining the nature of the molecular orbitals. The relative location of the molecular and ionic potential energy curves, which determine the Franck-Condon factors, depends on the nature of the orbital from where the electron is removed during ionization. This effect of the orbital involved, causes changes in the vibrational energy levels. For example, loss of a bonding electron in ionization reduces the charge distribution between the nuclei and hence decreases the force constant of the molecule. Since the vibrational frequency is proportional to the square root of the force constant, the effect of decreasing the force constant is also to lower the energy spacing between the vibrational levels. The effect of loss of an antibonding electron is just the opposite. Loss of an antibonding electron strengthens the bond, decreases the internuclear distance, increases the force constant and hence increases the spacing between the levels. Removal of nonbonding electron has little effect on the internuclear distance and the force constant, and hence the spacing between the vibrational energy levels remain unaffected. Thus a study of the changes in vibrational level spacings can be used to derive information on the nature of the orbital involved in ionization.

In addition to obtaining the bonding nature of the orbitals

involved in ionization, vibrational structure study in photoelectron spectroscopy is a valuable tool in determining the vibrational energy levels of those molecular ions where absorption and emission spectroscopic work have proved to be difficult. The study of photoelectron spectra obtained with higher energy photons gives information about the core electron binding energies. These binding energies are a function of the nuclear charge and hence this can be used to identify the atoms involved in the formation of a complex molecule. Thus X-ray photoelectron spectroscopy initiated by Seigbahn (1967) is now used extensively for chemical analysis.

The amount of autoionization and its effects in the photoionization process can be studied with photoelectron spectroscopy. When radiation of a fixed frequency is used, every ionic state in the energy interval $h\nu - I$ along with its continuum electron state contributes to the true wavefunction of the final state reached on photoabsorption. The contribution of a particular autoionization state is determined by its proximity to the photon energy and the strength of mixing of the neutral state with the ion state. A strong mixing implies a large continuum character for the autoionization state, and a dominant oscillator strength at $h\nu$. When the autoionization state contributes significantly to the true wavefunction, the photoelectron spectra show considerably distorted structure.

For example, in the ionization processes of xenon

$$Xe(5s^2 5p^6\ {}^1S_0) + h\nu \longrightarrow Xe^+(5s^2 5p^5\ {}^2P_{3/2}) + e^-$$

with threshold at 1022.1 Å and

$$Xe(5s^2 5p^6\ {}^1S_0) + h\nu \longrightarrow Xe^+(5s^2 5p^5\ {}^2P_{1/2}) + e^-$$

with threshold at 922.8 Å, the ratio of the two cross-sections to form $^2P_{3/2}$ and $^2P_{1/2}$ states is 1.60 for a large number of wavelengths in the range of 922.8 to 460 Å. But near the absorption resonances, this ratio has a value of 1.46, at 558.6 Å, 0.77 at 543.9 Å and 1.49 at 521.8 Å respectively.

In the case of molecules also, autoionization gives a different photoelectron intensity distribution from that when only direct ionization is present. Even in a single electronic state, the vibrational intensity distribution is found to change when autoionization is present. This can be seen from Fig 1.5 for molecular hydrogen (Doolittle and Schoen, 1965). In the figure the photoelectron spectra of molecular hydrogen obtained with a retarding potential analyzer at three ionizing wavelengths 772, 780 and 790 Å are given. The arrows on the figure mark the calculated appearance potentials of the vibrational states of H_2^+. A comparison of the three spectra shows the effect of autoionization in the 780 Å spectrum with a strong enhancement of the excitation of the $v' = 1$ state.

For autoionization, the vibrational intensity distribution of the ion does not depend on the Franck-Condon

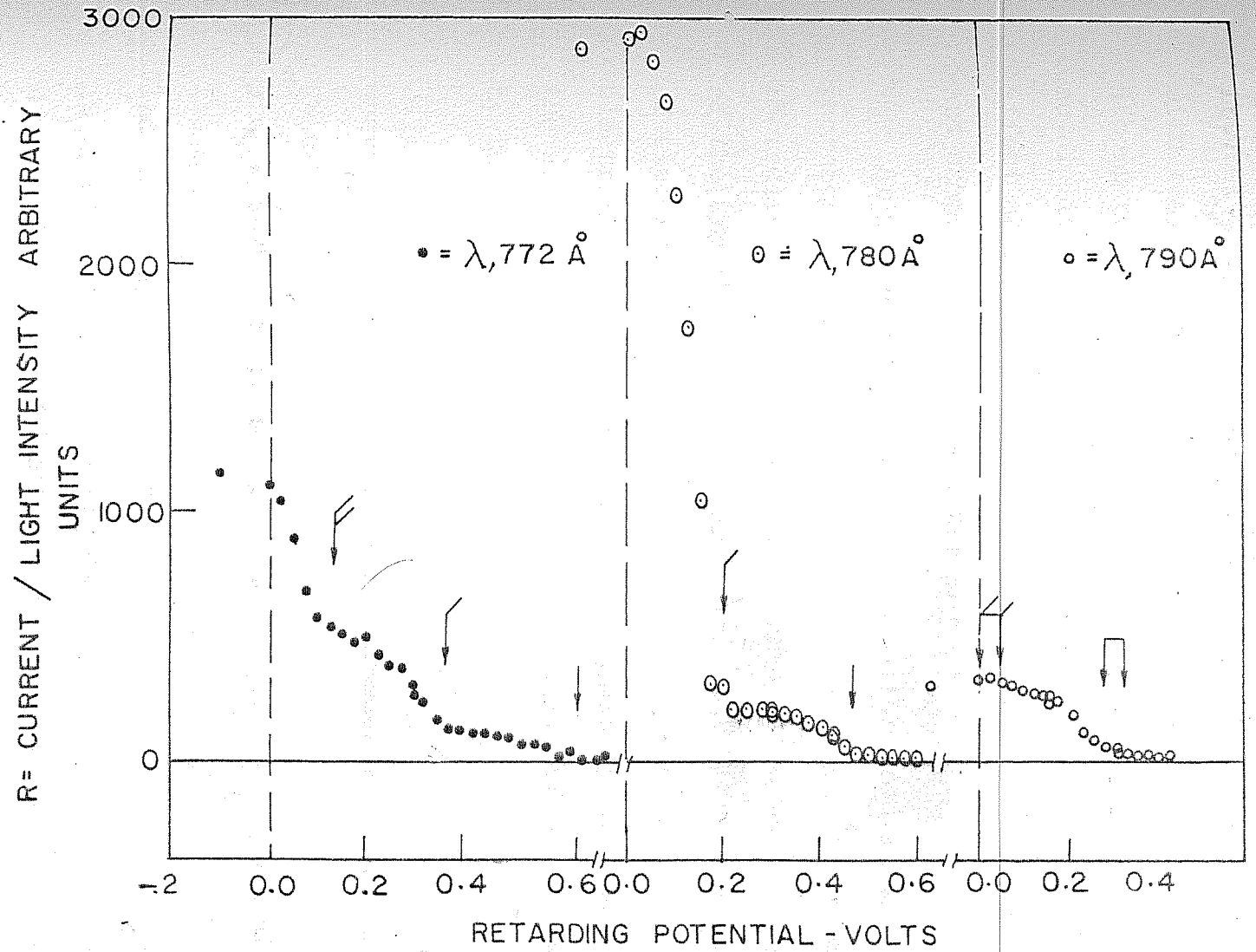


FIG. I.5 Effect of autoionization on the vibrational intensity distribution in the photoelectron spectra of H_2.

factors with respect to the neutral ground state; instead the intensity distribution is related to the Franck-Condon factors with respect to the excited autoionizing neutral state. Thus a comparison of the photoelectron spectra at and away from an autoionizing state can give contribution from the autoionizing effect alone and from this it is possible to study the nature and shape of the autoionizing state.

An important parameter to be determined in the study of photoionization is the angular distribution of the emitted photoelectrons. The photoelectron spectra taken as a function of the angle between the direction of the photon beam and that of electron ejection gives the angular distribution of the electrons. For a dipole transition with plane polarized light, the angular distribution of the photoelectrons is described by the differential cross-section

$$\frac{d\sigma_j}{d\Omega} = \frac{\sigma_j}{4\pi}\left[1 + \beta P_2(\cos\theta)\right] \qquad \text{I.24}$$

where σ_j is the photoionization cross-section for ejection of an electron from the j^{th} orbital, β is the asymmetry parameter and $P_2(\cos\theta)$ is the second order Legendre polynomial. The The asymmetry parameter β depends on the photoelectron energy and the nature of the orbital from which the photoelectron is ejected. Thus the measurement of β determines the nature of the orbital from where the electrons are emitted. The values of β are also used to study the possible electron correlation effects in the neutral.

I.6 Present Status of Photoionization Studies

I.6.1 Atoms

The photoionization of atoms have been studied both theoretically and experimentally to a reasonably good extent. Recent reviews by Starace (1979), Samson (1976, 1979), and Berkowitz (1979) give a very good account of the present status of photoionization studies. Photoionization cross sections and absorption spectra of the rare gases have been studied extensively, to the point where the absolute experimental cross-sections are known to an accuracy of ± 3% to ± 10% over the range from 100 Å to their respective ionization thresholds. The autoionizing structure of these gases has also been studied considerably. Apart from the rare gases, some work on about half of the elements in the periodic table with closed shell as well as open shell structure have been done. Theoretical studies with various forms of many body theory for atoms have been in good agreement with experimental data, particularly in the case of rare gases where an accurate comparison is possible. Partial photoionization cross-section measurements as a function of wavelength have been made so far only for the rare gases, cadmium and mercury. The angular distribution of photoelectrons ejected from the outermost shells have been measured only for the rare gases, Zn, Cd, Hg and O. The angular distribution of the rare gases have been studied over a large photon energy range, whereas, the

other atoms have been studied only at a few resonance lines like 584 (HeI), 304 (HeII), 736 (NeI) and 1048 Å (ArI).

I.6.2 Molecules

Most of the experimental as well as theoretical work on photoionization have been mainly confined to molecules of astrophysical significance. These are diatomic molecules like H_2, N_2, O_2, NO, CO, triatomics like CO_2, H_2O, N_2O, NO_2, CS_2, SO_2 and polyatomics like CH_4, NH_3, C_2H_2, C_2H_4 etc. Apart from these a few other organic as well as inorganic molecules have been studied using photoelectron spectroscopy for molecular structure determination. Experimental work on all the molecules listed above, is far from complete. Except in the case of H_2, whatever small amount of theoretical work has comeout show rather poor agreement with experimental data.

Photoabsorption and ionization cross sections for the diatomic molecules listed above as a function of wavelength have been measured by various groups. Near the ionization threshold, the continua of all these molecules exhibit large autoionization structure. Very little information is available for many of these molecules regarding the nature of the autoionizing states. Partial photionization cross-section or branching ratios have been measured by one or two groups on some of the molecules using photoelectron spectroscopy. Most of the photoelectron spectra have been obtained only at the resonance lines of 304, 584 and 736 Å. Even among these

measurements, except in the case of one or two, the techniques used have been far from satisfactory. In most cases, experiments were done without the use of a monochromator (Collins et.al,1972) This could have affected the spectra due to the presence of other lines from the light source. In many cases, the resolution of the electron spectrometer was quite poor (Bahr et al, 1971). A third drawback has been in neglecting the angular distribution effects. Neglect of the angular distribution could give rise to serious errors in the intensity distribution in the photoelectron spectra.

Samson (1979) has listed the main problems on photo-ionization of atoms to be undertaken in near future. The problems are virtually the same for molecules also. The most important part is the study of total and partial photo-ionization cross-sections as a function of the wavelength. Cross-section measurements have to be made within the continuum and across the resonances. The main difficulty in such a kind of work has been the nonavailability of a continuum source of radiation. The new synchrotron radiation facilities will have to be made use of for this purpose. In the absence of such a fecility, the BRV source could be of help. Care has to be taken to make the photoelectron spectra independent of the angular distribution of the electrons. This necessitates the use of a cylindrical mirror analyzer or the additional measurements of the degree of polarization

of the radiation and the asymmetry parameter β of the molecule.

The angular distribution studies involving the measurement of β as a function of the photoelectron energy (and hence as a function of the ionizing photon wavelength) is another important work to be carried out. One of the important reasons for measuring the asymmetry parameter β is to determine the deviations from the theoretical values predicted by the one-electron approximation. Deviations are expected when electron correlations are important. Dill et al (1974) have shown that for most open shell atoms, β is further influenced by anisotropic electron ion interactions. Dill (1973) has also shown that the photoelectron angular distribution should show pronounced variations with energy across autoionizing resonances. The prediction applies to both atoms and molecules. Finally, Manson (1971) has shown that oscillations in β are expected as a function of the electron kinetic energy. While measurements of β have been made for numerous molecules at the single wavelength of 584 Å, there have been no measurements as a function of wavelength. The prediction of Dill (1973) that the photoelectron angular distribution should show oscillations across discrete autoionizing resonances has been verified by Samson and Gardner (1973 b). Measurements of β across resonant structures provide a method to study the dynamics of photoionization.

Study of the photoionization of atomized species has

been one of the more recent developments. Atomized species include all those transient species like radicals, atoms, ions, and even the excited states of neutral atoms or molecules which are usually produced using an electric discharge. Photoionization studies of these transient species are extremely important in the fields of plasma physics, plasma chemistry, aeronomy and astrophysics. Probably the best technique for studying the transient species is that of photoelectron spectroscopy. In 1970 Jonathen and colleagues published the first photoelectron spectra of N, O, and H (Jonathen et al., 1970). Since then, several transient species have been studied and the progress in this area upto 1974 has been reviewed by Frost (1974). Again, most of these measurements have been carried out at certain resonance wavelengths only without the use of a monochromator. Also very little quantitative measurements have been done in this field which are independent of the angular distribution of the photoelectrons.

The work presented in this thesis has been oriented towards making some studies of photoionization in the above context. The above discussion very clearly shows the necessity of studying the photoelectron spectra of atomized as well as molecular species with scrupulously monochromatic radiation coupled with an electron energy analyzer which gives spectra independent of the angular distribution. The necessity of obtaining the photoelectron spectra of various gases as a

function of photon wavelength and of studying the effects of autoionization on the photoelectron spectra is apparent. Part of the work presented in this thesis are in these directions. A photoelectron spectrometer system with a monochromator and a cylindrical mirror electron energy analyzer has been built for this purpose and is discussed in the second chapter. The photoelectron spectra of O_2, H_2, and CO_2 have been measured at a number of wavelengths and the possible effects of autoionization are studied. In the photoelectron spectrum of CO_2 some new vibrational levels of the $X^2\Pi_g$ state of CO_2^+ have been detected. These have been dealt in the third chapter. Experiments on the study of photoionization of atomized species were also carried out and these form the fourth chapter.

I.7 Electron Scattering Studies using Photoelectron Spectroscopy

Just as important as the study of photoionization is the study of electron scattering with atoms and molecules. The electron scattering phenomena are distinguished as elastic, inelastic, superelastic and radiative. In an elastic scattering no energy exchange takes place between the internal motion of the atom or molecule and the electron. In an inelastic collision some kinetic energy is lost by the electron in exciting internal motion in the scattering species. Superelastic collisions occur only between an electron and an excited atom or molecule such that the electron gains energy from the internal motion of the atom/molecule. Collisions resulting

in the emission of electromagnetic radiation is called radiative.

The total electron scattering cross section has been measured by the Ramsuer technique which has been modified by Golden and Bandel (1965). Electron time of flight spectroscopy has also been used for low energy electron scattering studies as in the case of Ferch et al (1980). In the Ramsuer type experiments, the important part is in making monoenergetic electron beams. The electrons are generally produced thermionically and have a broad energy distribution. An electron monochromator which is essentially an electron energy analyzer is used to make the beam monochromatic. The resolution of the electron monochromator is restricted by the contact potentials present at the slits. This limitation in the electron energy resolution can be overcome if one uses electrons emitted by photoionization of atoms with monochromatic photons. The photoelectrons emitted will have an energy spread dependent mostly on the photon energy spread and the doppler motion of the atoms. The net spread is better than the resolution of the electron monochromators achieved so far. Moreover very small amount of scattering studies has been done at near-zero electron energies. The photoelectrons can be produced at these energies with better resolution as discussed above.

In the fifth chapter of the thesis, the experiment and results obtained for the electron scattering studies by

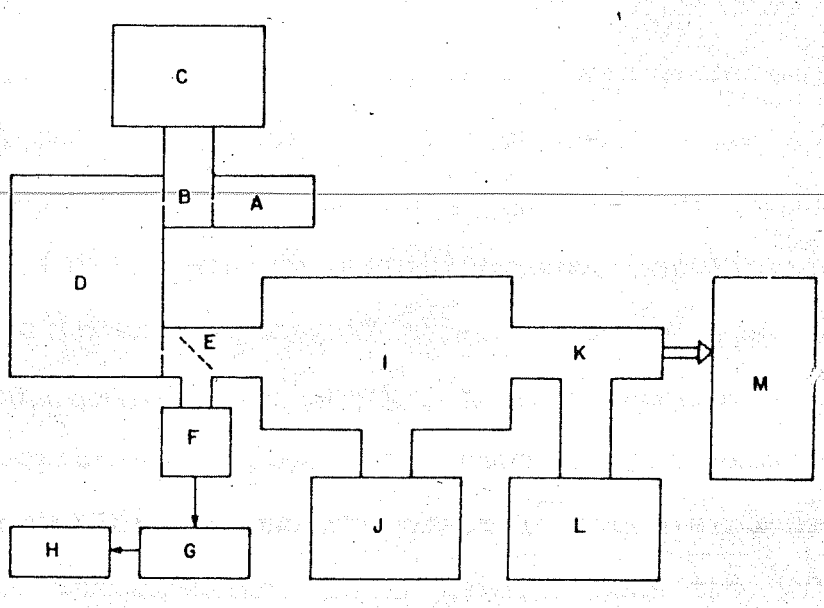
photoelectron spectroscopy are presented. The photoelectron spectrometer set up built for the photoionization study has been used as such for this experiment. Measurements were made for the relative total electron scattering cross-sections for H_2,

CHAPTER II

PHOTOELECTRON SPECTROMETER

II.1 INTRODUCTION

The necessity of studying the high resolution photoelectron spectra of gases as a function of the incident energy has been pointed out in the first chapter. The essential requirements for such a kind of work are a line emission/continuum light source, a vacuum ultraviolet monochromator and a high resolution, high sensitivity electron spectrometer. The experimental set-up used in the present work included a line source, a monochromator, an electron spectrometer and the necessary data acquisition system. The electron spectrometer consisted of the ionizing region, the electron energy analyzer and the electron detector. The block diagram of the photoelectron spectrometer assembly has been shown in Fig II.1. The details of the various parts and the operation and performance of the system is presented in the following sections.



A. LIGHT SOURCE
B. DIFFERENTIAL PUMPING STAGE
C. ROOTS PUMP + ROTARY PUMP
D. MONOCHROMATOR
E. BEAM SPLITTER
F. PHOTOMULTIPLIER
G. PICO AMMETER
H. CHART RECORDER
I. ELECTRON SPECTROMETER
J. DIFFUSION + ROTARY PUMP SYSTEM
K. DIFFERENTIAL PUMPING LINE
L. DIFFUSION + ROTARY PUMP SYSTEM
M. DATA AEQUISITION SYSTEM

Fig. II.1 BLOCK DIAGRAM OF THE PHOTOELECTRON SPECTROMETER ASSEMBLY

II.2 Electron Energy Analyzer

The electron energy analyzer is used to obtain the kinetic energy distribution of the photoejected electrons and is the most important part of the photoelectron spectrometer. In general, the energy distribution of charged particles is obtained by the proper use of an electric or a magnetic field. Usually, for low energy particles, the electric field analyzer is preferred to the magnetic field type because of its simplicity and direct analysis of the energy, rather than the momentum. In photoelectron spectroscopy for studying the valence electrons, it is convenient to use the electric field analyzers since the energy of the electrons is in general less than 40 eV, and in most of the cases in the range of 0 to 10 eV.

The electric field analyzers are classified into two main groups - the retarding potential analyzers and the deflecting field analyzers. In the retarding potential type, all the electrons above a certain threshold are collected and counted as a function of the threshold voltage, and as a result one obtains an integral spectrum. In the deflecting field analyzers, particles of various energies are spatially separated and focused on to different points in space and the number of particles at a particular point is counted as a function of the deflecting voltage, thus getting the differential spectrum. The deflecting field analyzers, therefore, have an advantage over the retarding potential

analyzers in providing the differential energy spectrum directly.

The deflecting field analyzers used commonly are parallel plate, cylindrical, spherical, and cylindrical mirror analyzers. A comparative analyses of these are given by Hafner et al (1968) and Heddle (1971). The various deflecting field analyzers have also been reviewed by Afanasev and Yavor (1975). A discussion of these analyzers are also available from Wannenberg et al (1974) and Roy and Carette (1977) where they have reviewed all the traditional types of electron energy analyzers and the criteria for their selection.

II.2.1 Choice of the Analyzer

Though there are various versions of electron energy analyzers available, the specific requirement of the experiment, and limitations of instrumentation precludes most of them from being used. The basic requirement of the analyzer in measuring the relative vibrational intensities is that the photoelectron spectra obtained should be independent of the angular distribution of the emitted photoelectrons. The angular distribution of the electrons in turn depends on the state of polarization of the ionizing radiation and the asymmetry parameter β of the molecule. When a monochromator is used along with the light source, the resulting photon beam is partially polarized because of the reflection at the concave

grating. The differential cross section for electric dipole transition with partially polarized light, leaving the residual ion in the j^{th} state is

$$\frac{d\sigma_j}{d\Omega} = \frac{\sigma_j}{4\pi}\left[(1 - \tfrac{1}{2}\beta) + \frac{3\beta}{2g+1}\left(g\cos^2\alpha + \cos^2\gamma\right)\right] \qquad \text{II.1}$$

as given by Samson (1969 a, '70), where the degree of polarization is defined by $g = I_x / I_z$, I_x is the irradiance of the radiant energy vibrating along the x-axis, and I_z is the irradiance vibrating along the z-axis, β is the asymmetry parameter of the molecule and α and γ are the angles between the direction of electron emission and x and z axes respectively. In the above expression, it is assumed that the photon beam is along the y-direction and that either the x or z axis is oriented along the direction of maximum polarization. It has been shown (Samson and Gardner, 1977 b) that for a cylindrical mirror analyzer with complete azimuthal symmetry, the intensity distribution of the photoelectron spectra is independent of the state of polarization of the ionizing radiation. It is also shown that (ibid), with such a geometry of the analyzer and with electrons analyzed at $54^{\circ}\ 44'$ to the direction of the photon beam, the photoelectron spectrum is also independent of the asymmetry parameter β of the molecule. This particular angle has conveniently been named as magic angle.

The only other analyzer which can give results independent of the angular distribution of electrons directly is the

spherical retarding potential analyzer covering all 4π solid angle.

Apart from giving an integral spectrum its usefulness is limited because of the difficulties in detecting and measuring the analyzed electron intensity. This drawback becomes more pronounced when the incident photon intensity reaching the ionization region drops substantially when a vacuum ultraviolet monochromator is used along with the light source. Thus for accurate measurement of vibrational intensities the choice is for the high resolution, high luminosity cylindrical mirror analyzer.

The focusing properties of the cylindrical mirror analyzer have been discussed in detail by Zashkvara et al (1966), Sar - El (1967) and Aksela et al (1970). It has been shown that a wide range of focusing conditions can be obtained by suitable choice of the angle Θ and of the deflecting potential applied to the outer cylinder. Aksela (1971) has compared in detail the energy distribution of electrons transmitted through a CMA at the location of both the minimum trace width and the image of the second order focus. When the effect of a large divergence in entrance angles is greater than the effect due to the size of the slit widths, Aksela found that the base width of the energy distribution was smaller at the minimum trace width location; however, FWHM was significantly smaller at the second order focus. Furthermore,

the distribution at the minimum trace width exhibited two sharp peaks. These double peaks could produce serious complications in spectrum analysis. When the effect due to the size of the source and exit slit is not negligible, the double peaks are smoothed out and the FWHM for both distributions are comparable.

Risley (1972) has presented design parameters for various geometrical arrangements of the CMA. From the curves for various parameters given by Risley it is seen that for second order focusing at $\theta = 55^{\circ}$, the sum d of the perpendicular distances of source and image from the surface of the inner cylinder should be about fifty times the radius of the inner cylinder. Even when $d = 2 r_i$ i.e, for axial focusing the second order focusing is possible for 42° only. Hence with the CMA operating at 55° angle only first order focusing is possible. Aksela (1970) has shown that the figure of merit which is the product of the resolving power and the entrance solid angle is better for a CMA with axial focusing than that with surface focusing when the source is not larger than the entrance aperture. In the case of an extended source, Heddle (1971) has redefined the figure of merit as luminosity or etendue which is the product of the entrance area and the solid angle and has also compared this figure of merit for three dispersive electron spectrometers in terms of the resolving power and a dimension. He has shown that the CMA with surface focusing has the largest etendue for a given resolution and dimension. For a CMA with a given radius

11490

and resolution of about 100, the etendue for surface focusing type is about four times that of the axial focusing type. Moreover in the axial focusing CMA, the electron detector has to be very critically positioned to collect the electrons. Also, the definite size of the detector might affect the energy resolution. Thus it was decided to use a CMA with surface of focusing property even though second order effect is greater in this type compared to that in the axial focusing type.

II.2.2 Cylindrical Mirror Analyzer - Design Aspects

In a cylindrical mirror analyzer with surface focusing, the distance between the entrance and exit slits is expressed as

$$\frac{L}{r_1} = \sqrt{4\pi k}\,\cos\theta\,\exp(-k\sin^2\theta)\,\mathrm{erf}.(\sqrt{k}\,\sin\theta) \qquad \text{II.2}$$

where L is the distance between the slits, θ is the angle at which the electrons enter the analyzer and k is the analyzer constant given by

$$k = \frac{E}{V} \ln \frac{r_2}{r_1} \qquad \text{II.3}$$

In the above expression, E is the electron energy in eV, V is the deflecting voltage applied to the outer cylinder, and r_2 and r_1, are the radii of the outer and inner cylinder respectively. The various parameters were fixed in the following way. The values of $\frac{L}{r}$, were plotted as a function of θ for various values of k. For each value of k, $\frac{L}{r_1}$ has a maximum at a particular value of θ. From these, the curve for which $\frac{L}{r_1}$ was

maximum at 54° 44' was chosen. This curve corresponded to $k = 1.03$, at $\theta = 54^{\circ}$ 44' giving $\frac{L}{r_i} = 3.232$. The luminosity or etendue of the analyzer as given by Heddle (1971) is $\epsilon \simeq \frac{50 r_i^2}{\rho^2}$ where $\rho = \frac{E}{\Delta E}$ is the resolution. From this it follows that the larger the radius r_i, the more the etendue. Hence a large radius of 2" was fixed for the inner cylinder. With this radius the distance between the slits was L = 6.264". The radius of the outer cylinder was selected to be 5". This is sufficiently larger than $r_m = 4.2$" where r_m is the maximum radial distance the electrons can achieve from the axis of the analyzer when they enter the analyzer at $55^{\circ} \pm 3^{\circ}$. The slit width of the analyzer as given by Heddle (1971) is

$$s = 1.5 L/\rho$$

where s is the slit width for the two slits. This is valid when $\alpha < 2(3\rho)^{-1/2}$ where α is the angular spread of the electrons. It was decided to restrict the angular spread to $\pm 3^{\circ}$, i.e., $\alpha = 6^{\circ}$, and the resolution was chosen to be 100. With these values of α and ρ the condition $\alpha < 2(3\rho)^{-1/2}$ was satisfied. Hence the slit width calculated was 2.4 mm. A slit width of 2 mm was fixed in the present CMA. The corresponding resolution turned out to be $\rho \simeq$ 120. The corresponding luminosity was $\epsilon = \frac{50 r_i^2}{\rho^2} \simeq 0.1$ sterad.cm^2.

Table II.1

Design Parameters of the Analyzer

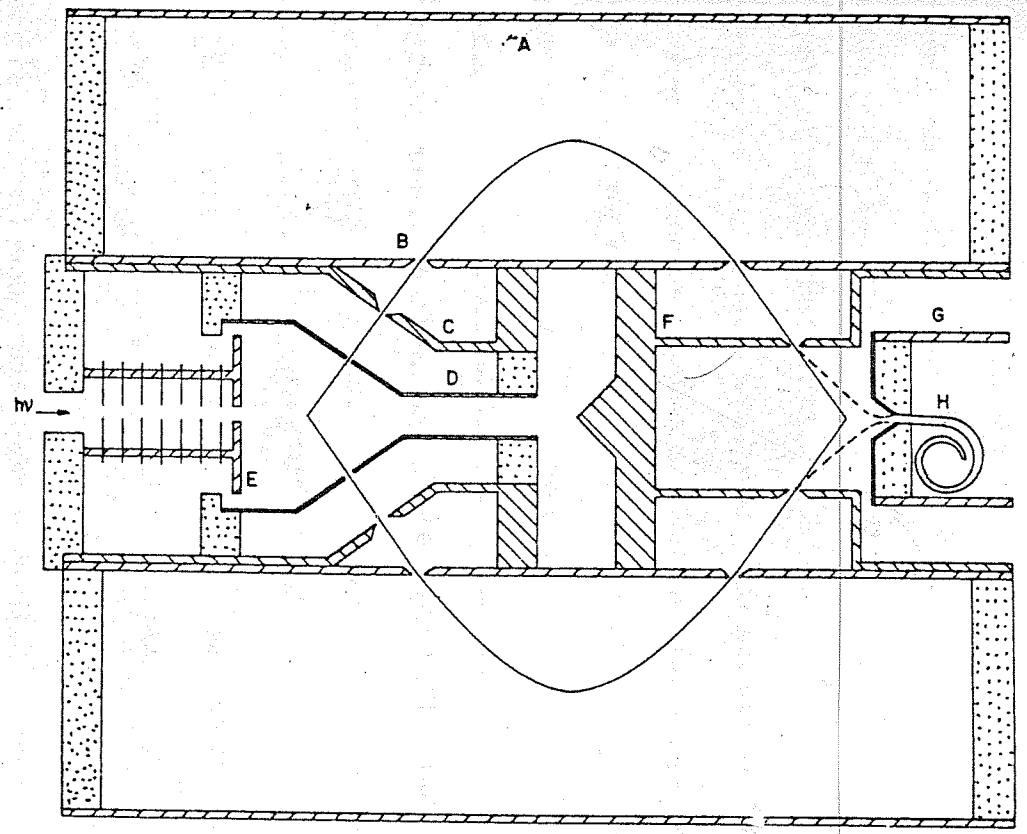
Radius of inner cylinder	r_1	=	2"
Radius of outer cylinder	r_2	=	5"
Distance between the slits	L	=	6.264"
Analyzer constant	k	=	1.03
Slit width	s	=	2 mm
Luminosity (etendue)	E	=	0.1 sterad.cm^2
Resolution	ρ	=	120

II.2.3 Analyzer Details

The cylindrical mirror analyzer was constructed with the parameters given in the previous section. The details of the analyzer are given in Fig II.2. The photoionization region is enclosed within the innermost electrode D of the analyzer and the photoelectrons could be accelerated or retarded by holding this electrode at a proper potential with respect to the inner cylinder before they entered the analyzing region enclosed within the outer cylinder A and inner cylinder B. Since the electrons travelled at an angle of 55° to the analyzer axis before they entered the analyzing region, the electrode D and the collimator C had to have the special geometry as shown in the diagram. The width of the slits on C and D are such that the angular divergence of the electrons is $\pm 3^{\circ}$.

The photon beam before entering the ionization region was made into a narrow pencil by a number of circular baffles E. These baffles were mounted on a machinable glass ceramic (MACOR) flange fixed to the end of the inner cylinder. To keep the source region (ionization region) free from any electric field, the baffles were kept at the same potential as D. The cylinder D was separated from C by MACOR flanges. C was machined in such a way so as to push-fit in B and was at the same potential as B. A collimator F was provided at the detector side also. This prevented the electrons from coming

A OUTER CYLINDER
B INNER CYLINDER
C COLLIMATOR
D ACCELERATING RETA- - RDING ELECTRODE
E LIGHT BAFFLES
F COLLIMATOR
G CHANNELTRON HOUSING
H CHANNELTRON



STAINLESS STEEL
INSULATOR

Fig. II. 2. ELECTRON SPECTROMETER

to the detector directly from the source region. It also prevented the electric field due to the voltage applied to the channeltron face from penetrating into the analyzing region. The photon beam after passing through the source region was blocked by the solid cone on F with a semivertical angle of 45°. This prevented the reflection of the photon beam into the source region. A small cylinder sufficiently screened from the source region and held at a few volts positive potential was fixed around the cone. This was to collect the metal electrons produced in that region. It was found that this did not have much effect and was subsequently removed. The inner cylinder was held in position and insulated from the outer cylinder by MACOR spacers at the ends. These spacers had large openings so as to facilitate rapid evacuation.

All the metal parts of the analyzer were made out of stainless steel 304. The outer cylinder was made from a sheet and hence had nonuniformity of about 2% in the diameter. Both the entrance and exit slits were about 5 inches away from the ends. This prevented the end field effects from affecting the resolution. The entrance and exit slits were cut almost through 360°, except for 3 small bridges on each slit spaced symmetrically around the surface to hold the cylinder together. The pieces C, D, and F where machined from single rods. Again slits were cut through almost 360° leaving three small bridges on each one. The light baffles were made from

thin sheets and mounted together with the help of three stainless steel screws. These baffles had apertures of 3 mm diameter and were kept 1 cm from each other.

II.3 Beam Splitter, Vacuum System and other details

The electron spectrometer was mounted in an 18" long 14" diameter stainless steel chamber which was evacuated by a 4 inch oil diffusion pump with an unbaffled speed of 500 lit/sec. This chamber was connected to the monochromator through a coupler which incorporated a beam splitter also. This coupler was provided with ports for detecting the reflected light from the beam splitter by a photomultiplier, for introducing the gas sample into the ionization region, and for the capacitance monometer connection. The beam splitter was made of thin wire mesh with about 80% transmission and was mounted at 45° to the direction of the photon beam. The reflected light from the beam splitter fell on the sodium salicylate coated face of a perspex light pipe.
The ultraviolet radiation was converted into visible light by the sodium salicylate and the visible light was transmitted through the light pipe to a photomultiplier. The PMT output was monitored using a picoammeter and a chart recorder. The whole analyzer was mounted onto the flange of the vacuum chamber with proper electrical insulation. This flange had an opening 4 inches in diameter, and an electron detector with a

separate mounting was introduced through this opening. Additional pumping of the gas leaking into the analyzing and detection regions through the narrow slits of the analyzer was achieved by a second 4" oil diffusion pump connected through a T-shaped line attached to the rear flange of the main chamber. This helped in maintaining the analyzing region and the detector at sufficiently low pressure even when the source region was at a high pressure of the order of 10^{-2} torr. The free end of the T-line was closed by a blanking plate to which the channeltron housing was mounted. This flange had a number of high voltage ceramic-metal seals also for the necessary electrical connections. The preamplifier and the amplifier were also mounted directly on this flange.

The pressure in the source region was monitored using an MKS Baratron Capacitance Manometer (head 310 MH-10) and the pressure in the main chamber was measured by an ionization gauge (gauge head-Veeco and unit - Veeco- RG 830).

It was found that the analyzer performance was greatly hampered by the earth's magnetic field. To reduce the effect of this field the whole experimental system was positioned in such a way that the axis of the analyzer was normal to the magnetic plane and the whole analyzer was covered by a number of mu-metal cylinders. These mu-metal cylinders were about 16" long and were made of 1/32"thick perfection annealed alloy.

conetic alloy. They were separated by thin aluminum foil in between. This mu-metal shield assembly was fitted inside the main chamber and was supported by the outer cylinder of the analyzer. The outer cylinder was insulated from this shield by a thin mica sheet.

II.4 Electron Detector

The electron detector used was a channeltron (Mullard B419 BL). The characteristics of the channeltron are given in the Table II.2. The channeltron was used in the counting mode, so that for each electron detected, it gave a saturated pulse at the output. These pulses went through a preamplifier and amplifier before getting stored in a computer controlled multichannel analyzer. The channeltron face was held at +100V so that it could attract the electrons onto it, and energize them sufficiently to produce secondary electrons. The end of the channeltron was kept at +3 KV potential.

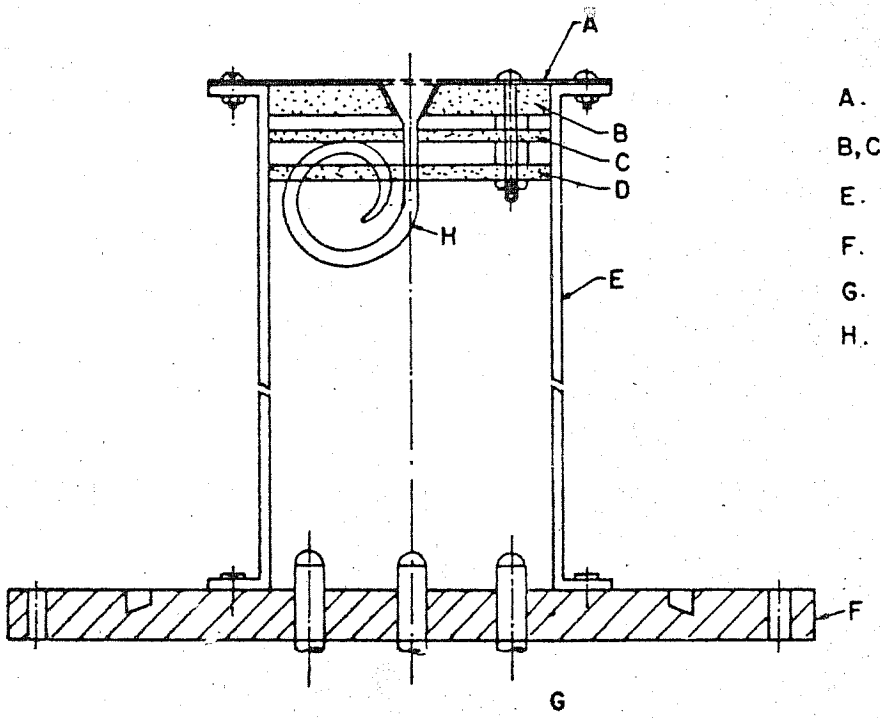
The channeltron was housed as shown in Fig II.3. Because of its asymmetric shape, special attention had to be given to mount it properly. Two teflon flanges to fit around its cone and neck and a third one with a slot to fit its helical position were made, each in two symmetric pieces. The channeltron was fixed in these pieces with proper spacers in between along with the thin stainless steel flange A. This set up was mounted on the cylindrical support E which in turn was fixed onto the

Table II.2

Characteristics of Mullard CEM-B419BL

Max.Operating Voltage	3.5 KV
Nominal Resistance	5×10^9 ohm
Gain	1.1×10^8 @ 2.5 KV
Noise (@ 2.5 KV)	2.0 p.p.s
Pulse Height Distribution Resolution (@ 10^8 gain and 1000 p.p.s)	0.6
Minimum effective cone diameter	9 mm

Note: The noise was found to be one order of magnitude less than the one given above.



A. Stainless Steel Flange

B,C,D. Teflon Flanges

E. Cylindrical Support

F. Stainless Steel Flange

G. Highvoltage Ceramic Metal Seals

H. Channeltron

Fig II 3 CHANNELTRON HOUSING.

flange F. A few highvoltage ceramic-metal seals were fixed on F for electrical connections. The cylindrical support E was provided with large holes on it for evacuation.

The voltage (+3 KV) given to the rear end of the channeltron was well shielded by the channeltron housing which was grounded. This was needed to prevent the electrons from coming to the rear end instead of the face and also to reduce the leakage of the field lines into the analyzing region. But it was found that there was some loss of resolution when the electrons were analysed at low energies, due to the field from the channeltron face. So it was found necessary to reduce the face voltage to 20-30 V to achieve better resolution. But this in turn, reduced the total count rate.

II.5 VUV Monochromator

An asymmetric type normal incidence 1 meter monochromator (Jobin-Yvon, France) was used to monochromatise the radiation coming to the electron spectrometer. The special holographic concave grating (Jovin-Yvon, France) used had a ruling of 1200 lines per mm and could be conveniently used in the spectral range from 300 to 1500 Å in the first order. The various photon energies could be selected by rotating the grating. The best beam width obtained was 0.1 Å. The monochromator was provided with a 4" oil diffusion pump and could be evacuated to a base pressure of $\sim 10^{-6}$ torr.

II.6 Light Source

The light source used was a microwave discharge lamp giving neutral emission lines characteristic of the gases used. Most of the work presented in this thesis was done using HeI 584 Å, NeI 736 Å, and 744 Å lines. Certain ArI and HI lines were also used. The gas from the cylinder was allowed to flow through a 1 cm diameter, 20 cm long quartz tube. The gas flow was controlled with a fine metering needle valve (Granville-Philips). The quartz tube was fixed on a metal flange with an 'O' ring seal. This flange was mounted on the differential pumping arrangement connected to the entrance slit side of the monochromator. The differential pumping arrangement included a roots pump backed by a rotary pump and a movable slit of width 1 mm and height 1 cm. The roots pump had a speed of 40 litres/sec and could give an ultimate vacuum of 10^{-3} torr. The slit could be moved for proper alignment. The diffusion pump of the monochromator acted as a second stage of the differential pumping.

The light source was powered by a 2450 MHz Kiva supply (Ophthos Instruments, MD) with a maximum output power of 100 watts. For certain experiments, modulation of the microwave power was needed. For that, another microwave generator, MR III (K.K.Ewig Shokai, Japan) was used. This had

a maximum output power of 200 watts, and could accept modulating pulses through an external circuit. As far as possible, the Kiva supply was used because of its smooth functioning. The microwave power was coupled to the discharge through an Evenson cavity which could easily be clamped around the discharge tube. The cavity and the discharge region were cooled by passing compressed air through the port provided in the cavity. The tuning of the cavity had to be done by the two tuning stubs provided and also by slight adjustment of the pressure in the discharge tube. The intensity of the radiation was found to be dependent on the pressure in the discharge tube and there was an optimum pressure at which the intensity was maximum. This optimum pressure varied from one gas to another. This effect could be due to the self absorption of the radiation.

The microwave discharge provided quite intense radiation. The main advantages in using this source were in its steady functioning, almost constant intensity and ease of operation.

II.7 Data Acquisition System

The data acquisition system included a preamplifier, an amplifier, a comparator, a 256 multichannel analyzer operated in the time mode and a staircase generator. The multichannel analyzer and the staircase generator were controlled by a microcomputer. The data display and recording were done by a cathode ray tube and a teleprinter respectively. All the data

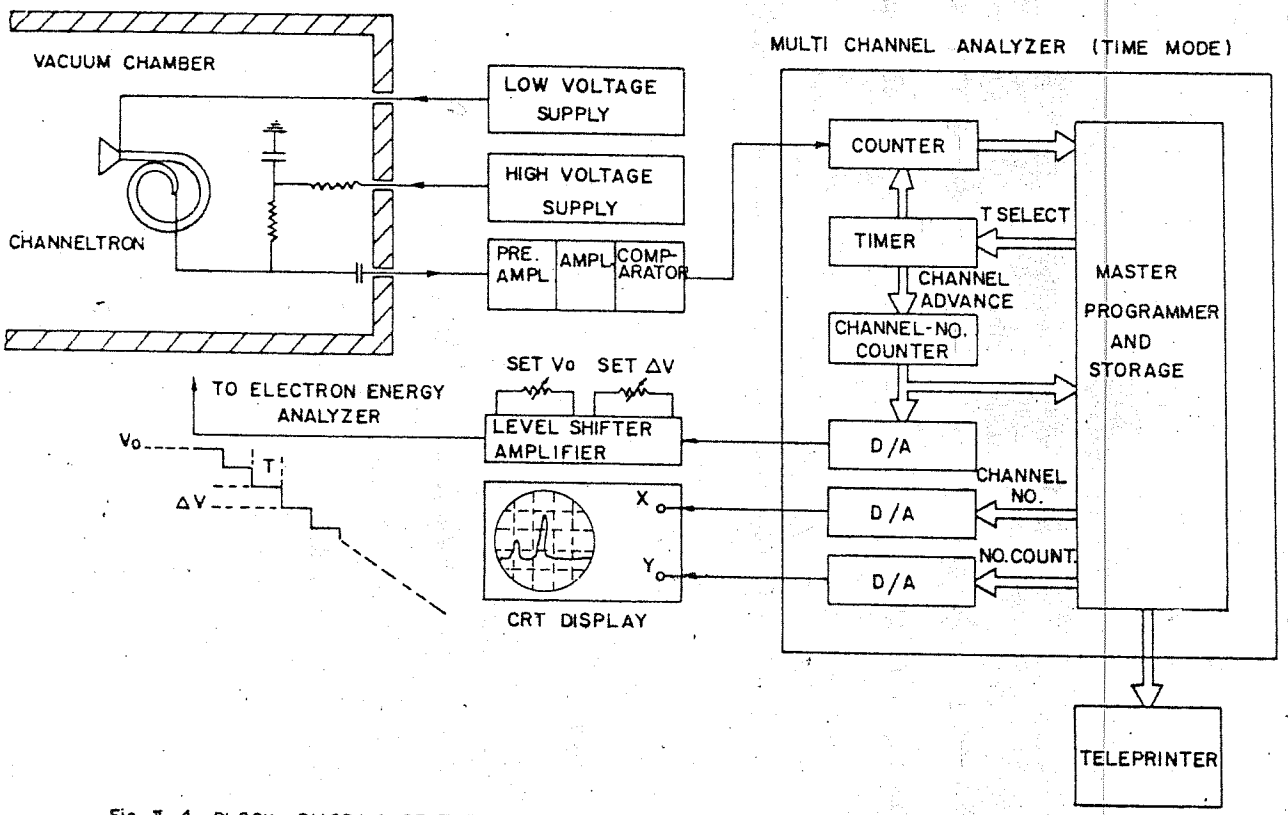


Fig. II. 4. BLOCK DIAGRAM OF THE DATA ACQUISITION SYSTEM

collection system was built in our own laboratory. The block diagram of the set up is shown in the Fig II.4.

The preamplifier was a high input impedance voltage pulse amplifier. The amplifier was AC coupled, linear wide band type with a gain of about 25. The comparator made the pulses TTL compatible.

The MCA included the pulse counter, oscillator or timer, the master programmer and storage, and the digital to analog (D/A) converters for the staircase and display. The pulses from the comparator go into the pulse counter and the number of counts for a definite time t is stored in the memory. The timer is used to fix the data collection time t per each channel. This time t is dictated by the master programmer which receives commands in the beginning of the experiment through the teleprinter. After each time interval t, the channel number is advanced and is counted by the channel number counter. This channel number goes into the memory as well as a D/A converter. The output of this D/A converter is proportional to the channel number and hence it produces the corresponding step of the staircase. This D/A converter has a range of 0 to 5 V only corresponding to the 256 channels of the MCA and has to be further amplified by a Level Shifter Amplifier. This Level Shifter Amplifier has provision to fix the initial voltage Vo in the range of +30 to - 30 volts and the stepsize ΔV. The

step size can be controlled continuously or in discrete values in the range from 2mV to 200 mV. From the memory, the channel number and the corresponding number of pulses stored in each channel go through two different D/A converters, the output of them being connected to the cathode ray tube display. The data at the end of each run is printed out or punched out on paper tapes by the teleprinter.

To start the data collection, first of all the initial voltage Vo and the step size Δ V are fixed manually. Commands are given through the teleprinter to select the data collection time t per each channel as well as the number of scans required. The time t can be set in any of the 0.1, 1, 10, 100, 200, 300 and 400 sec. intervals. The mode of operation, i.e., addition or subtraction of the data can also be fixed by the external command. Once the necessary commands are given, the system collects data automatically and displays it simultaneously until all the commands are fulfilled. The data collection can be stopped or restarted in between if needed. After each collection the data are printed out or punched out on the paper tapes by separate commands.

At times, large number of spurious pulses were observed at the output end of the channeltron. It was found that these pulses were due to some sort of leakage at the highvoltage seals when the atmosphere was very humid and the seals were unclean. To eliminate this a simple RC filter was used and this filter along with the load resistance and the coupling condenser were

enclosed in the spectrometer vacuum chamber itself. This completely eliminated the spurious pulses.

The output from the photomultiplier which monitored the intensity of the photon beam was fed into a picoammeter (ECIL). The picoammeter output voltage is given to a strip chart recorder (OMNISCRIBE). In the course of an experiment any change in the photon intensity was noted down from the chart recorder and the necessary corrections were made in the data.

II.8 Operation of the Spectrometer

When the electron source region of the photoelectron spectrometer was held at the same potential as the inner cylinder of the analyzer, the energy of the electrons entering the analyzing region was not modified in anyway. While analyzing the electrons in this way, it was found that the collecting efficiency of the analyzer was very small for electrons of energy from zero to about 1 eV. This was mainly due to the stray electric and magnetic fields remaining in the system. This collecting efficiency problem was partly overcome by a preacceleration of the electrons before they entered the analyzing region. Thus in general the analyzer was operated in two different ways. The first one was by keeping the source region at the same potential as the inner cylinder (usually both are kept at the ground potential) and the second one was by having a preacceleration. To distinguish these modes

the first one is named the grounded mode and the second one the accelerating mode.

Apart from having a large collecting efficiency for near zero energy electrons, the accelerating mode had a definite advantage over the grounded mode. In this mode all the electrons could be analyzed at a fixed energy, thereby maintaining the same resolution throughout the spectrum. Hence all the experiments were done in the accelerating mode by giving the staircase voltage to the source region and keeping the inner cylinder at the ground potential and outer cylinder at a fixed negative voltage. The constant negative voltage given to the outer cylinder was derived from a nickal-cadmium cell through a high resistance potentiometer.

II.9 Performance of the Spectrometer

The performance of the photoelectron spectrometer was studied with respect to the resolution, the collecting efficiency, the energy calibration and the shape of the peaks. It was found that all these characteristics were greatly affected by the earth's magnetic field and the small amount of the stray fields in the analyzer and also the electron scattering due to the parent molecules or atoms. The stray fields include the magnetic field due to any remnant magnetism present in the spectrometer material, the electric field due

to the contact potentials and the small amount of field leaking into the analyzer from any high voltage points like the channeltron inside the spectrometer. The effects of the various fields were studied in detail and are being described below.

II.9.1 Effect of the Earth's Magnetic Field

Initially, in the spectrometer, no magnetic field shielding or field compensation was used and the argon photoelectron spectrum with He 584 Å radiation was studied with the spectrometer in the grounded mode. But for a very weak hump nothing was discernible in the spectrum. After the introduction of three layers of μ-metal shield the hump became very pronounced and the two peaks $^2P_{1/2}$ and $^2P_{3/2}$ could be barely distinguishable. The introduction of three more μ-metal shields improved the spectrum to such an extent that about 80 meV resolution was obtained. A study of the molecular oxygen spectrum in the grounded mode at the same wavelength revealed that the collecting efficiency below about 1 eV was practically zero even with six layers of μ-metal shielding. Thus it was decided to introduce three more layers of μ-metal shielding. With this arrangement a final resolution of about 40 meV was obtained at an electron energy of about 5.5 eV in the grounded mode. In the same mode the collecting efficiency, especially below 1 eV was seen to improve drastically and the

$O_2^+ B^2\Sigma_g^-$ state could be seen with sufficient intensity in the O_2 584 Å spectrum.

It has been reported by Gardner and Samson (1973) that the presence of the magnetic field caused splitting of the peaks in the photoelectron spectra. They observed a splitting of the argon doublet into a pair of doublets separated by 360 meV in a 50 milli Gauss field with 584 Å radiation strongly polarized by a ½ m Seya-Namioka monochromator. In the present analyzer also the splitting of the peaks into two or more components was observed; but it never could be connected to the presence of the magnetic field. It was found that these splittings were only due to the contact potentials present due to impurities as discussed below.

II.9.2 Effect of Contact Potential

Whenever the spectrometer was exposed to humid atmosphere, corrosive or sticking gases or oil vapour the resolution degraded dramatically. The transmission of the analyzer reduced drastically and the analyzer constant was found to change and even presented multiple values resulting in more than one peak corresponding to each original peak. This problem was solved by extensive cleaning of the spectrometer parts followed by continuous evacuation of the system along with baking and plasma cleaning by making use of an RF discharge, the details of which will be given later in this section.

After obtaining a reasonably good performance of the analyzer, it was decided to see how exactly the 'poisonous' atmosphere affected the spectrometer. To see the effect of water vapour alone, the spectrometer was kept at about 25 torr pressure of water vapour for about 12 hours. The adverse effect of this on the performance of the spectrometer can be seen in Fig II.5, where the argon spectrum in the grounded mode of the analyzer at 584 Å is presented. In Fig II.5a is shown the spectrum before the exposure to water vapour and in Fig II.5b after the exposure. The overall intensity, the resolution, and the nature of the peaks are seriously affected by the exposure. A similar study was done by exposing the spectrometer to the atmosphere. A similar effect is seen in the two spectra in Fig II.6, one before exposure and the other after exposure to the atmosphere for about 2 hours. The performance of the photoelectron spectrometer was badly affected when the system got exposed to oil vapour and the worst thing happened when introduction of nitric oxide gas into the system was followed by water vapour. This happened accidentally. Right after taking a nitric oxide spectrum, the spectrum of H_2O was tried. Initially the performance was satisfactory, but as time elapsed the resolution and the intensity went down and after about two days no spectrum could be obtained. Extensive cleaning starting from abrasive cleaning to introduction of RF discharge only could restore the original performance.

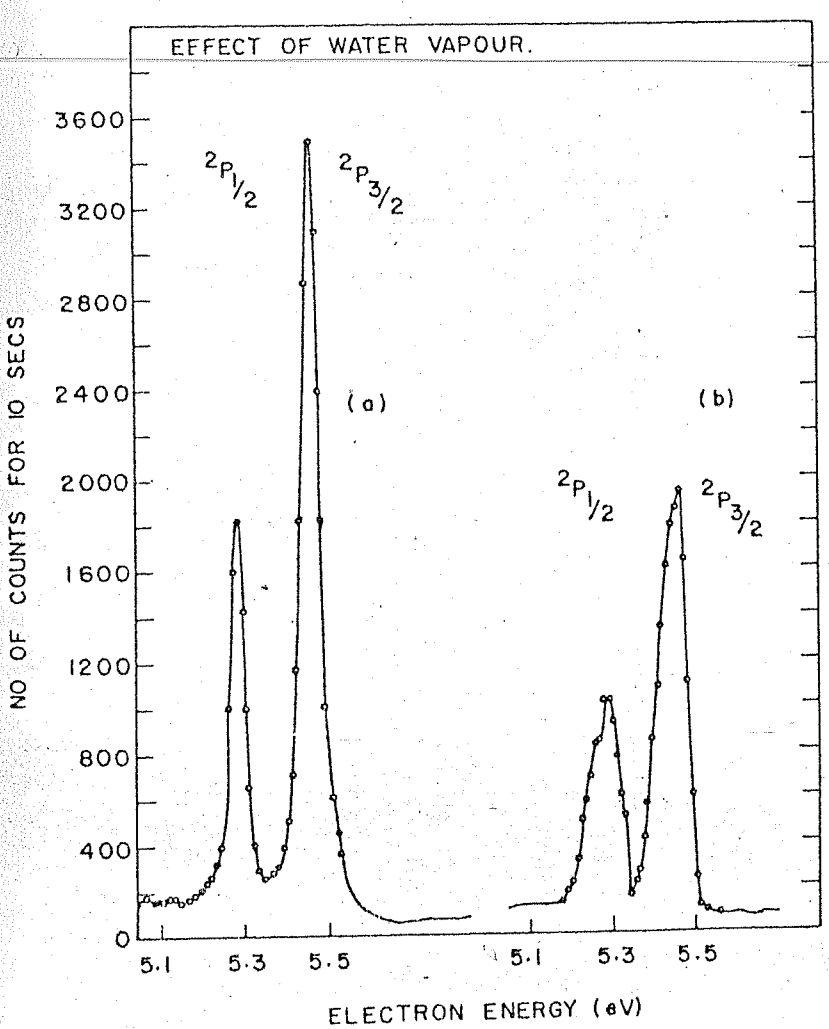


Fig II .5. Effect of moisture on the spectrometer performance.

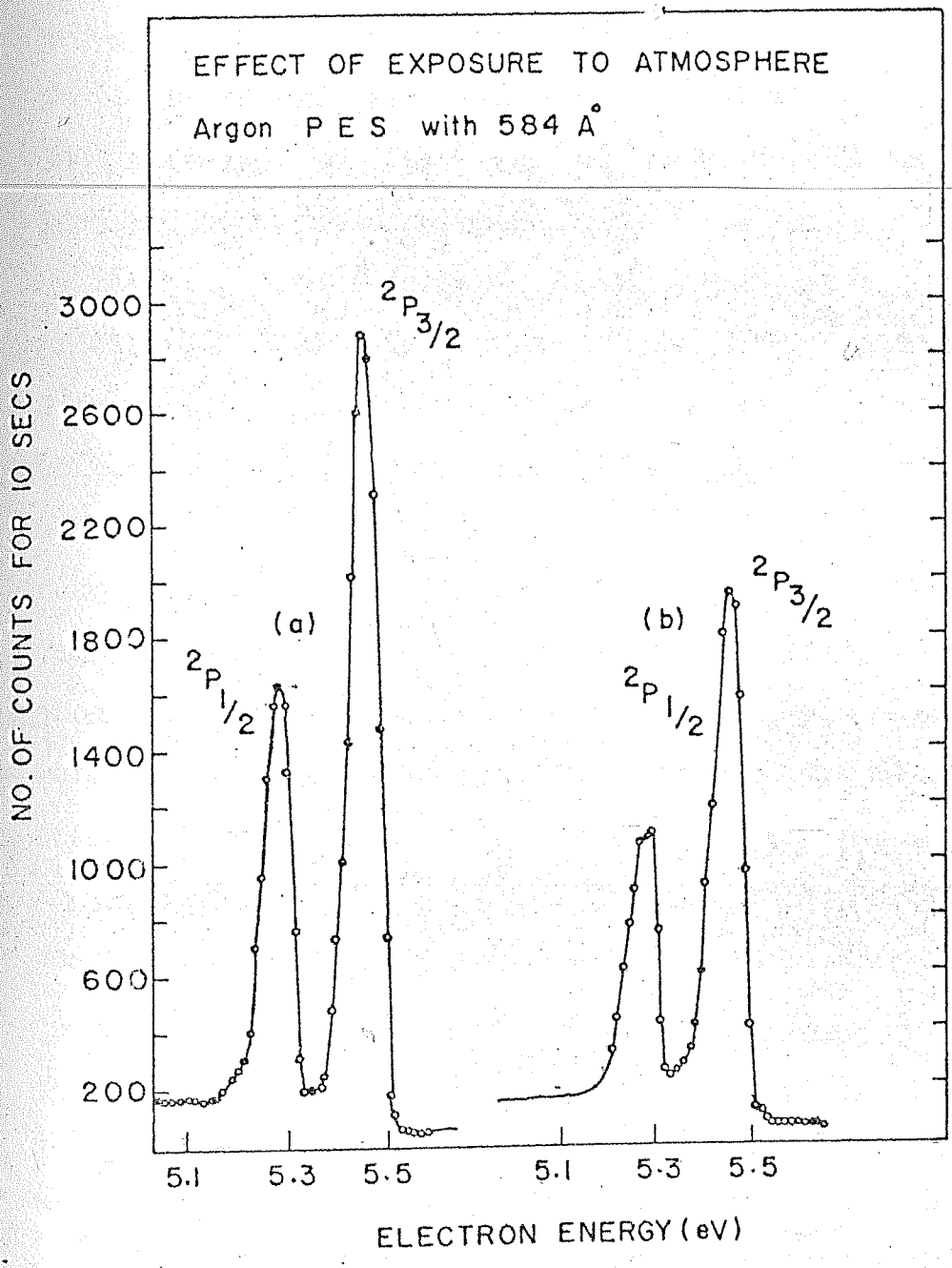


FIG. II . 6 Effect of exposure to atmosphere on the spectrometer performance

To reduce the effect of contact potential, the following procedures were adopted right from the beginning. As a first step, all the spectrometer parts were made from stainless steel 304. Moreover each part was machined and made in single pieces. Each piece was then degreased with trichloroethylene, followed by cleaning with detergent and distilled water. Other methods of cleaning using acid or alkali did not yield better results. After setting up the spectrometer the whole system was evacuated continuously for days together along with baking at about 100°C. using heater coils wrapped around the vacuum chamber. It was found that this baking time could be reduced drastically by using a plasma cleaning. The plasma was produced in argon at about 0.5 torr with the help of an RF supply. The accelerating/retarding electrode was used to introduce the RF power into the system. The effect of a typical plasma cleaning is shown in the Fig II.7. Even though the effect of this cleaning method was tremendous, this alone never gave satisfactory results. Always it had to be followed by further evacuation and baking. The main drawback was in the change in energy calibration after each discharge. After the plasma cleaning, it was necessary to wait for two or three days so that the analyzer constant k attained a steady value. Too much of discharge or discharge at very low pressures were found to degrade the performance on certain occasions. On most of the occasions it was found

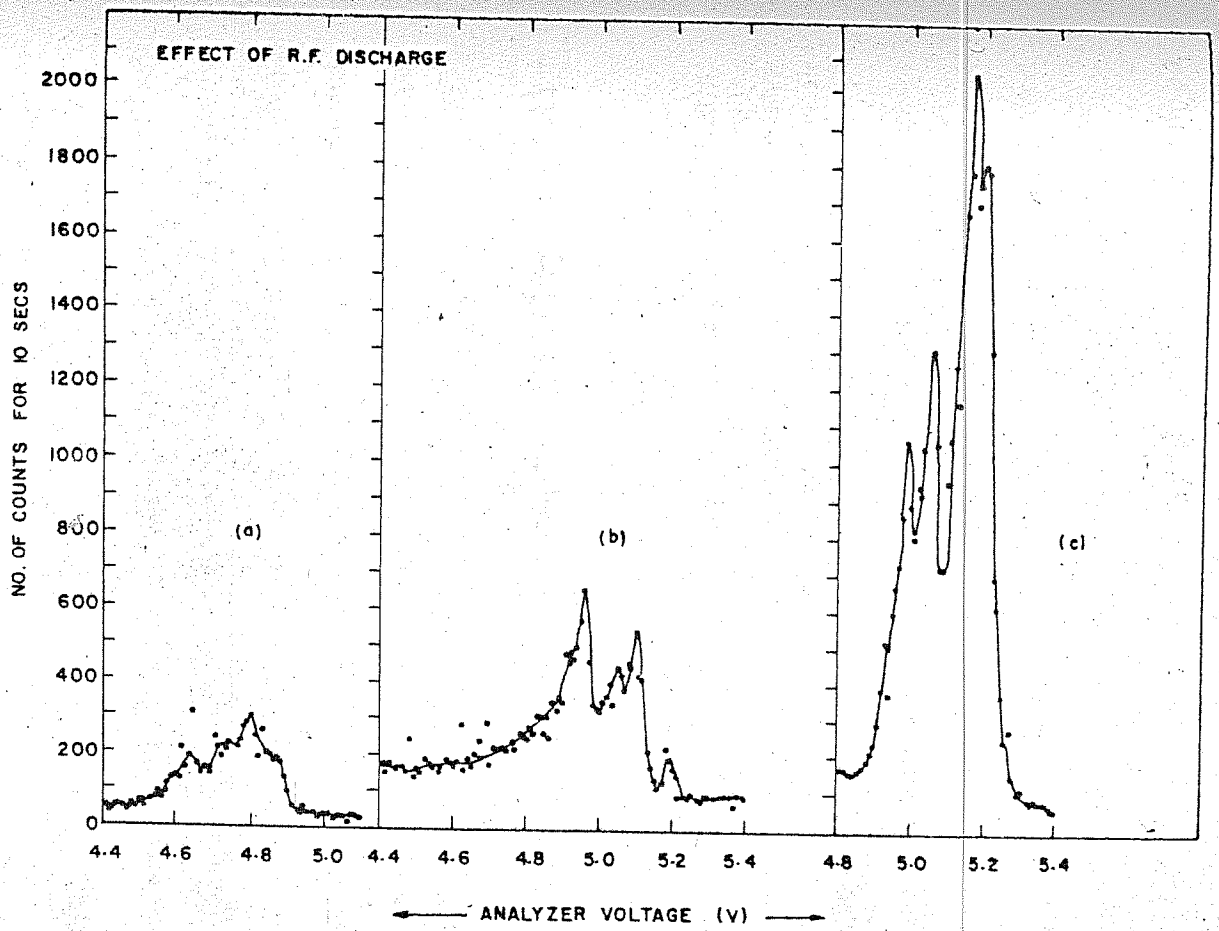


Fig. 1.7. EFFECT OF RF DISCHARGE ON THE SPECTROMETER PERFORMANCE.

(a) Before discharge. (b) After 5 minutes of discharge
(c) After 30 minutes of discharge

necessary to have an optimum use of the RF discharge for reducing the baking time.

It was also found that the R.F discharge affected the performance of the channeltron. Everytime after the discharge the number of dark current pulses were found to increase. It took a number of hours for the channeltron to heal and give the original dark current count rate. This adverse effect of the discharge on the channeltron was found to reduce by applying a negative potential of about 100 V to the channeltron face during the time of the discharge.

II.9.3 Effect of Draw-out Voltage

It was found that whenever the spectrometer was operated at very high resolution, the draw-out voltage applied to the channeltron face affected the performance. It was found that for a given resolution it was always necessary to find a draw-out voltage by trial which gave the maximum signal to noise ratio and the least distortion of the peaks.

II.9.4 Effect of Electron Scattering

The number of photoelectrons produced is proportional to the gas pressure in the ionization region. Thus it is good to have a high pressure to obtain large intensity for the peaks in the photoelectron spectrum. But this could not be the case, firstly because the channeltron has to be operated at less than

5×10^{-4} torr pressure and secondly because of the scattering of the electrons by the parent molecules. It was found that the scattering of the photoelectrons by the parent molecules decreased the intensity of the electron peaks as well as the resolution of the instrument. So before obtaining the spectrum of any gas, it was necessary to find the maximum pressure at which there was very little effect due to scattering. The photoelectron spectra were taken at this pressure.

II.9.5 Collecting Efficiency Calibration

The collecting efficiency of the analyzer is a function of the electron energy and also depends on the mode of operation of the analyzer. An exact calibration of the collecting efficiency of the analyzer is required to measure relative intensities of the various peaks in the photoelectron spectra accurately. The ideal way of calibrating for the collecting efficiency is to measure the intensity of a particular peak in an atomic photoelectron spectrum for a continuous range of photon energies. This requires the use of a continuum source like synchrotron radiation or a BRV light source. Another method is the inverted pass curve method described by Poole et al (1973) and modified by Gardner and Samson (1975b). In another paper (Gardner and Samson, 1976b), the relative vibrational intensities of strong vibrational peaks in the He(I) photoelectron spectra of N_2, CO, CO_2 and O_2 were

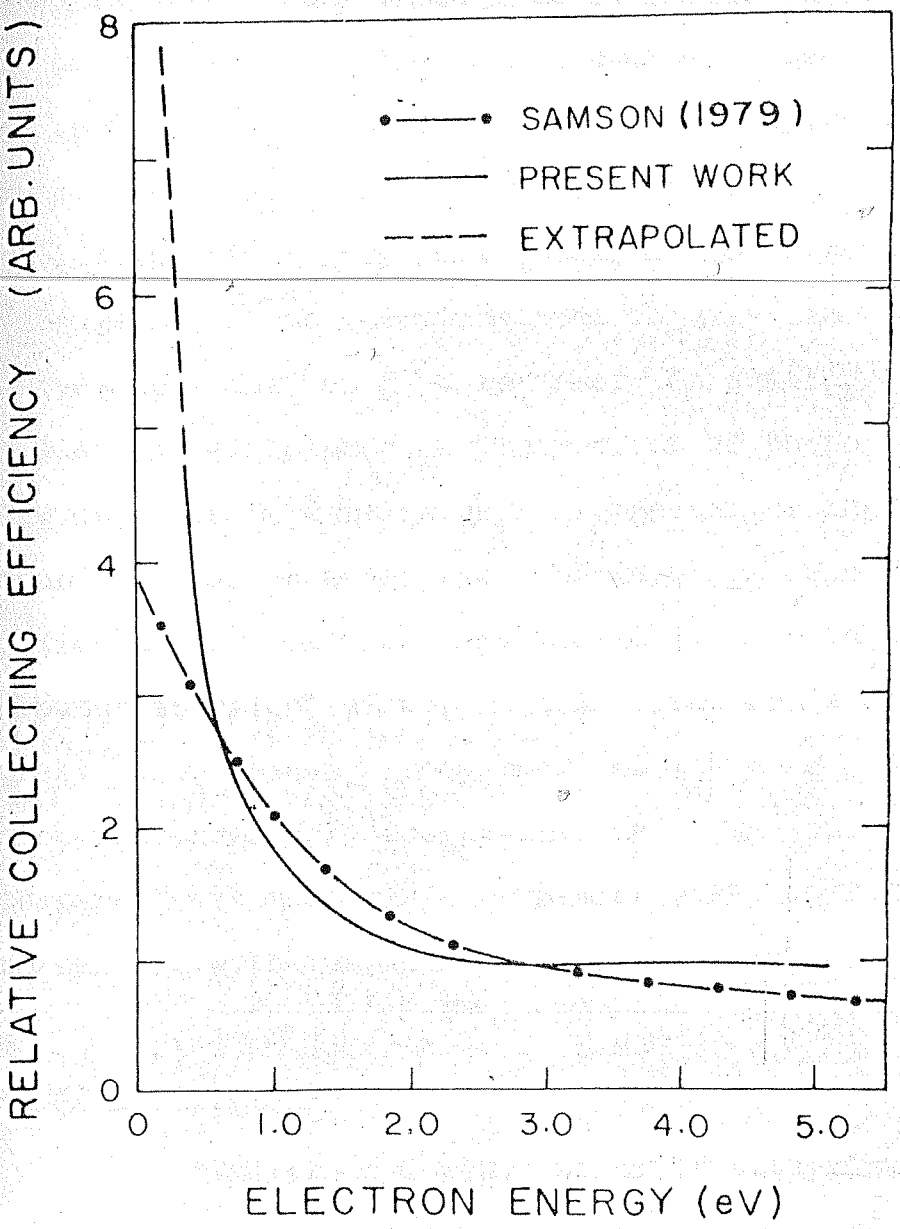


FIG. II 8 Collecting efficiency of the electron energy analyzer.

measured with a CMA whose relative luminosity was calibrated to an accuracy of ± 5%. These data were used to calibrate the collecting efficiency of the present analyzer by comparing the vibrational intensities observed for the various peaks. The collecting efficiency curve obtained for a particular analyzing voltage in the accelerating mode is given in the Fig II.8. The curve shows that at electron energies greater than 2.4 eV, the collecting efficiency is independent of photon energy, while at low energies, a varying gain in the collecting efficiency is found. It was observed that the gain (ratio of collecting efficiency at energies less than 2.4 eV to the constant value at greater energies) at a particular electron energy, was for all practical purposes, independent of the constant energy at which photoelectrons were energy-analyzed. The curve obtained is compared with that given by Samson (1979). This curve has been normalized with respect to the present one at 3 eV.

II.9.6 Energy Calibration

The energy calibration is determined by the analyzer constant k defined earlier by eqn. II.3. In the present analyzer, as discussed earlier k was selected to be 1.03. The value of k was experimentally determined by taking the photo-electron spectra of the monatomic gases Ar, Kr and Xe. The value of k was found to be in the range 1.01 to 1.05 on various

occasions. This value of k was measured when the performance of the spectrometer was reasonably good, and the small fluctuation could be due to changes in the contact potentials present at the analyzer slits. Usually before and after the collection of a spectrum the Ar spectrum was taken and from the $^2P_{1/2}$ and $^2P_{3/2}$ separation, the value of k was determined. Occasionally there was a small change in the value of k after a long experimental run.

II.9.7 Resolution

The resolution obtained for the spectrometer was a function of the operating conditions and the cleanliness of the spectrometer. Usually before and after every data collection, the argon spectrum was taken from which the resolution was determined. The spectrum of argon obtained with 736 Å radiation and analyzed at 1.5V in the accelerating mode is shown in Fig II.9. The FWHM was about 10 meV which corresponded to a resolution of 150. The symmetric nature of the peaks without any distortion and the intensity ratio of the $^2P_{1/2}$ and $^2P_{3/2}$ states was quite satisfactory. Also, the photoelectron spectrum of molecular hydrogen at 736 Å was studied in the accelerating mode and is shown in fig II.10. The figure shows only a small portion of the photoelectron spectrum corresponding to $v' = 6$ vibrational level of the ground electronic state of

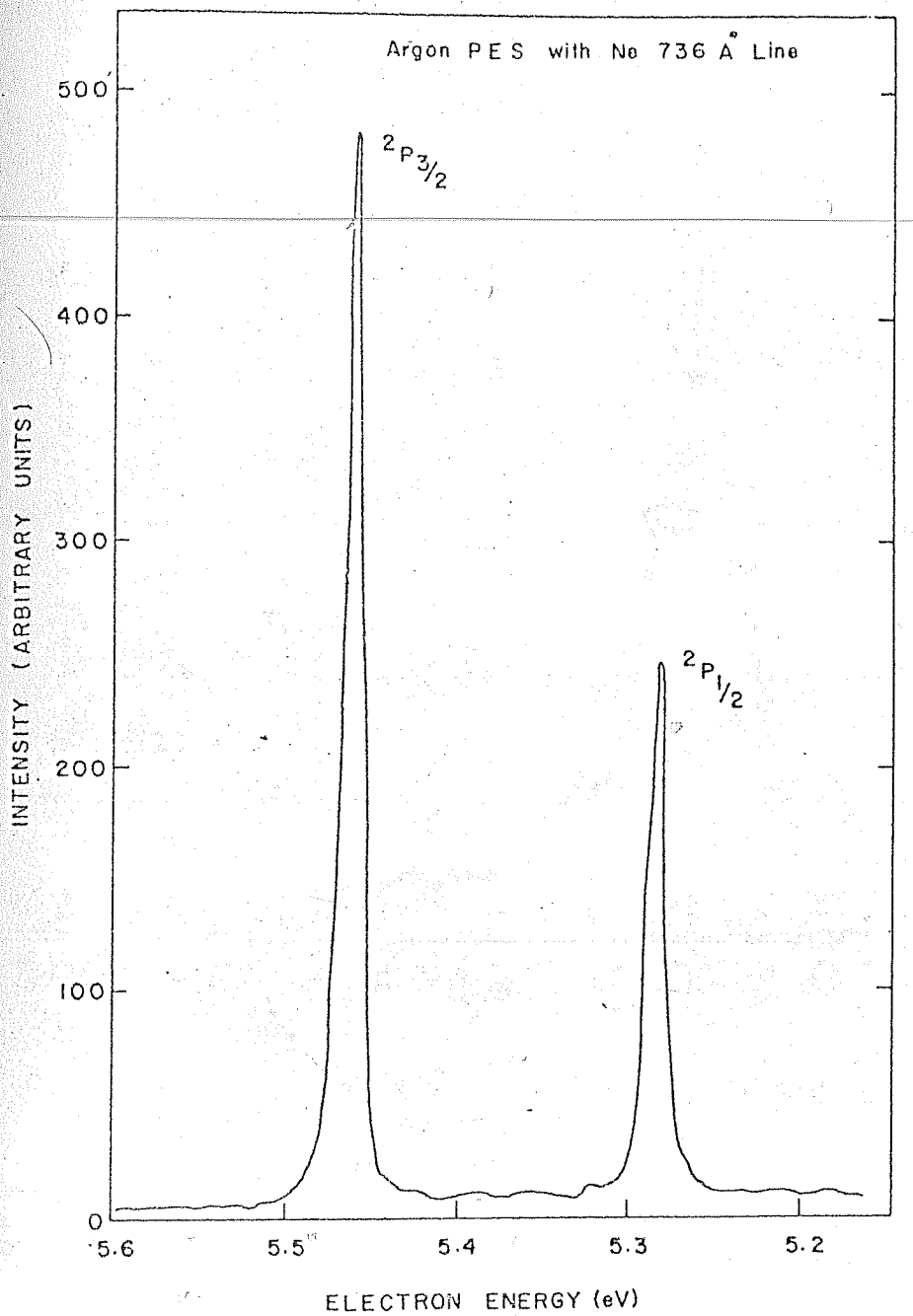


Fig. II. 9 ARGON PES WITH Ne 736 A° LINE

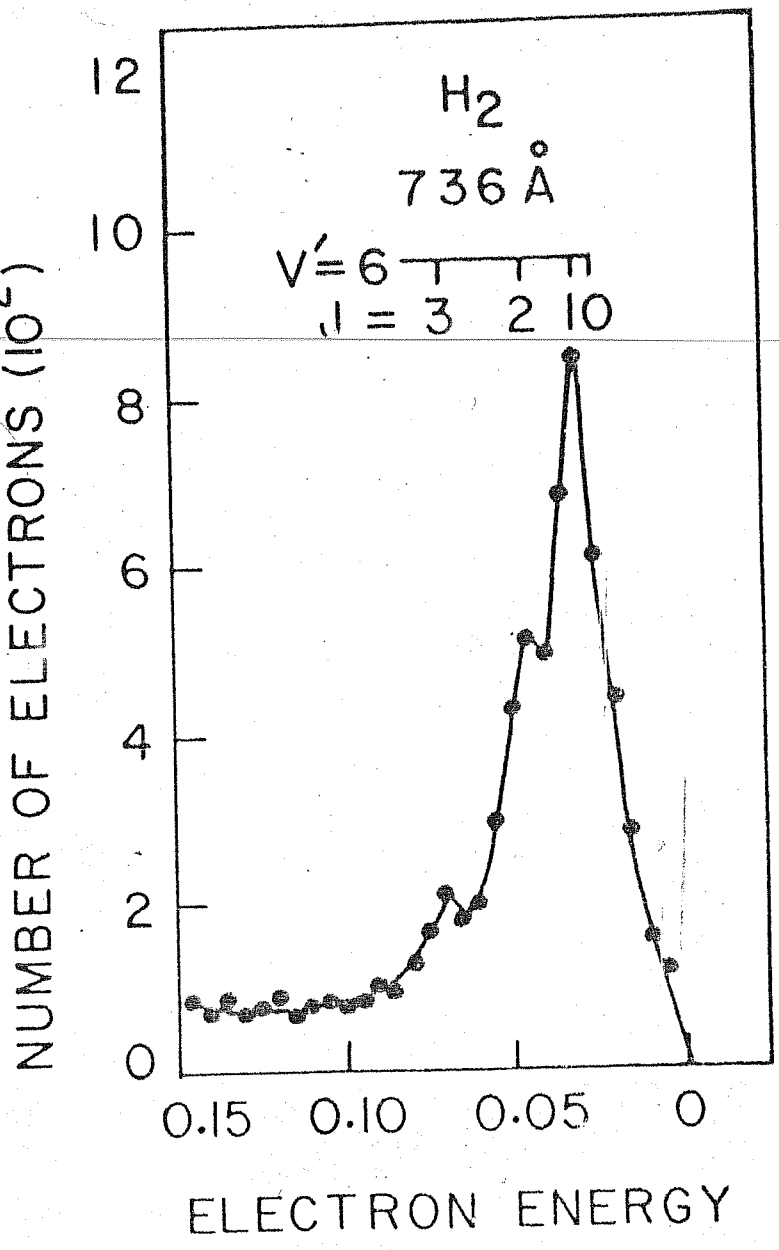


FIG II 10 Rotational levels in the H_2 PES

the molecular ion. The rotational states corresponding to $J = 1,2,3$ in $v' = 6$ vibrational state are clearly resolved with an energy resolutions of about 9 to 10 meV.

CHAPTER III

PHOTOELECTRON SPECTROSCOPY AND AUTOIONIZATION OF O_2, H_2 and CO_2

III.1 Introduction

The importance of photoelectron spectroscopy in the study of photoionization has been discussed in detail in the first chapter. The photoelectron spectra give the relative intensity distribution of vibrational peaks in the various electronic states of the molecular ion. Presence of autoionization causes strong perturbations in the vibrational intensities. Thus the study of the vibrational intensities in the photoelectron spectra at and away from the autoionizing wavelengths contributes to the knowledge of the autoionizing states. The vibrational states of the ion which are not observed otherwise in direct ionization could be observed in the photoelectron spectra at autoionizing wavelengths. This provides detailed information about the vibrational parameters

of the ionic state.

In this chapter results are presented regarding the effect of autoionization in the photoelectron spectra of O_2, H_2 and CO_2. Also presented are the values of the vibrational constants for the three normal modes of the ground state of CO_2^+.

III.2 Molecular Oxygen

The photoelectron spectra of molecular oxygen have been studied at a number of wavelengths between 300 Å and the threshold by various investigators. Natalis (1976) has listed about 40 experimental values of the photoelectron intensity $I(v')$, with $v' = 0$ to 6 for the O_2^+, $X^2\Pi_g$ photoelectron vibrational series. Most of these data are for the ionizing wavelengths of 584 Å and 736 Å. The vibrational intensity distributions produced during photoionization, for the $X\,^2\Pi_g$, $a\,^4\Pi_u$, $b\,^4\Sigma_g^-$, and $c\,^4\Sigma_u^-$ states of O_2^+ have been determined by Gardner and Samson (1978) for a number of wavelengths between 745 and 304 Å. The branching ratios and absolute values of the total and partial photoionization cross-sections for producing O_2^+ in its various electronic states in the wavelength range 100-800 Å have also been measured (Samson et al, 1977). The effects of autoionization on the vibrational intensity distribution of O_2^+ has been observed at various wavelengths, and particularly at 736 Å (Collin et al, 1972; Bahr et al, 1971b; Gardner and Samson, 1978).

Numerous experimental data at 736 Å exist for the vibrational intensities of the photoelectron bands corresponding to the $X^2\Pi_g$ and $a^4\Pi_u$ states of O_2^+ (Collins et al., 1972; Branton et al., 1970; Carlson, 1971; Price et al, 1972; Kirsinger and Taylor, 1973; Samson and Gardner, 1975, 1977a). Large descrepancies in the results have been discovered, which could be attributed to instrumental effects and/or to differing operating conditions in different experiments. Except for Samson and Gardner (1975, 1977a) rest of the investigations have used retarding-potential-type as well as deflecting type electron energy analyzers, with photoelectrons analyzed at various angles from 20 to 127°. In some of these experiments, neon emission lines (which occur at both 736 and 744 Å) were used as the photon source without any monochromator, with the result that the data reported for 736 Å may have some additional contribution due to the 744 Å line. Also, the data reported from these experiments were uncorrected for angular distribution or analyzer transmission. Samson and Gardner (1975, 1977a) used an electrostatic cylindrical mirror analyzer (CMA) for the energy analysis of photoelectrons produced by the interaction of monochromatic photons with molecular oxygen, collecting the photoelectrons at an angle of 54°,44'. It has been discussed in Section II.2.1, that for such an experimental arrangement, the vibrational populations are independent of the asymmetry parameter and the degree of polarization of the incident photon beam. It appears

that the only reliable data available so far at 736 Å on the intensity distribution of the vibrational levels in the O_2^+ photoelectron spectrum are those of Samson and Gardner. It is thus clear that more experiments using the same collection angle with CMA are necessary to have a better understanding of the effect of autoionization on the vibrational intensity distribution. With this point in view the photoelectron spectra of O_2 were studied at the wavelengths 584, 736 and 744 Å.

The photoelectron spectra of molecular oxygen at 584, 736 and 744 Å were taken at an energy resolution of 45 meV. The spectra at 736 and 744 Å are shown in Fig III.1. The 744 Å spectrum shows the first six vibrational levels, from $v' = 0$ to $v' = 5$, of the $X^2\Pi_g$ state of the molecular ion. The vibrational intensity distribution shows maximum population at the $v' = 1$ level. The vibrational levels of the $X^2\Pi_g$ state corresponding to $v' = 15$ to $v' = 20$ can also be seen in this spectrum. These levels do not appear in the 584 Å spectrum (The spectrum at 584 Å has not been shown in fig III.1). The presence of these vibrational levels from $v' = 15$ to $v' = 20$ in the spectrum at 744 Å does not in any case indicate even weak autoionization The presence can be explained in terms of the high collecting efficiency of the analyzer in this electron energy region (1.5 eV to 0.7 eV) as shown in Fig II.8. Also seen in the spectrum are the vibrational levels $v' = 0$ to $v' = 4$ of the $a^4\Pi_u$ state.

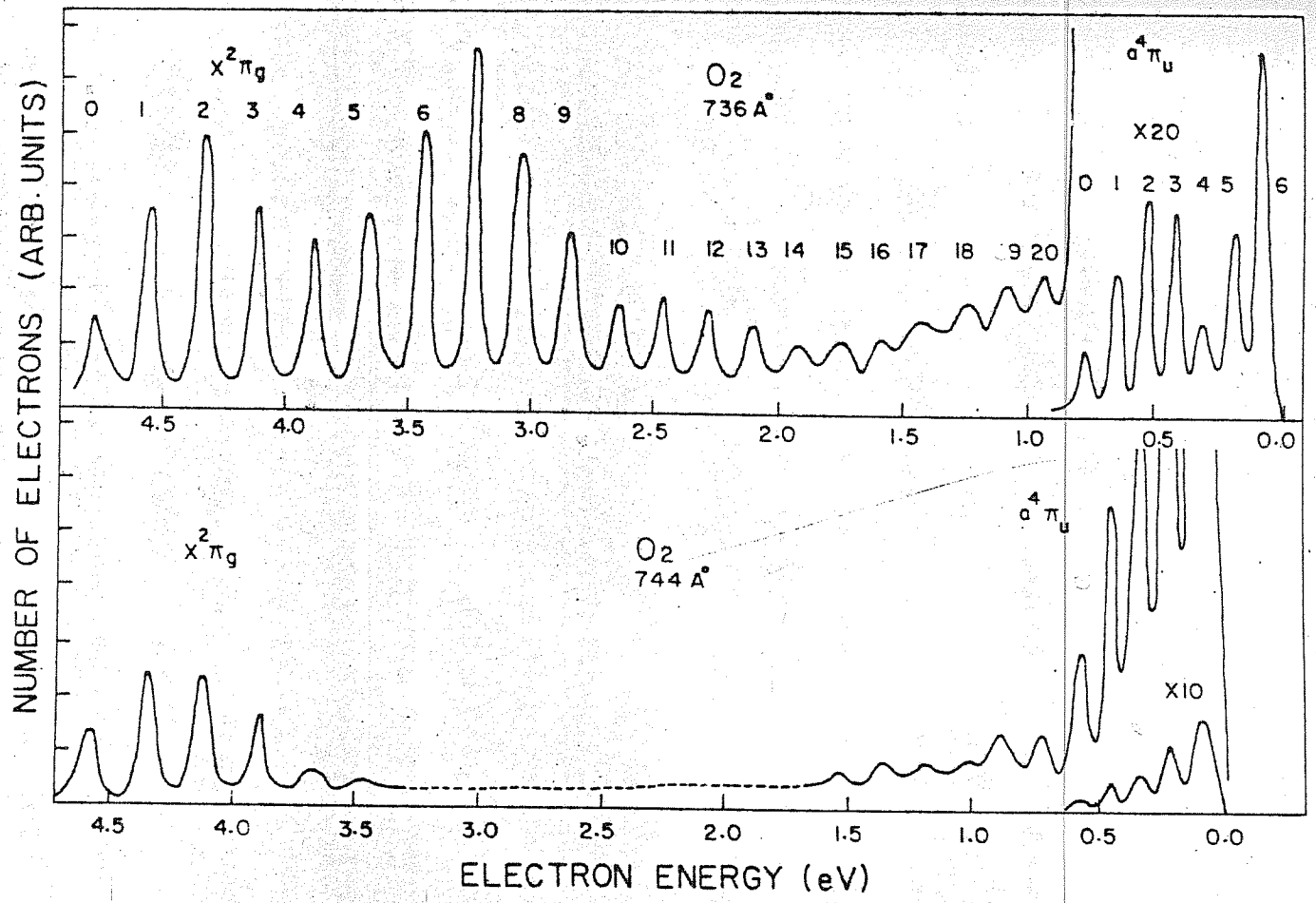


Fig III. 1: O_2 P.E.S AT 736 & 744 Å LINES

In the photoelectron spectrum at 736 Å, twenty one vibrational levels from v' = 0 to v' = 20 for the $X^2\Pi_g$ state can be seen with the intensity maxima at v' = 2, v' = 7, v' = 11 etc. The shift in the maximum from v' = 1 (744 Å spectrum) to v' = 2 (736 Å spectrum) can be noticed without any ambiguity. Also, the intensity of the maximum at v' = 7 is higher than the intensity at v' = 2. All seven (from v' = 0 to v' = 6) energetically possible vibrational levels at 736 Å for the $a^4\Pi_u$ state can also be seen with their intensities much higher than the highest intensity maximum for $X^2\Pi_g$ state.

The vibrational populations at the two incident wavelengths, as shown in Fig III.1 have not been corrected for collecting efficiency at different electron energies. After making the corrections, the vibrational intensities for the $X^2\Pi_g$ state have been tabulated alongwith values reported by Samson and Gardner (1977 a) Table III.1. In both cases, the data has been normalized keeping the vibrational intensity for v' = 1 as 100. In the present work, the intensity maxima are observed at v' = 2, 7,11 and 19 while Gardner and Samson have reported maxima at v' = 1, 6/7 and 19 respectively. Also the vibrational populations as reported in the two cases are not the same. Differences in the two sets of values may be because of slightly different operating conditions. Such a difference is qualitatively explained later in this section.

TABLE III.1

RELATIVE VIBRATIONAL INTENSITY DISTRIBUTIONS[a] FOR THE $X^2\Pi_g$ STATE (O_2^+) AT 736 Å

Vibrational level	Relative intensity	
	Present work	Samson and Gardner (1977 a)
0	45	52
1	100	100
2	137	89
3	101	56
4	85	57
5	98	65
6	141	82
7	182	82
8	129	64
9	90	45
10	54	32
11	59	24
12	48	15
13	40	10.5
14	29	5.8
15	29	2.3
16	28	3.2
17	31	6.7
18	33	6.8
19	34	7.9
20	33	4.8

[a] Normalized to a value of 100 for the v' = 1 level in both cases.

TABLE III.2

RELATIVE VIBRATIONAL INTENSITY DISTRIBUTIONS[a] FOR THE $a^4\Pi_u$ STATE (0_2^+) AT 736 AND 744 Å

Vibrational level	Relative intensity	
	736 Å	744 Å
0	1.0	1.0
1	1.9	1.3
2	2.4	1.3
3	1.5	1.6
4	0.5	1.6
5	0.8	
6	1.2	

[a] Normalized to a value of unity for the v' = 0 level in both cases.

The corrected vibrational intensities for the $a^4\Pi_u$ state as measured at both 736 and 744 Å are presented in Table III.2. The intensities are normalized to a value of unity for the $v' = 0$ level. The 736 Å spectrum shows intensity maxima at $v' = 2$ and 6; but the data at 744 Å shows that the intensity may still not have reached its maximum value in the spectrum where only first five vibrational levels are energetically possible. A comparison between the 584 (not shown in the figure) and 744 Å spectra leads to the fairly safe conclusion that in the 744 Å spectrum there is no effect of autoionization and that the spectrum is contributed by direct ionization only. This is in accordance with the conclusions of Price et al (1972) and Morgenstern et al (1971). The intensity ratio of the $v' = 2$ vibrational level of the $a^4\Pi_u$ state to the $v' = 1$ level of the $X^2\Pi_g$ state gives a value of 5.95. A value of 5.8 has been reported for this ratio by Natalis et al (1977).

The direct ionization spectrum at 744 Å is subtracted after proper normalization from the direct ionization plus autoionization spectrum at 736 Å to give the net effect of autoionization alone. The normalization is done in such a way that the resultant effect of autoionization for $v' = 0$ vibrational level for the $X^2\Pi_g$ state of the ion leads to zero vibrational intensity. This assumption seems to be valid because the vibrational intensity ratio of $v' = 0$ level as measured at 736 Å and 744 Å is essentially the same as the

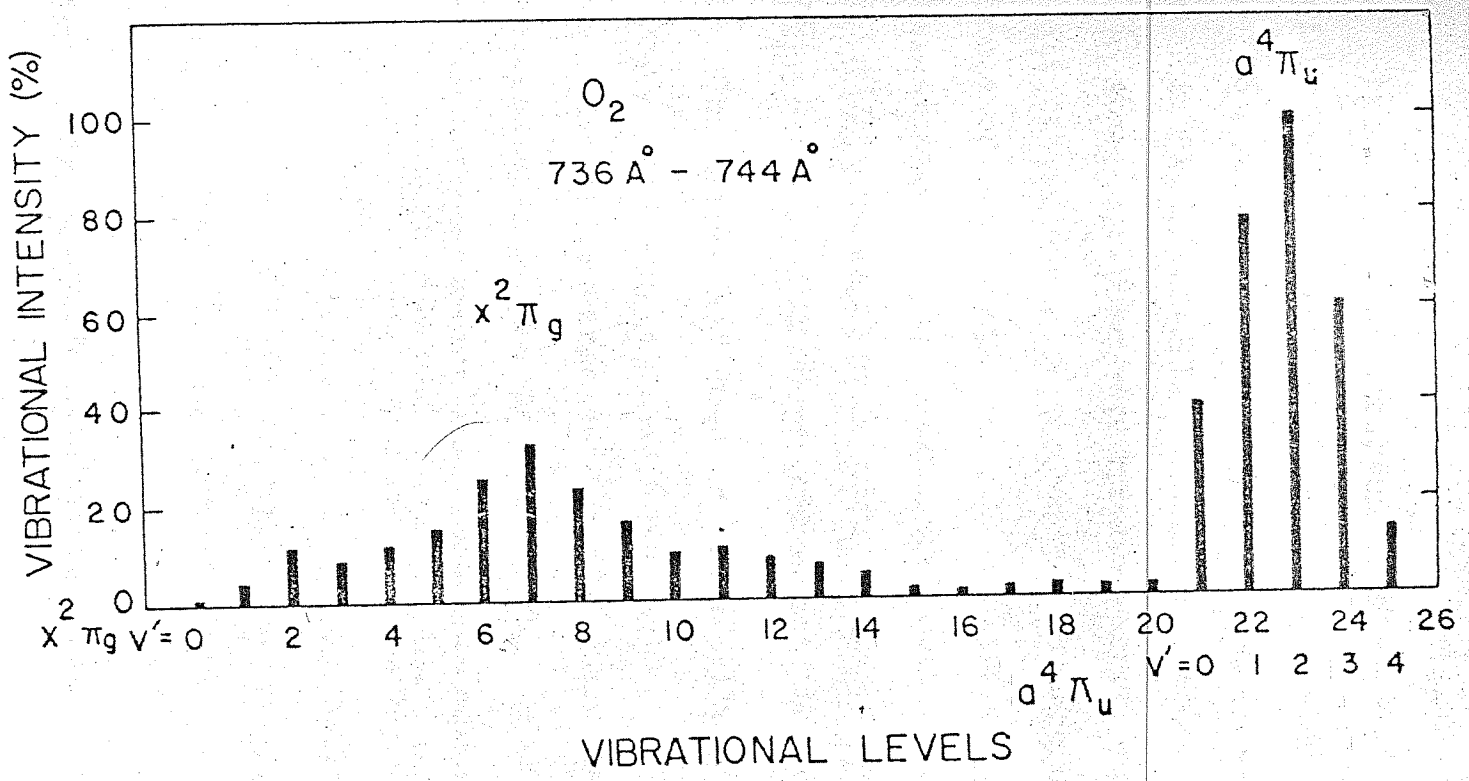


Fig. Ⅲ. 2 Autoionization contribution in O_2 PES at 736 Å

photon intensity ratio at the two emission lines, even though the total absorption cross-section at 736 Å is 50% higher than that at 744 Å (Samson et al., 1977; Gardner and Samson, 1978). The 736 Å minus the 744 Å spectrum after such normalization is shown in Fig III.2. The vibrational intensity for v' = 2 of the $a^4\Pi_u$ state has been kept hundred and the relative intensities of all other levels in the two electronic states have been calculated accordingly. Fig III.2 clearly shows the effect of autoionization on the vibrational population of both the $X^2\Pi_g$ and $a^4\Pi_u$ states. It is also seen that the effect on the $a^4\Pi_u$ state is much more pronounced than on the $X^2\Pi_g$ state.

The nature and shape of this strong autoionizing state at 736 Å which contributes to both the states $X^2\Pi_g$ and a $a^4\Pi_u$ have not been obtained so far. The important points which have come up from the present as well as other experiments are (1) The autoionization contributes to almost all the vibrational levels in $X^2\Pi_g$, with a number of maxima at v' = 2, 7, 11, and 18. The contribution to the $a^4\Pi_u$ state is much more, with the maximum at v' = 2. (2) The relative photoionization efficiency from 727 to 742 Å as measured at wavelength resolution of 0.07 Å by Dehmer and Chupka (1975) as shown in Fig III.3, does not show any discrete autoionizing state at the exciting wavelength of 735.895 Å. The well-established Rydberg state with n = 5 and converging to the v' = 0 level of the $b^4\Sigma_g^-$ state of the molecular ion at about 732 Å seems to be too

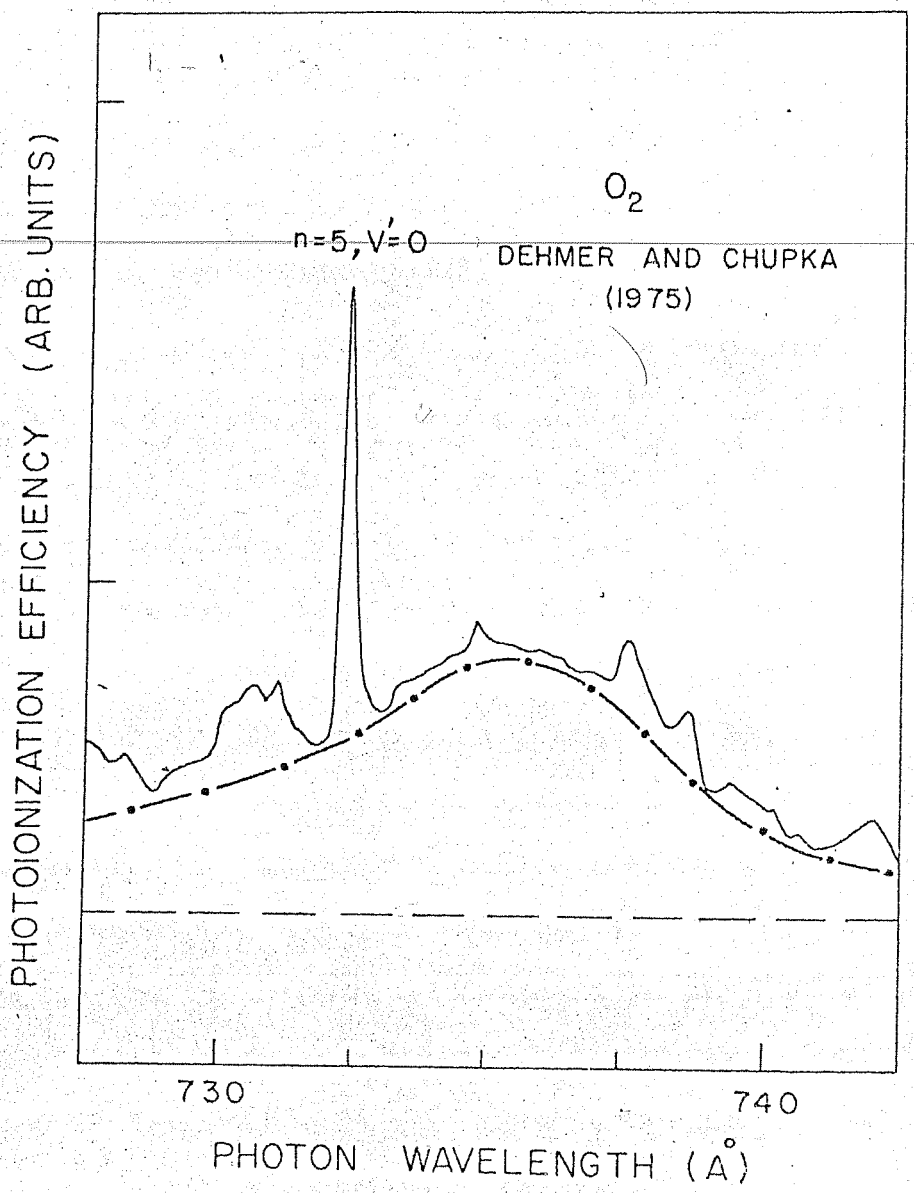


Fig. III.3 Photoionization efficiency curve of O_2
(Dehmer and Chupka, 1975)

far away to contribute to the autoionization effect observed here. But the important point to be noted is that the Rydberg state at 732 Å along with other weak features is superimposed on a broad peak with maximum at about 736 Å. This peak is indicated by the dashed-dotted line in Fig III.3. The dashed line shows the background level.

A qualitative explanation of the vibrational intensity distribution for the $X^2\Pi_g$ state of O_2^+ in the 736 Å photoelectron spectra has been given by Smith (1970). He has assumed that the autoionizing state is a Rydberg state leading to O_2^+, $A^2\Pi_u$. Accordingly, he has obtained various maxima in the vibrational intensity distribution by adjusting the line profile index and the vibrational level of the autoionizing state. Two of the assumptions made in his calculation do not seem to be right. The first one is regarding the nature of the autoionizing state, which he attributes to a Rydberg state leading to the O_2^+, $A^2\Pi_u$. In the high resolution photoionization efficiency curve obtained by Dehmer and Chupka (1975), no sharp feature has been observed corresponding to this state. Again, to explain the observed vibrational intensities, Smith has taken a large value of the line profile index. This may not be possible since the only feature present around 736 Å is a broad hump for which the line profile index cannot be large. Another drawback in this calculation is that the autoionizing

contribution to the $a^4\Pi_u$ state has not been considered simultaneously. If the autoionization to the $X^2\Pi_g$ and $a^4\Pi_u$ states are from a single state, which in all likelyhood is correct, then the nature of the autoionizing state should satisfy the distribution of the vibrational intensities in both the $X^2\Pi_g$ and $a^4\Pi_u$ states.

The Franck-Condon factors connecting the autoionizing state and the ionic state have been calculated by Blake et al (1970), and Bahr et al (1971 b) to explain the vibrational intensity distribution at the autoionizing wavelengths corresponding to the M and I vibrational progressions of O_2. Various vibrational intensity distributions were obtained by adjusting the change in internuclear distance Δr_e during autoionization and also the vibrational level v of the autoionizing state. It was shown by Bahr et al (1971 a) that if the autoionization takes place from a vibrational state v, the vibrational intensities in the resulting ionic state would be modulated to have $v + 1$ maxima.

This formulation could be used to obtain the nature of the autoionizing state from the observed vibrational intensity distribution. But there is a drawback in this method. The $(v + 1)$ maxima rule cannot be applied quite often because most of the vibrational levels in the ionic state may not be energetically possible. This is clearly seen from the intensity

distribution in the $X^2\Pi_g$ and $a^4\Pi_u$ states. In the $X^2\Pi_g$ state the first 21 vibrational levels are seen in which there are four maxima at $v' = 2, 7, 11$ and 18. But in the $a^4\Pi_u$ state only two maxima can be seen since the vibrational levels with $v' > 6$ are energetically forbidden. Even for the $X^2\Pi_g$ state it may not be possible to observe all the $v + 1$ maxima, since the vibrational levels can extend upto $v' = 60$ (Samson and Gardner, 1977 a).

Price et al (1972) have tried to explain the autoionization at 736 Å due to the presence of the Rydberg state at 732 Å. (Yoshino and Tanaka, 1968; Dehmer and Chupka, 1975) with $n = 5$ and converging to the $^4\Sigma_g^-$ state of the ion. According to them the excited neutral state is a $^3\Sigma_u^-$ state with a $^4\Sigma_g^-$ core and a $p\sigma_u$ electron which autoionizes into the $X^2\Pi_g$ and $a^4\Pi_u$ states of O_2^+ with the emission of $2p\pi_g$ and $2p\pi_u$ electrons respectively. This explanation does not hold good on the sole criterion that the Rydberg state discussed is at 732 Å and is too far away to have any effect at 736 Å. As a matter of fact, using the electric dipole selection rule, the autoionizing state can be a $^3\Sigma_u^-$ or a $^3\Pi_u$ state since the initial ground state of O_2 is $^3\Sigma_g^-$. Each of these two states can give rise to a number of Rydberg series depending on the initial and final orbitals of the excited electron. Thus the autoionizing state at 736 Å could be due to a Rydberg state converging to any higher lying ionic state. The following discussion will show that this ionic state is most probably a repulsive state

resulting in dissociation.

The broad hump around 736 Å as shown in Fig III.3 giving rise to autoionization is possibly due to absorption of photons from the neutral ground state to the autoionizing state which is repulsive in nature. A repulsive state cannot have discrete vibrational levels. But it can be assumed that it has a continuous set of pseudo vibrational levels. Hence when the upper state is repulsive with such a continuous set of pseudo vibrational levels, the absorbed photons can have continuous energies. This continuous absorption is limited to a small range of energies obeying the Franck-Condon principle. After absorption of the photon the molecule tend to break apart. But, before it could do so the excited molecule undergoes autoionization ejecting an electron and forming an ion. This is possible if the autoionizing time is small compared to the nuclear motion. The molecule after autoionization is no more repulsive and forms a stable ion. The emitted electron could be a $2p\pi_g$ or $2p\pi_u$ to form the $X^2\Pi_g$ or $a^4\Pi_u$ state of the ion respectively.

It is quite logical to expect similar features in the photoionization efficiency curves corresponding to absorption to repulsive excited neutral states which undergo autoionization giving stable ions. In fact, the photoionization efficiency curves for O_2 given by Dehmer and Chupka (1975) show several

such broad features, eventhough they are less prominent as compared to that at 736 Å.

The above nature of the autoionizing state also explains the descrepancy in the vibrational intensity distribution obtained by the author and by Samson and Gardner (1977a) using identical experimental arrangements. In both the experiments the effect of the angular distribution of the electrons as well as the collecting efficiency of the analyzer has been taken care of. The only factor which could give arise to the discrepancy is the energy of the ionizing radiation. If the photon energy is slightly different, the excited neutral will be formed in a different pseudo vibrational level and this, on autoionization could lead to different vibrational intensities in the ion. A small difference in the photon energy is quite possible if the resonant line from the light source is broadened due to self absorption. The width of the resonant line due to self absorption could be as much as 0.18 Å for a gas pressure of about 0.5 torr (Samson, 1969b). Thus a difference in the gas pressure in the ultraviolet source could give rise to the different vibrational intensity distribution as in this particular case.

III.3 Molecular Hydrogen

The photoelectron spectra of H_2 have been studied by a number of authors (Frost et al, 1967; Turner, 1968; Berkowitz and

Spohr, 1973; Asbrink, 1970; and Gardner and Samson, 1976 a). Work has been mainly done at 584 Å and 736 - 744 Å wavelengths. In the 584 Å spectrum the vibrational levels upto v' = 15 have been observed. The rotational structure in the photoelectron spectra has been obtained by Asbrink(1970) and Niehaus and Ruf (1971) using undispersed neon 736 - 744 Å lines and by Samson (1976) using monochromatic Ne 736 Å line. The effects of autoionization on the photoelectron spectra of H_2 has been reported by Doolittle and Schoen (1965) and Berkowitz and Chupka (1969) at a number of wavelengths between threshold and 760 Å. Samson (1976) reported the effect of autoionization on the 736 Å photoelectron spectrumof H_2. But the photoionization efficiency measurements for H_2 shows only very weak autoionization features below about 750 Å (Chupka and Berkowitz, 1969; Dehmer and Chupka, 1976), thus necessitating further study of the possible effect of autoionization at 736 Å.

The photoelectron spectra of molecular hydrogen at 736 Å was obtained with an energy resolution of about 12 meV. The spectrum is shown in the Fig III.4. It shows the seven energetically possible vibrational levels from v' = 0 to v' = 6 of the $X^2\Sigma_g^+$ state of the molecular ion. The rotational structure could be seen for v' = 5 and 6 vibrational levels. In this spectrum, the vibrational intensities have not been corrected for the analyzer transmission. The photoelectron spectrum at 584 Å was also taken (not shown in figure) and the vibrational populations at 736 Å and 584 Å levels v' = 0 to v' = 6 were

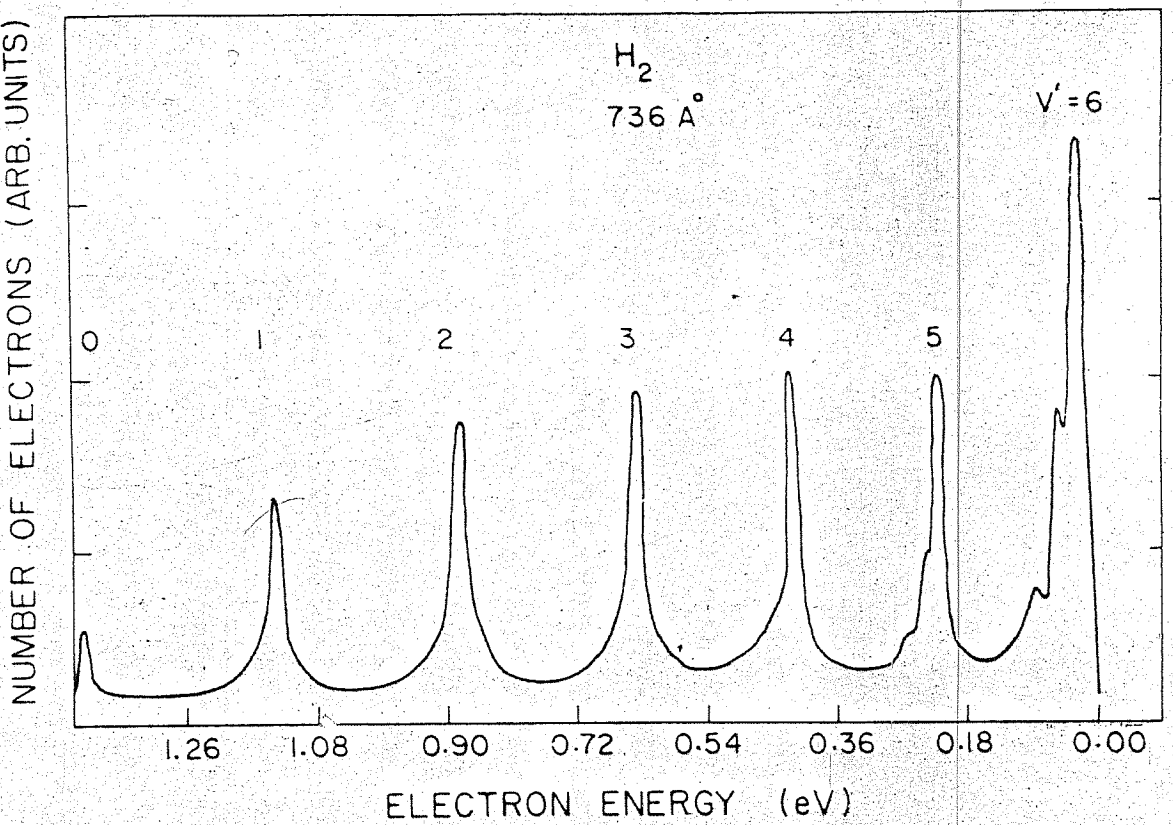


FIG. III 4 H_2 PES at 736 Å

compared after proper correction for the transmission of the analyzer. The result is shown in Fig III.5. The values measured in the present work are shown above (Fig III.5a) and those obtained by Samson (76) below (Fig III.5b). The intensity in the vibrational level having maximum population has been made cent percent and the relative populations of all other levels have been calculated accordingly. From Fig III.5a, it is evident that the vibrational intensity distributions at both 736 Å and 584 Å are the same for all practical purposes. Fig III.5b evidently shows the effect of autoionization. The high resolution photoionization efficiency measured by Dehmer and Chupka (1976) does not show any autoionizing feature in para - H_2 in the vicinity of 736 Å. For ordinary hydrogen, no data has been reported by them below 745.3 Å. However the absorption cross-sections measured by Lee et al (1976) do not show any autoionizing feature at the exciting wavelength. It is possible that the results obtained by Samson at 736 Å are not corrected for the transmission of the analyzer. Recently Berkowitz(1979) has reported that no effect due to autoionization in H_2 at 736 Å could be observed using experimental set up similar to that used by Samson. All these results seem to point out that even weak autoionizing features are not present at this wavelength. This is in accordance with the results presented by the author.

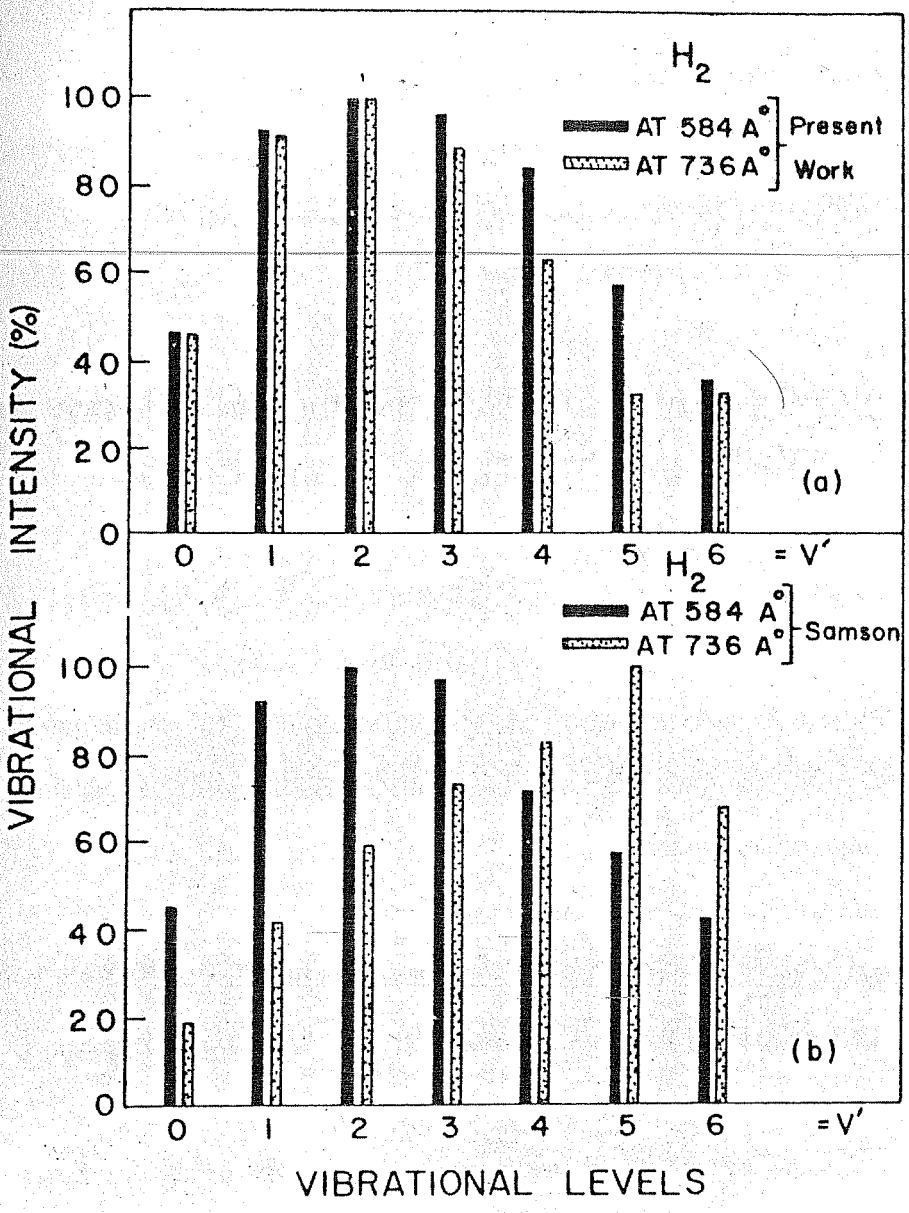


Fig. III. 5 Comparison of H_2 PES at 584 & 736 A°

III.4 Carbon Dioxide

The photoelectron spectra of CO_2 have been studied by Bahr et al (1969,72), Brundle and Turner (1969), Eland and Danby (1968), Collin and Natalis (1968), Samson and Gardner (1973a) etc. Some of the work except in the case of Bahr et al, was done at high energy resolution with a view to have a thorough analysis of the vibrations of the ionic states. The band corresponding to the ground state $X^2\Pi_g$ of the ion has been resolved to an extent that only the levels (0,0,0), (1,0,0), (2,0,0) and (0,0,2) have been observed so far. However the levels (2,0,0) and (0,0,2) have not been completely resolved. A few more vibrational levels have been observed in the threshold photoelectron spectra (TPES) of CO_2 by Batten et al (1976) and Frey et al (1977). A somewhat similar picture has evolved from the ionic fluorescence experiments of Lee and Judge (1972), Judge and Lee (1973) and Sroka and Zietz (1973) also. It appears that the data available so far regarding different vibrational levels of the ion is insufficient even though a good deal of work has been done using three different techniques was mentioned above. Even though Bahr et al studied the spectra at a number of wavelengths in the range 584 Å to 720 Å at a rather very poor resolution and Samson and Gardner in the wavelength range of 185 to 716 Å at high resolution, no work has been done to study the effect of autoionization on the photoelectron spectra of CO_2. Thus it was decided to study

the photoelectron spectra of CO_2 at different ionizing wavelengths.

The photoelectron spectra of CO_2 were studied at 584, 736, 744, and 876 Å incident wavelengths at an energy resolution of 40 meV. The spectra were taken in a single scan with electron pulses being stored for 300 seconds to give a single data point. The spectra had to be taken in a single scan since the constant voltage given to the outer cylinder was not really constant. It was found to decrease by about 50 mV from an initial value of 2V in about 12 hours. Proper corrections for energy scale were done to take care of this small change. Extreme care was taken to maintain the gas pressure in the ionization region constant during the experiment.

The photoelectron spectra at 584, 736, and 744 Å showed the vibrational levels (0,0,0), (1,0,0), (2,0,0) and (0,0,2) of the $X^2\Pi_g$ state of CO_2^+. In the 736 Å spectrum apart from these four levels many more vibrational levels were seen. Some of these additional levels were seen with very weak intensity in the 744 Å spectrum also. In the 876 Å spectrum, apart from the allowed levels (0,0,0), (1,0,0) and (2,0,0), the level (0,1,0) could also be observed. In the 736 Å spectrum, the effect of autoionization was seen not only by the presence of the additional vibrational levels, but also by the change in the intensity distribution of the levels (0,0,0), (1,0,0) and (2,0,0). The vibrational structure and the effect of

autoionization on the vibrational intensities of the $X^2\Pi_g$ state were analyzed in detail and are presented below.

The photoelectron spectra at 736 Å has been shown in Fig III.6 for electron energies from about 2.25 to 3.20 eV and in Fig III.7 for electron energies ranging from 1.35 to 2.6 eV. In Fig III.6 is also shown the photoelectron spectrum at 744 Å. The vibrational levels observed in both the spectra have been assigned the quantum numbers as shown in the two figures. For assigning the new levels, the vibrational constants ν_1 and ν_3 as measured from the first four prominent levels (ν_1 ,0,0) with ν_1 = 0,1,2 and (0,0,2) were made use of. Also, while assigning the vibrational quantum numbers, care has been taken not to violate the selection rules. According to the selection rules discussed by Sharp and Rosenstock (1964), the transitions from the ground vibrational state of a linear symmetric triatomic molecule like CO_2, to a similar ion are restricted to final states in the bending and antisymmetric stretching modes which have an even number of quanta. Thus the vibrational levels are limited to (ν_1 ,0,0) with ν_1 = 0,1,2, ..., (0,0, ν_3) with ν_3 = 0,2,4, ...; and (0, ν_2 , 0) with ν_2 = 0,2,4 .... There can also be combination levels like (ν_1, ν_2, ν_3) with ν_1 being an integer and ν_2 and ν_3 being even integers.

In the photoelectron spectra at 736, 744, and 584 Å no vibrational level could be clearly seen corresponding to the

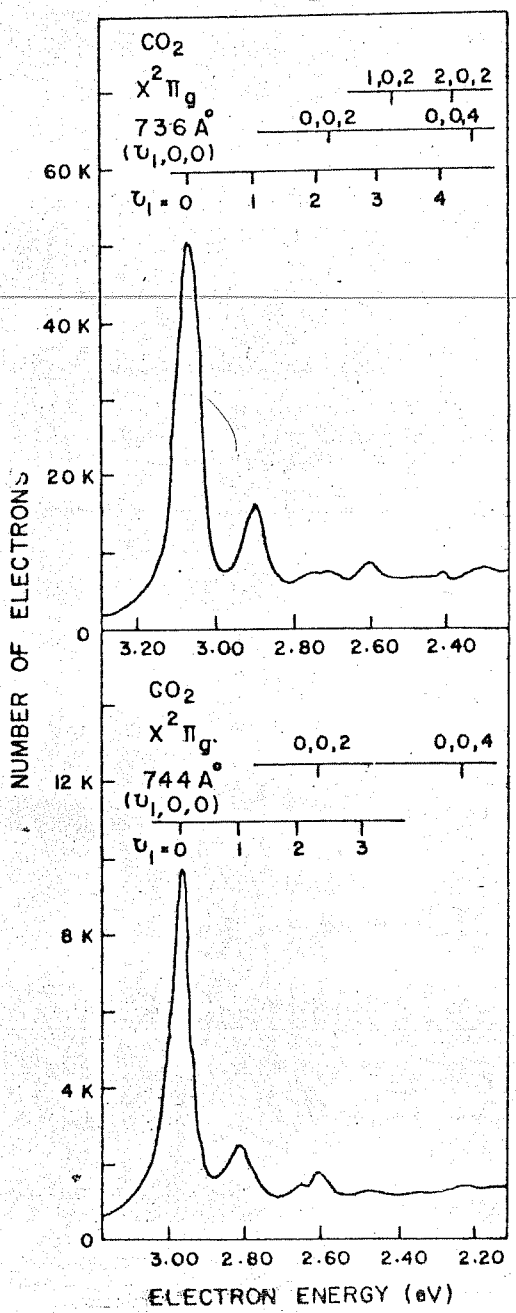


Fig. III 6 CO_2 PES at 736 & 744 A°

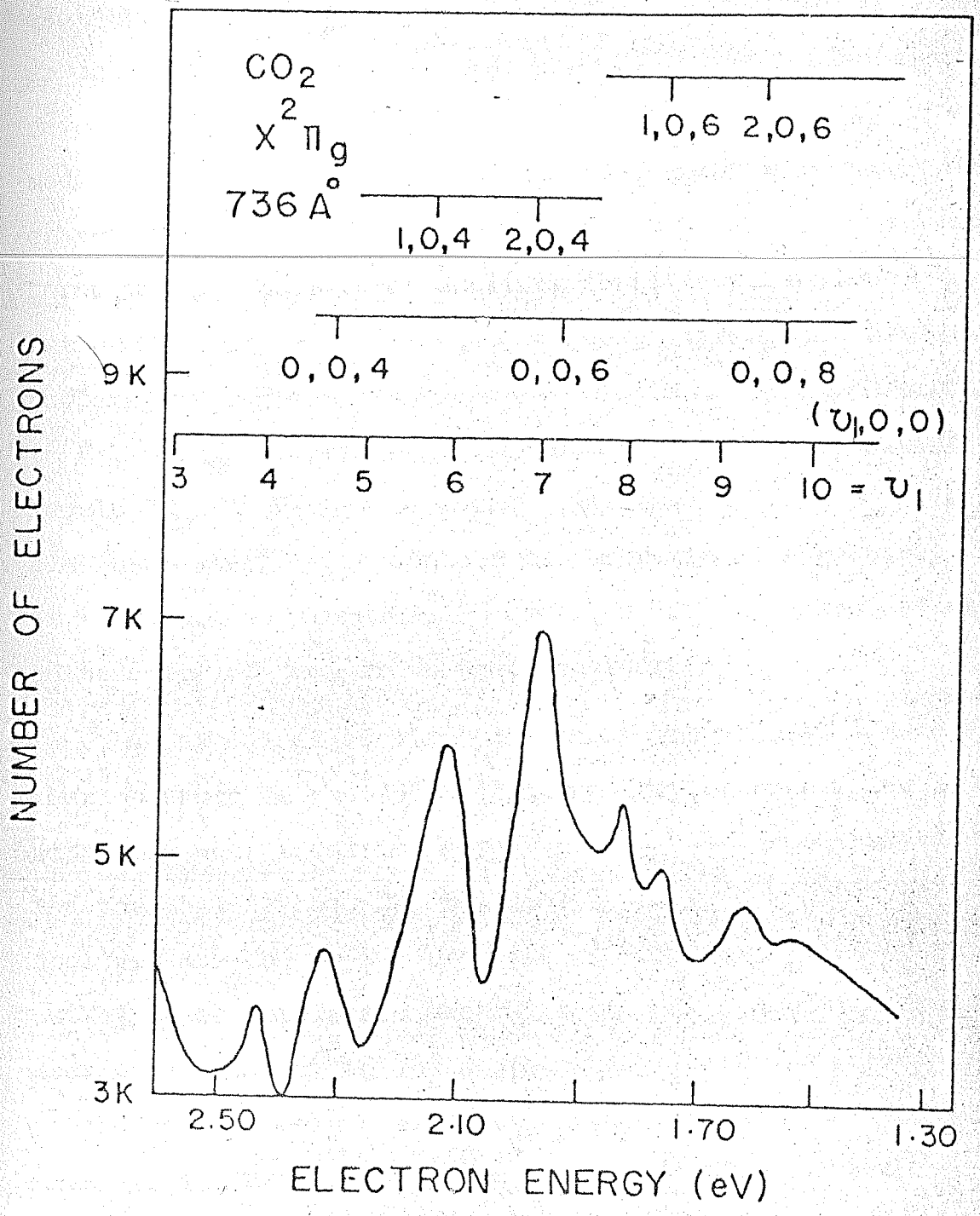


FIG. III. 7 Continuation of CO_2 PES at 736 Å

excitation of the ν_2 mode. Even the (0,2,0) level is absent as compared to the (2,0,0) and (0,0,2) levels. Also since the value of ν_2 is very small as compared to ν_1, and ν_3, the mode would have very large values of quantum numbers in the energy range, where most of the new levels are observed and hence the probability of exciting these levels would be extremely small. As a result, while assigning the quantum numbers, it has been assumed that only the modes corresponding to ν_1, and ν_3 are present in the spectra. The combination levels (ν_1, 0, ν_3) with nonzero values of ν_1, and ν_3 have also been assigned to explain the vibrational structure. Many of the assigned vibrational levels are clearly resolved, but quite a few of them are merged together.

As explained earlier, all these vibrational levels have been observed in the 736 Å spectrum only, though a few levels with very weak intensity appear in the 744 Å spectrum also. The possibility that the new levels observed in the 736 Å spectrum are due to the presence of some impurities is ruled out as these levels are absent in the 584 Å spectrum and very weak or absent in the 744 Å spectrum. In fact a comparison of the 736 Å spectrum with 744 Å spectrum shows two things. Firstly, the additional peaks are due to CO_2^+ only and secondly, these levels are present as a result of autoionization at 736 Å.

III.4.1 (ν_1,0,0) levels

The different vibrational levels corresponding to the symmetric stretching mode (ν_1,0,0) have been observed in the photoelectron spectra at 584, 736 and 744 Å. In the 584 Å spectrum only (0,0,0), (1,0,0) and (2,0,0) could be observed. This is in agreement with the observations of Brundle and Turner (1969), Eland and Danby (1968) and Collin and Natalis (1968). The vibrational intensities of the three levels in the present work at 584 Å also match with those given in these experiments. The levels (2,0,0) and (0,0,2) are practically locked together as observed in the spectra at both 584 Å and 736 Å, but in the 744 Å spectrum, the two levels are better resolved because of the increase in intensity of the (0,0,2) level compared to that at both 584 and 736 Å. In the 736 Å spectrum, the level (1,0,0) is much intense and sharp as compared to that in the 584 and 744 Å spectra. This could be due to the additional contribution due to autoionization. The assigned level (3,0,0) is displaced from the nearby peak by about 30 meV. The vibrational levels (4,0,0), (6,0,0), (7,0,0) and (8,0,0) are clearly seen in the spectrum in Fig III.7.

The value of vibrational frequency ω_1 of the symmetric stretching mode has been calculated from the data at 736 Å shown in the Fig III.6 and Fig III.7. In this calculation,

only those peaks which are clearly resolved have been considered and the average value of ν_1 was measured to be 1309 ± 40 cm^{-1}. A smaller value of 1210 ± 50 cm^{-1} has been reported for the vibrational spacing using photoelectron spectroscopy by Turner et al (1970). The confidence level of the present measurement is higher than that quoted by Turner et al., since the measurement has been made from a larger number of vibrational levels. The different values of ν_1 reported using different techniques are 1240 ± 10 cm^{-1} by Frey et al (1977) using TPES, 1250 cm^{-1} Tanaka et al (1960) and, 1280 cm^{-1} by Johns (1961,64) using optical methods and 1280 cm^{-1} by Gauyacq (1975) by ionic fluorescence respectively. The present measurement of ν_1 agrees well with these within the stipulated experimental errors.

III.4.2 (0,0, ν_3) and (ν_1, 0, ν_3) levels

The vibrational levels (0,0,2), (0,0,4), (0,0,6), and (0,0,8) are shown in the 736 Å spectrum (Fig III.6,7). Also shown are the combination levels (1,0,2), (2,0,2), (1,0,4), (2,0,4), (1,0,6) and (2,0,6). The asymmetry of the peaks and also the complexity of the spectra could be due to these as well as other combination levels. From the different levels of the (0,0, ν_3) series, the vibrational frequency ν_3 has been found to be 1476 ± 40 cm^{-1}. A value of 1420 ± 50 cm^{-1} has been reported by Turner et al (1970) in their photoelectron

spectroscopy experiment and of 1469 cm^{-1} by Johns (1964) in his optical spectroscopy experiment. The value obtained in the present work seems to be in good agreement with the results obtained by optical technique.

III.4.3 (0,1,0) level

According to the selection rules discussed previously, it is not possible to have direct ionization to (0,1,0) level in a perfectly symmetric triatomic molecule. Thus, the population of (0,1,0) level is forbidden by direct ionization, assuming the ion is linear. Koryashkin (1966) has reported that the O-C-O angle in the $^2\Pi_{3/2}$ CO_2^+ ion is 168 $\pm$ 3°. Thus there is some nonlinearity in the ion. This nonlinearity could vitiate the selection rules. Nor would the selection rules apply if the population of the ion is by way of autoionization from a neutral bent state.

The photoelectron spectrum at 876 Å (Fig III.8) clearly shows the partially resolved vibrational level (0,1,0) in addition to the levels (0,0,0), (1,0,0) and (2,0,0). Since the (0,1,0) level has not been observed in the ground state of CO_2^+ at other ionizing wavelengths (as is obvious from the photoelectron spectra at 584, 736, and 744 Å), it is a safe conclusion that the presence of (0,1,0) level is not due to the small nonlinearity of CO_2^+ ground state as observed by Koryashkin(1966).

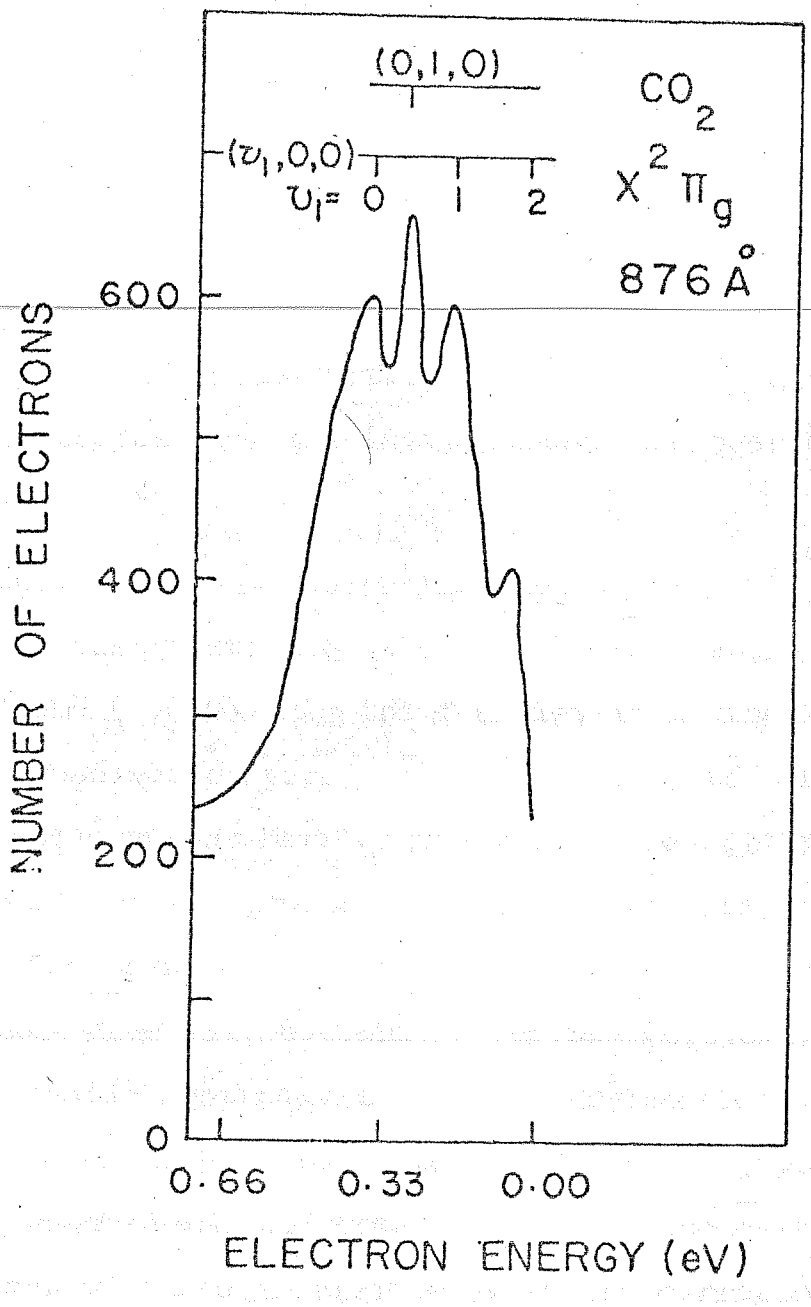


FIG. III. 8. CO_2 PES at 876 Å

Thus the only possible explanation for the presence of the (0,1,0) level is the autoionization at 876 Å through a bent neutral state. It is interesting to note that in the threshold photoelectron spectrum obtained by Batten et al (1976) the (0,1,0) level has been observed at 895.45 Å. They have also observed a peak in the total photoionization curve at 896.35 Å. Thus the presence of the (0,1,0) level has been closely connected to autoionization.

The presence of autoionization at 876 Å is seen by the intensity distribution of the other three levels (0,0,0), (1,0,0) and (2,0,0). As the four levels in the 876 Å spectrum are not resolved properly, it is difficult to make an exact quantitative measurement of the vibrational intensities. A rough value of the intensity could be obtained from the peak heights and these after the correction for collectiong efficiency give 100, 60, and 27 for the (0,0,0), (1,0,0) and (2,0,0) levels respectively. The corresponding intensity of the (0,1,0) level is 92. The intensity of the (0,0,0) peak has been kept as hundred and the other intensities calculated accordingly. Comparison of these intensities with the corresponding intensities obtained in the 584 Å spectrum (given in Table III.3) shows that the 876 Å spectrum is purturbed to a large extent by autoionization.

The presence of autoionization at 876 Å can also be seen from the photoionization efficiency curves given by McCulloh (1973) and Batten et al (1976) in this energy range. The curve given by McCulloh shows a steady increase in the photoionization efficiency from 870 Å onwards and dropping down rather steeply at the threshold of ionization with a large amount of fine structure superimposed on it. Between 870 and 880 Å, the fine structure is not so prominent, but definitely there are some small peaks. The photoionization curve given by Batten et al between 874 and 884 Å shows a definite peak at 876.35 Å. No assignment of this peak has been done so far. The ionizing wavelength used, 876.056 Å is fairly close to this peak and hence the effect of autoionization observed at this wavelength could be due to this state only.

From the separation of the (0,1,0) level from the (0,0,0) level, the vibrational frequency ν_2 was calculated and a value of 605 ± 60 cm^{-1} was obtained. No value for ν_2 in any other photoelectron spectroscopy experiment has been reported so far. A value of 492 ± 35 cm^{-1} by Batten et al (1976) and 508 ± 10 cm^{-1} by OFrey et al (1977) using TPES, 531 cm^{-1} by Koryashkin (1966) using optical methods and 498 cm^{-1} by Gauyacq (1975) using ionic fluorecence has been reported. The present value is on the higher side as compared to the values measured by other techniques.

III.4.4 Vibrational Intensities and Autoionization

Vibrational intensities for the (ν_1,0,0) levels with ν_1 = 0,1, and 2 have been measured in the photoelectron spectrum at 584 Å, 736 Å, and 744 Å respectively. The vibrational intensities are shown in Table III.3. The intensity for the (0,0,0) level in all the three spectra is kept at 100 and the intensity for other levels has been calculated accordingly. The vibrational populations at 736 Å show a clear departure from those at 584 and 744 Å. Therefore, contribution from strong autoionization at 736 Å (actual wavelength = 735.895 Å) cannot be ruled out. Incidentally, there is a well-established Rydberg series with n = 5 and converging to the v' = 3 level of the $A\,^2\Pi_u$ state of the molecular ion, at a wavelength of 735.2 Å as reported by McCulloh (1973). The two wavelengths are very close with the result that the effect of autoionization becomes apparent at the incident photon wavelength of 735.895 Å.

The values of the vibrational intensities for the (1,0,0) level as shown in the Table III.3. at the wavelengths 584 and 744 Å are the same for all practical purposes. But the intensity of the (2,0,0) level is about 36% higher at 744 Å as compared to that at 584 Å. This could be an indication of a weak autoionization at 744 Å.

In the 736 Å spectrum even though the effect of

TABLE III.3

RELATIVE VIBRATIONAL INTENSITY DISTRIBUTION[a)]

FOR THE $X^2\Pi_g$ STATE OF CO_2 ION

Level	RELATIVE INTENSITY		
	584 Å	736 Å	744 Å
(0,0,0)	100.0	100.0	100.0
(1,0,0)	26.4	32.7	25.8
(2,0,0)	11.4	14.9	15.5

a) Normalized to a value of 100 for the (0,0,0) level.

autoionization is clearly seen, the vibrational level (0,1,0) is not excited as compared to the 876 Å spectrum discussed earlier. This only shows that the autoionizing level at 736 Å is a linear neutral state.

CHAPTER IV

PHOTOELECTRON SPECTROSCOPY OF ATOMIZED SPECIES

IV.1 Introduction

High resolution vacuum ultraviolet photoelectron spectroscopy has provided valuable information about the electronic structures and the orbital arrangements in small molecules. The technique has potential importance in similar investigations of transient species like dissociated atoms, radicals and ions, and excited neutrals. In these cases, not enough experimental data are available. Probably the best technique so far for studying the transient species is photoelectron spectroscopy.

In 1970, Jonathen and colleagues reported the first photoelectron spectra of N, O, and H (Jonathen et al, 1970). Since then several transient species like O_2 ($a\,^1\Delta_g$), CH_3, SO, CS etc. have been studied and the progress in this area upto 1974 has been reviewed by Frost (1974). Most of the work on photoelectron spectroscopy of the atomized species has been

confined to measuring the ionization potentials and observing new energy levels. Very few measurements for the intensities of vibrational and electronic states in the photoelectron have been made, which are independent of the angular distribution of the electrons. Also, most of the spectra have been obtained only at certain resonant wavelengths without the use of a monochromator. Hence it was decided to develop a system to measure the accurate branching ratios of the atomized species. The phase sensitive detection technique used by Jonathen et al (1974) and later modified by DeLeeuw et al (1976) was used for this purpose in conjunction with the photoelectron spectrometer discussed in Chapter II.

IV.2 Experimental Details

IV.2.1 The Phase Sensitive Detection Technique

In general the transient species to be studied are produced in an electrical discharge. Also the concentration of the transient species after the discharge is very small compared to that for parent molecules. As a result the photoelectron spectra is dominated by the parent species, and a very weak spectrum is obtained for the transients. To overcome this problem, Jonathen et al (1974) used the phase sensitive detection (P.S.D) technique alongwith modulation of the electrical discharge producing the transient species. The P.S.D technique although widely used in other types of spectroscopy,

had not been previously used in photoelectron spectroscopy. In this application, the phase sensitive technique requires a regular and reproducible variation of partial pressure of the species, i.e., deviation from the normally highly desirable steady-state conditions. Ideally, partial pressure of the species should vary between zero and a maximum value. It is not possible to achieve this by mechanical interference with the flow rate of molecules either into or out of the photoionization chamber. Such a procedure would lead to loss of resolution because of pressure variation - the so-called " pressure-shift" effect. Thus the partial pressures of the atomized species and the parent molecules are best varied by means of modulating the electrical discharge used for atomization. Usually the electrical discharge is powered by a microwave generator. There is an optimum range of modulation frequency, the upper limit of which is determined by the pumping speed of the system. If the frequency is too high, steady state conditions will be approached because the reciprocal of the modulating frequency becomes less than the residence time of the species in the photoionization chamber. The lower frequency limit is governed by questions of stability of the apparatus and time taken to record a spectrum. Jonathen et al (1974) found the optimum modulation frequency to be in the range of 10-20 Hz for their spectrometer. They used this technique successfully to obtain the $O_2(a\,^1\Delta_g)$ photoelectron spectrum.

In this technique since the phase-sensitive detector is only sensitive to the amplitude of partial pressure fluctuations, signals arising from transients and parent molecules will be approximately equal in magnitude. Moreover, since the variations in partial pressures show a 180 degree phase difference, positive and negative spectra, with respect to the base line result. In this way, parent molecules and transients are distinguished. Although the technique enhances the intensity of the photoelectron spectra of the transients relative to parent molecules, in general, the value of the method is still limited by the extensive overlap between lines from transients and parent molecules. This limitation can be removed using a double modulation technique (De Leeuw et al, 1976) where the intensity of the ultraviolet light source also is modulated with proper phase difference with respect to the microwave discharge producing the transients, thus supressing the spectrum due to parent molecules.

During the period when the microwave discharge producing the transients is off, the photoelectrons arise only from the parent molecules. The modulation of the intensity of the ultraviolet source is done such that when the concentration of the parent molecules is large, the intensity of the ionizing radiation is less and vice versa. Equalizing the number of photoelectrons arising from parent molecules in both on and off periods by adjusting the phase and depth of the lamp modulation

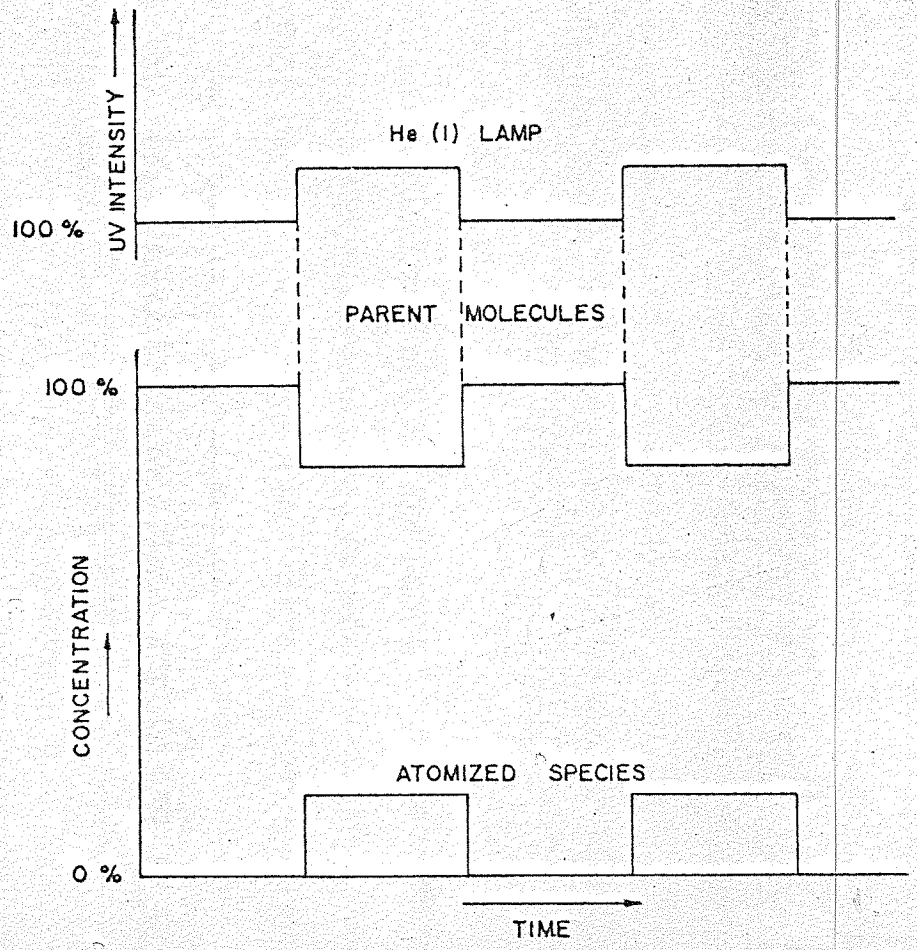


FIG IV. 1. Amplitude diagram showing double modulation for the suppression of photoelectron spectra due to parent molecules

yields a zero P.S.D output. Photoelectrons from transients are produced only during the period when the discharge is on and when the lamp intensity is maximum. Therefore the PSD output of the atomized species remains virtually unchanged. The modulation of the microwave discharge which produces the atomized species and the intensity of the lamp is shown in Fig IV.1. The variation of the concentrations of the atomized species and the parent molecules in time is shown by the two lower curves. The uppermost one shows the variation of ultraviolet light intensity.

IV.2.2 Instrumental Details

The photoelectron set up discussed in Chapter II was used with suitable modifications, especially in the data acquisition part. The ultraviolet light source was powered by a microwave supply with maximum output power of 200 watts. (MR III, KK Ewig Shokai, Japan). This supply had an additional facility for modulating the output power.

In the electron spectrometer, modification was made to have a microwave discharge in the gas entering the ionization chamber. The gas coming through the needle valve was taken through a 5 mm i.d., 15 cm long quartz tube subjecting it to a microwave discharge. [The concentration of atoms produced in a 2450 MHz microwave discharge with the help of an Evenson cavity was found to be maximum for a discharge tube with internal diameter of 5 mm (Vijaykumar and Krishnakumar, 1979)].

This quartz tube was connected to a 1 cm diameter pyrex tube which conducted the gas into the ionization chamber. The pyrex tube was coated with orthophosphoric acid to reduce the loss of the atomized species due to collision with the wall. The microwave discharge was produced in the quartz with the help of an air-cooled Evenson cavity and a microwave generator. This microwave generator was identical to the one used in the light source and had similar arrangement for modulating the output power.

The data acquisition system discussed in Chapter II was replaced by the phase sensitive detection system except for the staircase generator and the channeltron voltage supplies. The block diagram of the PSD set up is shown in Fig IV.2. The pulses from the channeltron after proper amplification and discrimination were fed into a rate meter. The rate meter output was connected to the phase sensitive detector. The PSD system was the lock in amplifier (Keithley, Model 840 Autolock Amplifier). From the function generator square pulses of amplitude - 10V and frequency f_o were fed into the two phase shifters and also to the level shifter amplifier II. This level shifter amplifier increased the depth of the square pulses to a value V_2 before they entered the microwave generator II. The phase shifter I and the level shifter amplifier I were used to adjust the phase and amplitude of

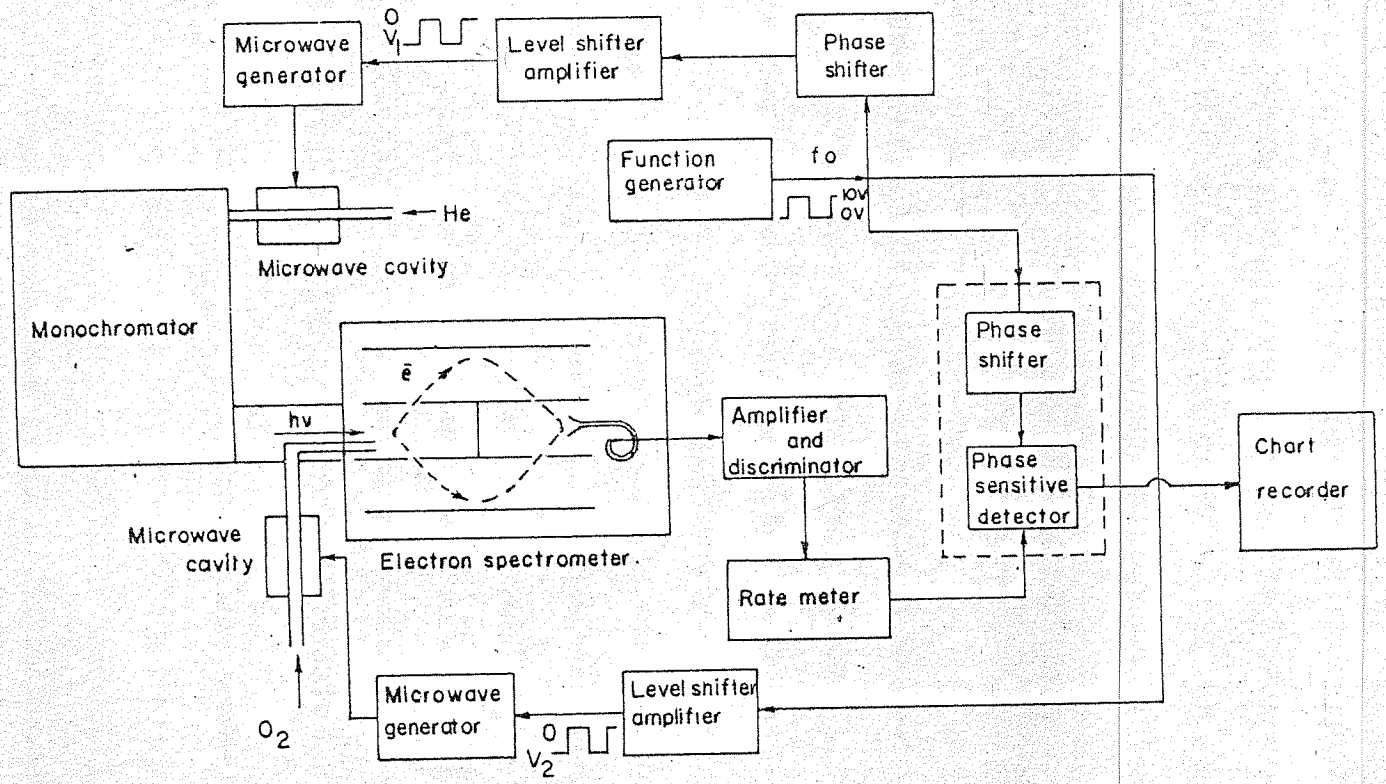


Fig. IV 2 Block diagram of the experimental arrangement

modulation of the lamp intensity. The phase shifter II adjusted the phase by an amount $\ominus$ which corresponded to the time lag between the production of the transient species in the discharge region and detection of electrons emitted by those species. The PSD output was fed to a chart recorder for recording the spectra directly.

IV.2.3 Operation and Performance

The photoelectron spectrometer was operated in the acceleration mode as discussed in Chapter II. The staircase voltage given to the innermost electrode was derived from the computer controlled multichannel analyzer as already discussed. The initial voltage of the staircase and the step size were fixed manually and the energy scanning was done automatically by giving the initial commands through the teleprinter to the MCA. The single scan mode was used with the time for each step being decided by the time constant selected in the PSD which in turn was decided by the frequency of modulation.

The performance of the set-up was tested by trying to obtain the photoelectron spectrum of O_2 ($a\,{}^1\Delta_g$) produced in the microwave discharge of O_2. Initially modulation of the transient species only was tried. The microwave generator could take a maximum modulating signal height of 75 volts and and this gave about 30% modulation of the power. Experiment

was done using various modulating frequencies in the range of 1 to 30 Hz and using different pressures in the discharge tube. But in no case a spectrum could be obtained. Since the single modulation did not work out, the double modulation, with the modulation of the lamp intensity also, was not tried.

There could be various reasons for the failure of this experiment. Probably the pumping speed employed was not sufficient resulting in a large residence time of the species in the ionization chamber. The failure could be partly due to this since a large residence time necessitates the use of low frequencies and at these frequencies, the stability of the apparatus is very poor. But the most important problem could be the low count rate of the electrons. Since a monochromator was used along with the light source, the intensity could go down by about two orders of magnitude. Thus using this method, it seems, at present, impossible to obtain the photoelectron spectra of transients using an ultraviolet monochromator until and unless light sources of sufficient intensity to cope with the loss in the monochromator are available.

IV.3 $O_2(a\ ^1\Delta_g)$ Photoelectron Spectra

Since the PSD method did not work, it was decided to study the photoelectron spectra of the atomized species by the conventional method. Experiment was done to obtain the photoelectron spectra of $O_2(a\ ^1\Delta_g)$. The main problem in this was

the large background counts due to particles other than photoelectrons. The probable source of these counts were the excited neutral molecules which impinged on the channeltron face producing electrons and hence the pulses. These counts due to the so called 'hot particles' could be reduced by reducing the pressure. Passing the discharge products through a cold trap before allowing to enter the ionization chamber also reduced these counts to a good extent. But this directly affected the concentration of the species to be studied. For molecular oxygen it was possible to find an optimum pressure where the counts due to the 'hot particles' were almost negligible and the photoelectron counts were appreciable. The spectra of the discharged O_2 were studied at 584 Å as well as at 736 Å. The intensity due to the $a^1\Delta_g$ state was very small. The photoelectron spectra obtained for the ground state of O_2^+ due to $O_2(a^1\Delta_g)$ at 584 Å and 736 Å are shown in Fig IV.3.4, Figure IV 3 gives the 584 Å spectrum. The vibrational levels $v' = 0$ to 3 of $O_2^+(X^2\Pi_g) \leftarrow O_2(a^1\Delta_g)$ it can be seen with small intensity along with $O_2^+(X^2\Pi_g) \leftarrow O_2(X^3\Sigma_g^-)$. This spectrum has been taken in the grounded mode of the analyzer. This explains the poor resolution of the spectrum. Figure IV.4 gives the 736 Å spectrum taken in the accelerating mode of the analyzer and analyzed at -2 volts. The resolution is about 30 meV. In this spectrum it is possible to see the vibrational levels $v' = 0$ to 5 of $O_2^+(X^2\Pi_g) \leftarrow O_2(a^1\Delta_g)$ eventhough $v' = 4$ and 5 are

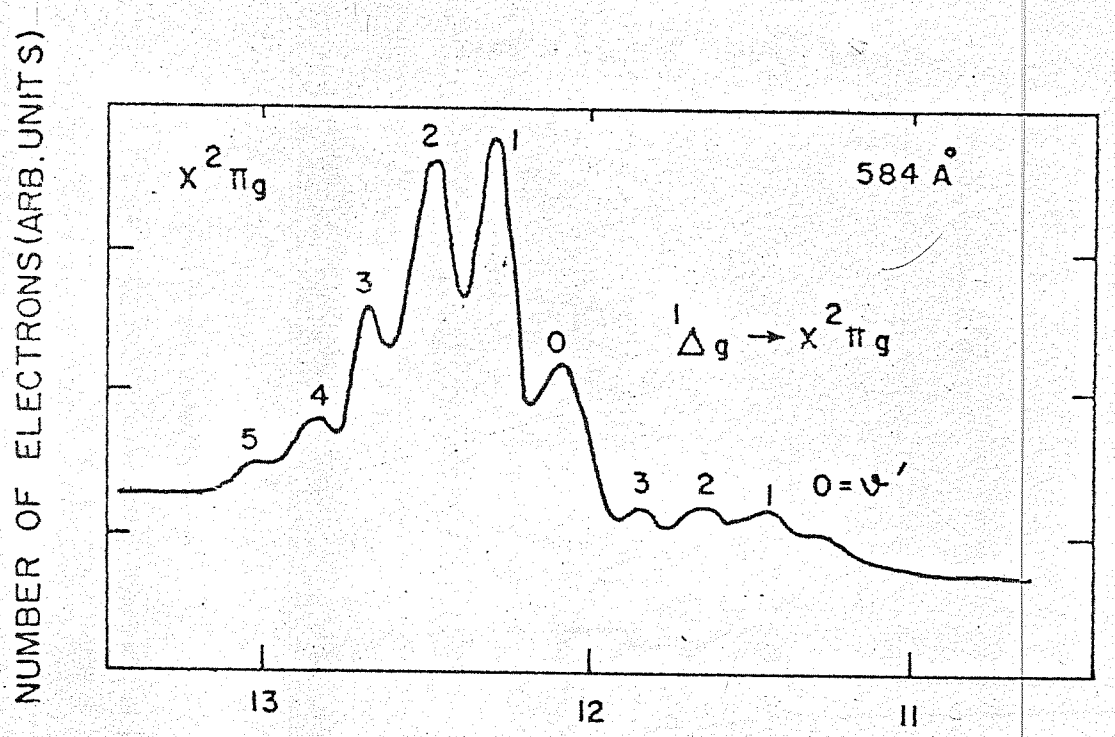


Fig. IV.3 Photoelectron spectrum of O_2 ($a^1\Delta g$) at 584 Å

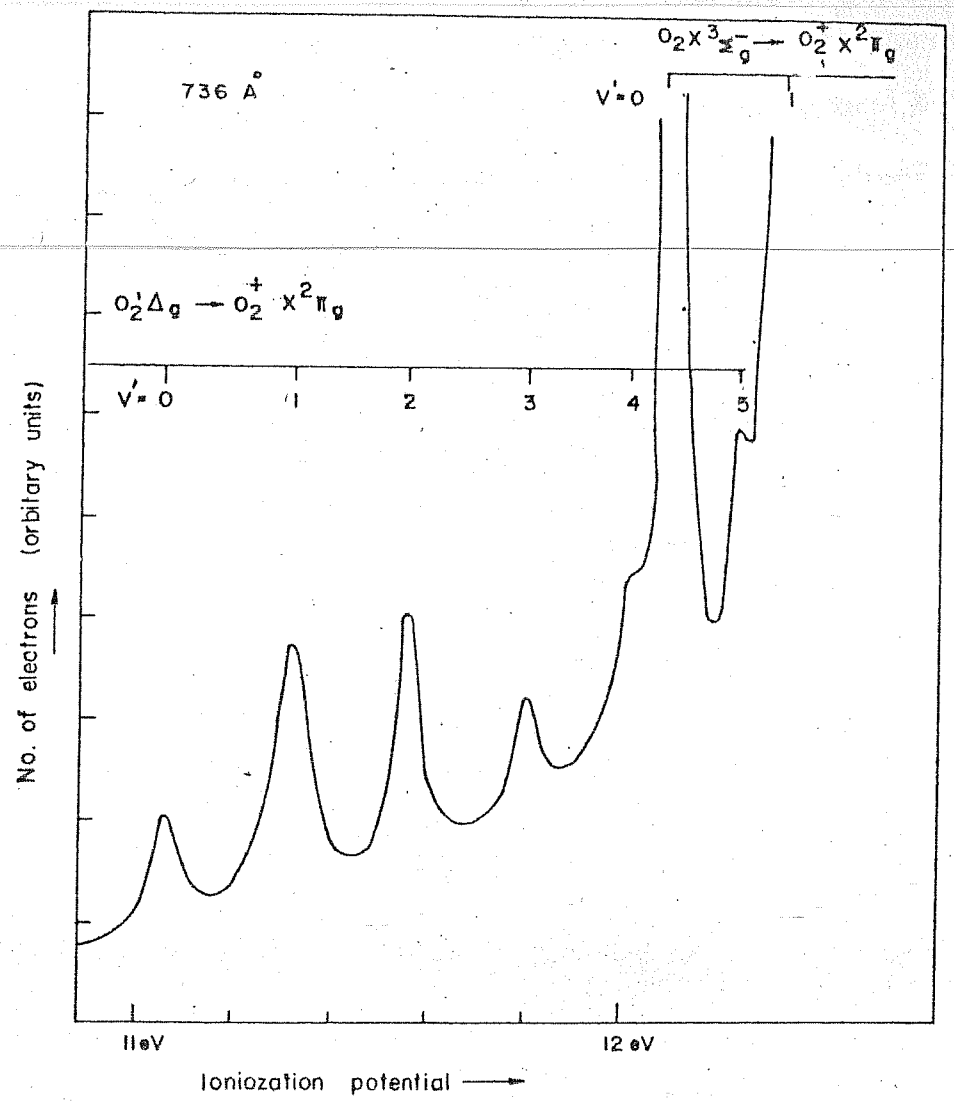


Fig IV. 4. Photoelectron spectrum of O_2 ($a\,^1\Delta_g$) at 736 Å

overlapped by the $O_2^+(X^2\Pi_g) \leftarrow O_2(X^3\Sigma_g^-)$ peaks. The levels $v' > 5$ from $O_2(a^1\Delta_g)$ could not be seen probably because of small intensity coupled with the overlap due to peaks from $O_2(^3\Sigma_g^-)$ state and hence that part of the spectrum is not shown in the figure.

CHAPTER V

TOTAL ELECTRON SCATTERING CROSS-SECTION FOR MOLECULAR HYDROGEN AT LOW ENERGIES BY PHOTOELECTRON SPECTROSCOPY

Introduction

While studying the photoelectron spectra of certain gases using the set up discussed in Chapter II, it was found that the photoelectron intensities varied at different pressures. This effect as pointed out in Section II.9.4 was due to the scattering of electrons by the parent molecules. The effect of scattering was particularly significant in the case of molecules like H_2 for which the electron scattering cross-sections are, in general, quite large. It was decided to make a systematic study of the electron scattering in the system with a view to establish the use of photoelectron spectroscopy in measuring the electron scattering cross sections. The scattering effects on the photoelectron spectrum of molecular hydrogen at 736 Å were studied and the relative total scattering cross sections for hydrogen from zero to 1.14 eV were obtained.

The details of the procedure used to obtain the cross sections and the comparison of results with the existing data are presented in this Chapter.

The earliest measurement of total $\bar{e}$ - H_2 scattering cross-section with discrete low energy electrons were made by Ramsauer (1921 a,b), Brode (1925) and Bruche (1927 a,b,c) for energies greater than about 0.25 eV. The cross sections were later remeasured by Normand (1930) and Ramsauer and Kollath (1929) to detect fine structure, if any, using an apparatus with higher velocity resolving power for electrons. It was found that there is, in general, some agreement as to the shape of the total scattering cross section curve for various electron energies. The magnitudes of the cross sections at some energies, however, were found to differ by a large factor in some experiments. Again, sharp peaks at electron energies around 2.5eV and 4.9 eV were reported by Normand (1930) alone while there is no evidence for this structure in the earlier investigations. In 1966, Golden et al (1966) measured the absolute total e^- - H_2 scattering cross section as a function of electron energy from 0.25 eV to 15 eV with an estimated probable error of $\pm$ 3%.

Some indirect methods have been used to measure the momentum transfer cross sections for molecular hydrogen. The results of Englehardt and Phelps (1963) and Bekefi and Brown (1958) clearly show an agreement in shape only of the

cross section versus electron energy curve as compared to the direct methods as discussed above. However, a large descrepancy in magnitude is observed, especially at the extremely low values of electron energy.

V.2 Experimental Details

The photoelectron spectrometer discussed in the second chapter was used as such for the electron scattering studies. It may be mentioned here that an additional pumping system with a four inch oil diffusion pump at the detector side as discussed in Section II.3 was incorporated specially for the scattering studies. This pumping system was directly connected to the analyzing region (i.e., region between the inner and outer cylinders of the CMA) also. The gas throughput into this region as well as the detectorside was only through the analyzer slits. Thus it was possible to maintain a high pressure difference between the ionization chamber and these regions. (This set up was used for all the previous experiments also). This helped in maintaining a low pressure necessary for the smooth functioning of the channeltron and also kept the scattering of electrons in the analyzing region to a minimum, thereby confining the electron scattering up to the entrance slit of the energy analyzer. Pressures upto $\sim 3.5 \times 10^{-2}$ torr could be maintained in the ionization chamber without affecting the performance of the channeltron.

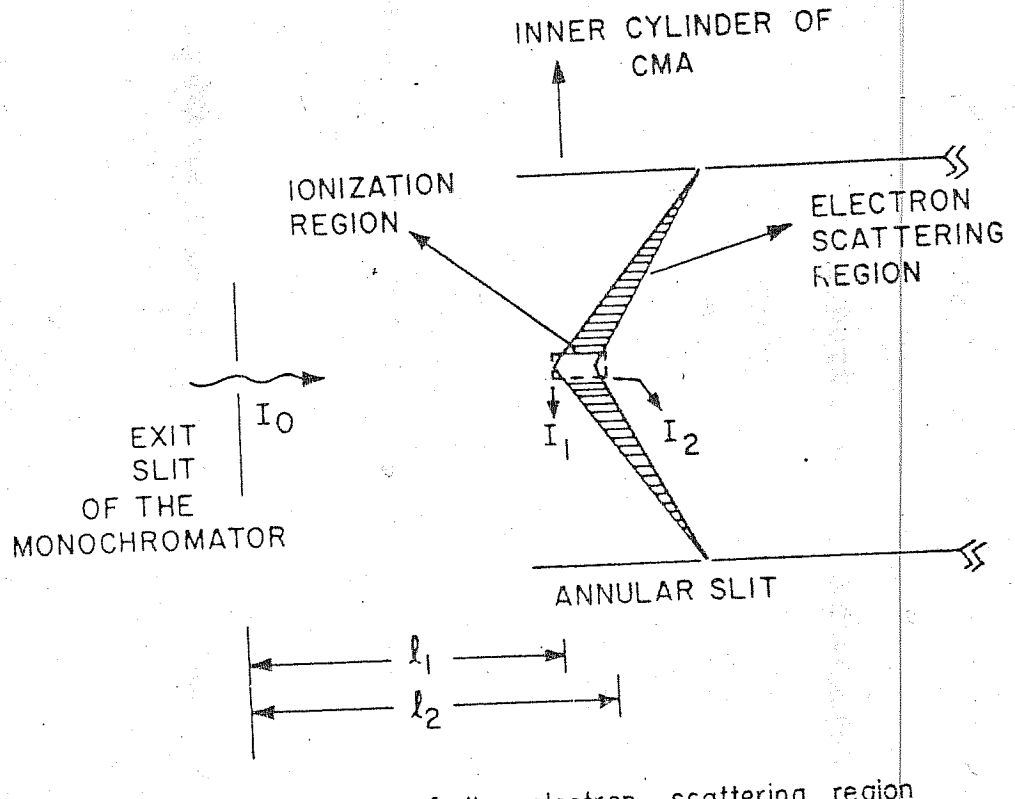


FIG V 1 Schematic of the electron scattering region

In the present experiment, the photoelectrons were produced all along the photon beam which was 3 mm in diameter. The electron produced in a small length Δl and travelling at 55° angle to the photon beam axis were collected by the analyzer. The length Δl was defined by the $\pm 3^{\circ}$ angular spread of the electron entering the analyzer. As the electrons travelled towards the entrance slit of the analyzer they underwent scattering with the parent molecules present. The scattering region is schematically shown in Fig V.1. In the figure, Io denotes the intensity of the light at the exit slit of the monochromator. The ionization region with length Δl is bounded by the lengths, l_1 and l_2 from the exit slit of the monochromator. I_1 and I_2 are the photon intensities at l_1 and l_2. In the experiment l_1 was kept about 20 cms.

V.3 Measurement of the Cross-section

The photoelectron spectrum of H_2 at 736 Å gives 7 vibrational levels from $v' = 0$ to $v' = 6$. Each of these vibrational levels represents a monoenergetic beam of electrons. Thus the seven peaks represented seven points in the energy scale from 0.02 to 1.14 eV with almost equal separation.

The photoelectron spectra of H_2 at 736 Å were obtained with 12 meV resolution at a large number of pressures in the ionizing region. From the spectra, the amplitudes of the photoelectron peaks at different energies were measured as a function of the

gas pressure. The initial intensity of the electrons at each energy depends on the partial photoionization cross section for producing electrons at that energy and the intensity of the light and the number of molecules at the ionizing region from where the electrons are collected for analyzis. The measured intensities of the photoelectron peaks give the final intensity after scattering. At small pressures in the ionization chamber the scattering is negligible and the electron production process, which is proportional to the pressure assuming the photon intensity to be constant, is dominant. Thus at small pressures, the measured photoelectron intensities increase with pressure. Afterwards the intensities of the peaks tend to saturate, reach a maximum and start decreasing very fast at higher pressures. The dependence of the intensity of the photoelectron peaks is clearly shown in Fig V.2. In the figure, a typical set of photoelectron spectra for $V' = 3$ vibrational level of the ground electronic state of molecular hydrogen ion, obtained at 736 Å is shown. The spectra were taken at various gas pressures from 8.4×10^{-1} to 1.04×10^{-2} torr. The amplitudes for the $V' = 3$ peak at different pressures are measured and after necessary corrections for noise, the values are plotted as a function of pressure (curve III of Fig V.3). The number of electrons increases linearly upto about 3.5×10^{-3} torr, reaches a maximum at about 5×10^{-3} torr, and starts decreasing at higher pressures. The initial number of electrons participating in the scattering process at different gas

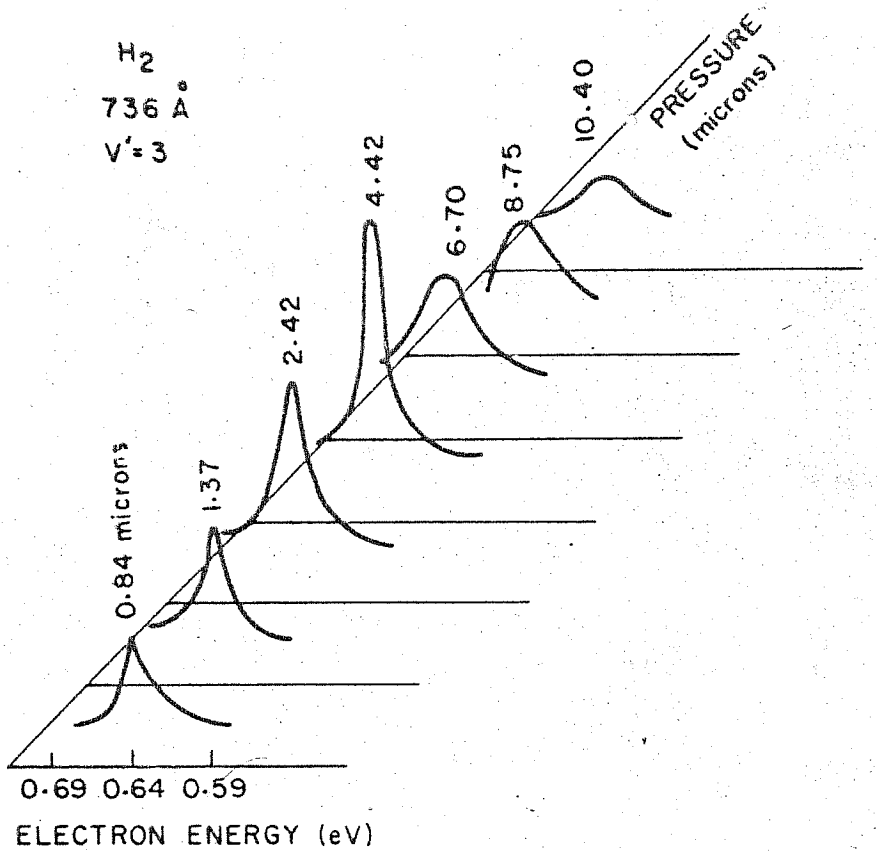


Fig. V. 2 Effect of increasing gas pressure on the photoelectron spectrum

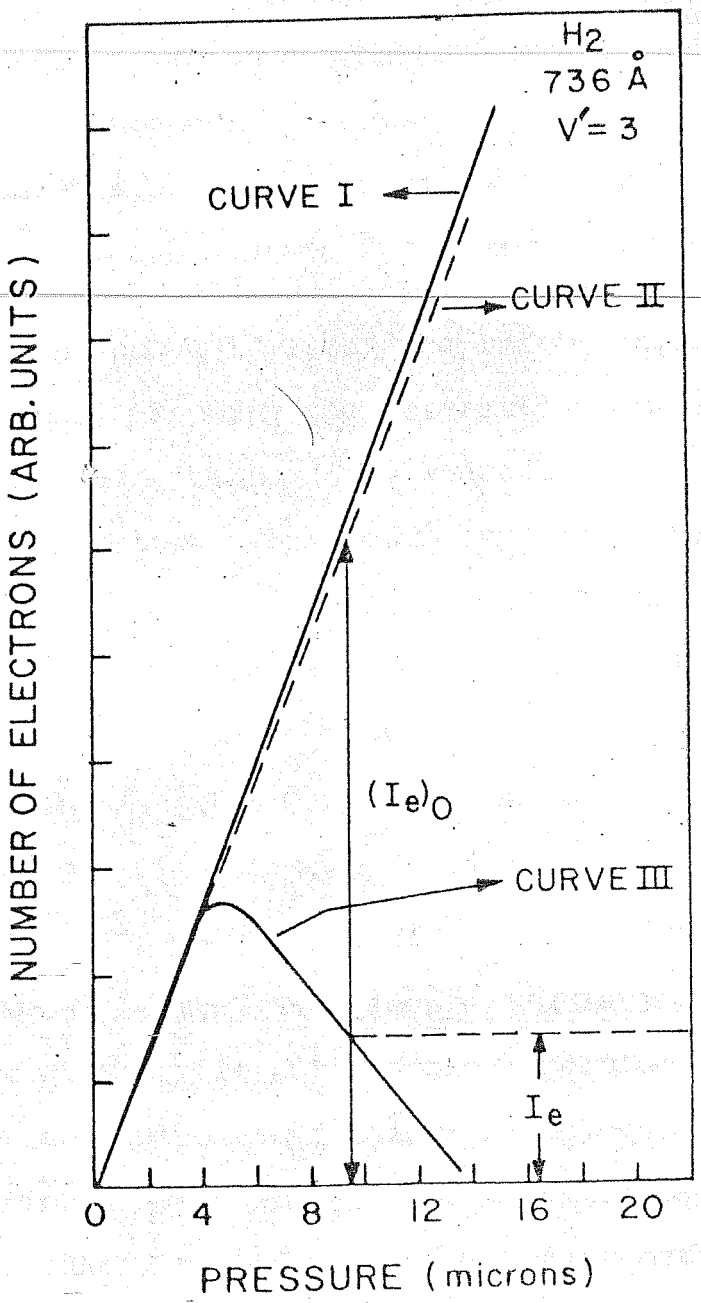


FIG. V. 3. e^- - H_2 scattering; pressure v s intensity of photoelectron peak.

pressures is obtained by producing the straight line given by the linear region between 8.4×10^{-4} and 3.5×10^{-3} torr. This is characterised by curve I in Fig V.3. Thus the intensities of the electrons before scattering and after scattering are represented by curves I and III respectively.

The curve I giving the initial number of electrons is obtained, assuming the intensity of the photon beam reaching the ionizing region from where the electrons are collected, to be constant. But actually this decreases as the pressure increases due to absorption in the gas column ahead. Calculations have been made to get the exact intensity at the ionizing region. The number of electrons produced in the small region $\Delta l = l_2 - l_1$ (Fig V.1) is given by

$$Ne = I_0 e^{-\frac{k\rho l_2}{760}} \left[e^{\frac{k\rho \Delta l}{760}} - 1 \right] \qquad \text{V.1}$$

where ρ is the gas pressure, I_0 is the intensity of the photon beam at the exit slit of the monochromator, and k is the photoabsorption coefficient of molecular hydrogen at the particular wavelength. The photoionization efficiencies have been taken as unity at 736 Å. As a matter of fact, the ionization efficiency is very slightly less than unity (Cook and Metzger, 1964). The total photoabsorption cross section at the incident wavelength have been taken from Lee et al (1976). The number of electrons available for scattering at different pressures could be obtained from eqn.V.1 for a particular

electron energy. Curve II (Fig V.3) obtained after normalizing the curve I at pressures below 3.5×10^{-3} torr gives the actual initial number of electrons before scattering, at various pressures. In the present case of molecular hydrogen the difference between the two curves is negligible.

For each value of the pressure in the scattering region curve II defines $(I_e)_o$, the number of electrons before scattering and curve III defines I_e, the number of electrons measured after scattering. The absorption coefficient, α of the gas for the electron beam can be defined as

$$I_e = (I_e)_o \exp(-\alpha x) \qquad \text{V.2}$$

where

$$x = \frac{p \cdot d}{760} \qquad \text{V.3}$$

d is the scattering path length and p is the pressure in torr. A graph of $\ln \frac{(I_e)_o}{I_e}$ against pressure is a straight line, the slope of which gives a measure of α, in a relative way at a particular electron energy. With number of molecules/cm^3 available for scattering known, one can derive from α, the effective collision cross section or the total electron scattering cross section of the target species.

This method could yield absolute cross sections provided the pressure is measured absolutely in the collision region. Unfortunately, the pressure has been measured absolutely at a place slightly away from the collision region and there is some impedance introduced in between because of the presence of a

large number of circular light baffles used to collimate the photon beam. Also, the path length in the scattering region cannot be exactly defined in the experiment. This point has been discussed in later part of the text. Thus, the relative cross sections only could be measured.

V.4 Results and Discussions

The results of the measurement of the relative total electron scattering cross section for molecular hydrogen at electron energies ranging from 0.02 to 1.14 eV are shown in Fig V.4 along with the results of Ramsauer and Kollath (1929) and Golden et al (1966). The results have been normalized at an electron energy of 0.94 eV where the two curves reported by Ramsauer and Kollath (1929) and Golden et al (1966) give the same absolute cross section of 13 A^2. The present results seem to agree with those of Ramsauer and Kollath in a better way than with the results of Golden et al. The cross sections given by Golden et al in the lower electron energy region seem to decrease much faster but the measurement by Normand (1930) show a steep increase in the cross section below 1 eV. The results of Normand have not been shown in Fig V.4.

Recently, total cross section measurements for $e^- - H_2$ scattering at low energies have been reported by Ferch et al (1980) using an electron time-of-flight method. The results in the electron energy range from 0.02 eV to 1.2 eV have been shown

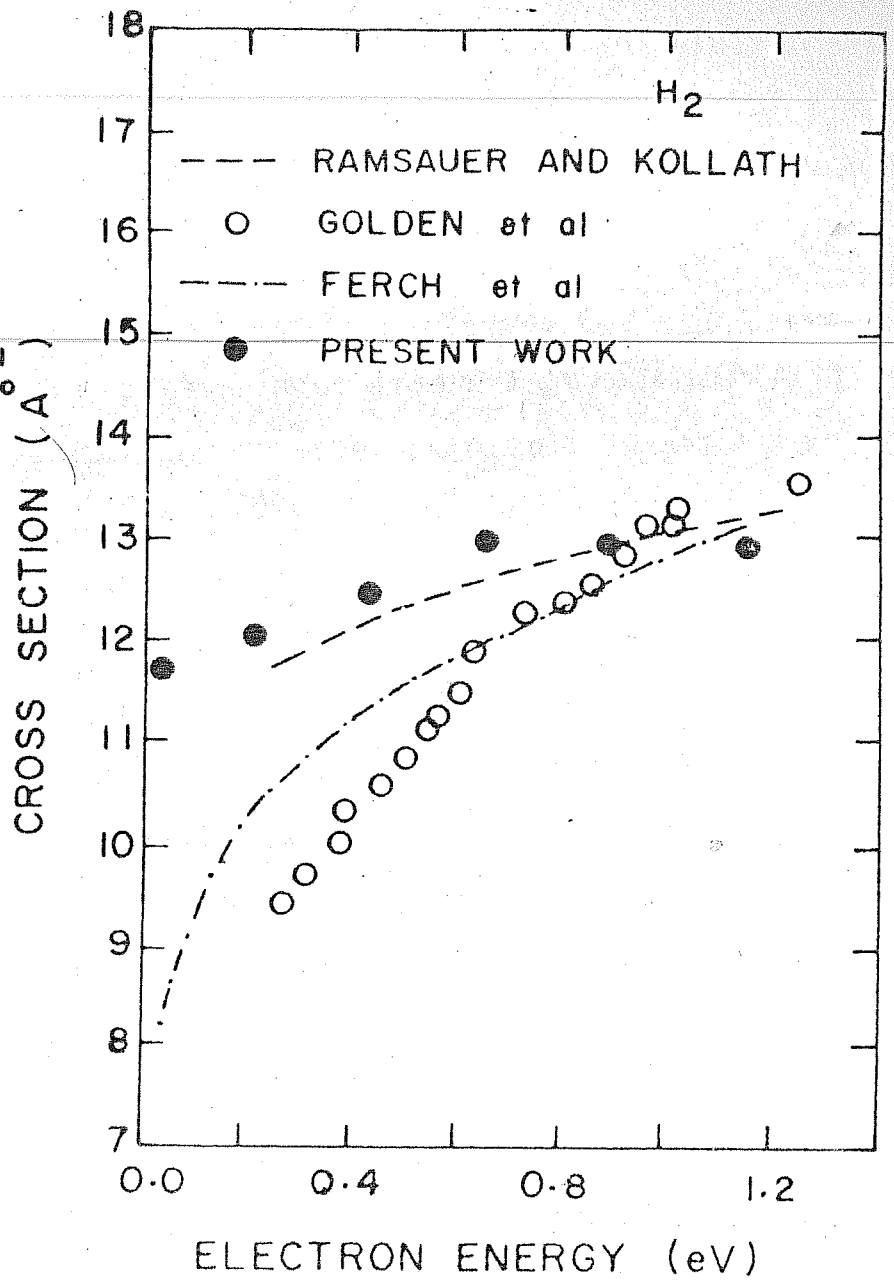


FIG. V. 4 Relative total electron scattering cross section for H_2

in Fig V.4. The cross section values are, in general lower than those obtained in the present experiment but are higher than those given by Golden et al at electron energies below 0.7 eV.

V.5 Major Sources of Errors

One of the major errors in the measurement could be due to the scattering of electrons in the analyzing region. In the analyzing region the energy of the electron varies and hence it is not possible to treat the scattering electrons as monochromatic. The experimental system has been designed in such a way that the pressure in the analyzer region, in general, is 10 to 12 times less than that in the ionization region. But since the electrons have to travel a larger distance before coming out of the analyzer, the scattering in this region could contribute some error. A similar error would result in the region enclosed by the retarding/accelerating slit and the main slit of the CMA through which the electrons enter the analyzer region, when the CMA is used in the accelerating mode. In the present experiment the accelerating mode was used with the electrons being analyzed at 1.5 V. A third source of error could be due to the extrapolation of the scattering curve from low pressure to high pressure region. The error might result from the inaccuracy in determining the extent of the linear portion of the scattering curve.

V.6 Conclusion

In the experiment discussed above, the relative total scattering cross sections of molecular hydrogen have been measured using photoelectron spectroscopy. This is the first time this technique has been used to measure the electron scattering cross section. The results obtained have been in fairly good agreement with those reported by other methods.

Apart from giving only relative values and not absolute values of the cross sections, the drawback of the present set up has been the errors due to scattering in the accelerating and analyzing regions. But these are all mere technical problems which can be solved by improved instrumentation. The cross section values can be made absolute by measuring the pressure and the scattering path length absolutely. Defining the path length as well as eliminating the scattering in the accelerating and the analyzing regions can be simultaneously accomplished by introducing a much faster differential pumping arrangement.

In the present experiment, measurements were made only at seven discrete energies. Also the energy resolution was limited by the analyzer energy resolution since the photoelectrons peaks were all due to vibrational levels. The resolution can be improved by using any rare gas with large photoionization cross-section to produce the photoelectrons. The photoelectrons produced from atoms with monochromatic photons have very small energy spread and the energy resolution of the experiment is

equal to this spread since the scattering process takes place before the electrons enter the analyzer and hence are not affected by the contact potential or any other similar problems. The photoelectrons produced from the atomic gas are allowed to be scattered by the target gas introduced in the system. The pressure of the target gas is varied and the intensities of the photoelectron peaks due to the atomic gas are measured. The scattering cross section is obtained by following the procedure discussed as in the case of H_2. To obtain the energy dependence of the scattering cross sections electrons have to be produced in a wide range of continuous energies. This could be achieved by using a continuum source of photons and carrying out the experiment as a function of photon energy. Thus using photoelectron spectroscopy, total electron scattering cross sections at very high energy resolution can be measured as a continuous function of energy. This method seems to be very promising particularly for very low electron energies.

CHAPTER VII

SCOPE FOR FURTHER WORK

Part of the work presented in this thesis has been to study the photoelectron spectra of simple molecules as a function of the wavelength of the ionizing radiation. The work has been strongly limited due to lack of a continuum light source. But the limited work which has been carried out as in the case of molecular oxygen, clearly points out the need for studying the photoelectron spectra as a function of energy of the ionizing radiation especially in the vicinity of resonances in the photoionization continuum. This necessitates the use of a synchrotron radiation source which is ideal for this type of work. In the absence of synchrotron radiation, BRV source could be a good substitute. The main drawbacks with the BRV source have been its pulsed operation with small repetition frequency and large fluctuation in the intensity. Also, the uranium electrode which is generally used as the anode erodes after certain number of operations (about 10000 pulses

and has to replaced or reshaped frequently. But it seems to be possible to eliminate these problems with certain compromises. With the BRV source built in our laboratory it has been possible to limit the intensity fluctuation within a factor of two operating at 1 pulse per second. The problems due to the erosion of the uranium electrode can be eliminated by replacing it with a tungston electrode. But in this case, the continuum may not be very strong in the shorter wavelength region. But the lamp with tungston electrode can be used with a repetition frequency of about 100/sec, without much fluctuation in intensity with the result that the photoelectron spectra as a function of the ionizing wavelength could be effectively studied. Efforts are being made at present in this direction.

So far, most of the photoelectron spectra of the transient species has been obtained at certain resonant line emissions from rare gases without the use of a monochromator. Also very few measurements of the relative peak intensities in the photoelectron spectra have been made so far which are independent of the angular distribution of the photoelectrons. With this point in view, a study of photoelectron spectra of transient species was undertaken in the laboratory and an effort was made to collectively use the various sophisticated techniques which have been so far used independently. In Chapter IV of the thesis, an experiment has been described in which a photoelectron spectrometer incorporating a VUV monochromator and a cylindrical mirror electron energy analyzer has been used to obtain the photoelectron

spectra of the transient species with the help of the phase sensitive detection technique. Unfortunately this experiment did not succeed. The possible reasons for the failure seems to be the lack of very fast transportation of the transient species produced in the discharge into and out of the ionization region of the photoelectron spectrometers and the low count rate of electrons. The lack of fast transportations of the transient species directly affects the modulation frequencies employed for the purpose of phase sensitive detection. It is possible to transport these species into and out of the ionization region by having a very fast pump connected directly to that region thus enabling one to have a much larger modulation frequency. The low count rate of the electrons is due to the less intensity of the ionizing radiation after monochromatization. Thus as long as a VUV monochromator is used, it is absolutely necessary to have a much intense light source. In the case of a microwave discharge lamp which is usually used in this type of experiments, intensity could be increased by having a better power coupling into the discharge plasma. There has been certain amount of work going on in this direction. Glangetas (1980) has obtained an intensity of about 10^{16} photons/sec at about 1200 Å from microwave discharge in Xe and Kr. It is possible that such a lamp could be used to obtain helium and neon emission lines with larger intensities and at wavelengths shorter than 1000 Å.

One very significant aspect of the work presented in the thesis has been the use of photoelectron spectroscopy for electron scattering studies. It has already been explained in Section V.6 how the present set up could be improved to obtain the absolute total electron scattering cross section at very high energy resolution. With the use of a continuum photon source, this method could be extended to a larger range of electron energies than is possible with the line source.

LIST OF PUBLICATIONS

Publications related to the work presented in this thesis,

(1) Autoionization of O_2 by photoelectron spectroscopy

Vijay Kumar and E.Krishnakumar

J.Electron Spectrosc. 22, 109-118 (1981)

(2) Total electron scattering cross section for molecular hydrogen at low energies by photoelectron spectroscopy

Vijay Kumar and E.Krishnakumar

J.Electron Spectrosc. 24, 1-9 (1981)

(3) Photoelectron spectroscopy of CO_2

Vijay Kumar and E.Krishnakumar

To be published.

Publications not included in the thesis,

(1) Measurement of concentration and study of recombination of atomic hydrogen by Wrede-Harteck method

Vijay Kumar and E.Krishnakumar

Rev.Sci.Instrum. 50, 776 (1979)

(2) Production and absolute concentration measurement of O, O_2 ($^1\Delta_g$) and O_2 ($^1\Sigma_g^+$)

Vijay Kumar, E.Krishnakumar and Ajay Kumar

REFERENCES

1 Afanasev, V.P., and Yavor, S.Ya., 1975,
Soviet Phys - Tech.Phys., 20, 715

2 Aksela, S., 1971,
Rev.Sci.Instrum., 42, 810

3 Aksela, S., Karras, M., Pessa, M., and Suoninen, E., 1970,
Rev.Sci.Instrum., 41, 351

4 Al-Joboury, M.I., and Turner, D.W., 1962,
J.Chem.Phys. 37, 3007

5 Al-Joboury, M.I., and Turner, D.W., 1963,
J.Chem.Soc., 5141

6 Asbrink, L., 1970,
Chem.Phys.Letters, 7, 549

7 Auger, P., 1925,
J.Phys.Radium, 6, 205

8 Bahr, J.L., Blake, A.J., Carver, J.H., and Kumar, V., 1969,
J.Quant.Spectrosc.Radiative Transfer, 9, 1359

9 Bahr, J.L., Blake, A.J., Carver, J.H., Gardner, J.L., and Kumar, V., 1972,
J.Quant.Spectrosc.Radiative Transfer, 12, 59

10 Bahr, J.L., Blake, A.J., Carver, J.H., Gardner, J.L., and Vijay Kumar, 1971 a,
J.Quant, Spectrosc.Radiative Transfer, 11, 1839

11 Bahr, J.L., Blake, A.J., Carver, J.H., Gardner, J.L., and Vijay Kumar., 1971 b,
J.Quant.Spectrosc.Radiative Transfer, 11, 1853.

12 Batten, C.F., Taylor, J.A., and Meisels, G.G., 1976,
J.Chem.Phys. 65, 3316

13 Bekefi, G., and Brown, S.C., 1958,
Phys.Rev. 112, 159

14 Bekowitz, J., 1979
in Photoabsorption, Photoionization and Photoelectron Spectroscopy (Academic Press, New York)

15 Berkowitz, J., and Chupka, W.A., 1969,
J.Chem.Phys. 51, 2341

16 Berkowitz, J., and Spohr, R., 1973,
J.Electron Spectrosc., 2, 143

17 Berry, R.S., 1966,
Chem.Phys. 45, 1228

18 Beutter, H., 1935,
Z.Physik, 93, 177

19 Blake, A.J., Bahr, J.L., Carver, J.H., and Vijay Kumar, 1970
Phil.Trans.Roy.Soc.London, A268, 159

20 Branton, G.R., Frost, D.C., Makita, T., McDowell, C.A., and Stenhouse, I.A., 1970,
Phil.Trans.Roy.Soc.London, Ser.A., 268, 77

21 Brode, R.B., 1925,
Phys.Rev., 25, 636

22 Bruche, E., 1927 a,
Ann.d.Physik, 82, 912

23 Bruche, E., 1927 b,
Ann.d.Physik, 83, 1066

24 Bruche, E., 1927 c,
Ann.d.Physik, 84, 279

25 Brundle, C.R., and Turner, D.W., 1969,
J.Mass Spectry. Ion Phys., 2, 195

26 Carlson, T.A., 1971,
Chem.Phys.Letters, 9, 23

27 Chupka, W.A., and Berkowitz, J., 1969,
J.Chem.Phys., 51, 4244

28 Collin, J.E., and Natalis, P., 1968,
J. Mass Spectry. Ion Phys., 1, 121

29 Collin, J.E., Delwiche, J., and Natalis, P., 1972,
in Electron Spectroscopy, ed. Shirley, D.A., (North Holland, Armsterdam) P.401

30 Cook, G.R., and Metzger, P.H., 1964,
J.Opt.Soc.Am., 54, 968

31 Dehmer, P.M., and Chupka, W.A., 1975,
J.Chem.Phys., 62, 4525

32 Dehmer, P.M., and Chupka, W.A., 1976,
J.Chem, Phys., 65, 2243

33 DeLeeuw, D.M., De Lange, C.A., and Maclean, C., 1976,
J.Electron Spectrosc., 9, 185

34 Dill, D., 1973
Phys. Rev., 7, A1976

35 Dill, D., Manson, S.T., and Starace, A.F., 1974,
Phys. Rev.Letters, 32, 1971

36 Doolittle, P.H., and Schoen, R.L., 1965,
Phys, Rev.Letters, 14, 348

37 Ederer, D.L., and Tomboulian, D.H., 1964
Phys.Rev., 133, A 1525

38 Eland, J.H.D., and Danby, C.J., 1968,
J.Mass Spectry.Ion Phys., 1, 111

39 Englehardt, A.G., and Phelps, A.V., 1963,
Phys, Rev., 131, 2115

40 Fano, U., 1935,
Nouvo Cimento (Ser.8) 12, 154

41 Fano, U., 1961,
Phys.Rev.,124, A 1866

42 Fano, U., Cooper, J.W., 1965,
Phys.Rev., 137, A 1364

43 Ferch, J., Raith, W., and Schroder, K., 1980,
J.Phys.B.Atom.Molec.Phys., 13, 1481

44 Frey, R., Gotchev, B., Kalman, O.F., Peatman, W.B.,
Pollak, H., and Schlag, E.W., 1977,
Chem.Phys., 21, 89

45 Frost, D.C., 1974,
J.Electron Spectrosc., 5, 99

46 Frost, D.C., McDowell, C.A., and Vroom, D.A., 1967,
Proc.Roy.Soc.(London) A296, 566

47 Gardner, J.L., and Samson, J.A.R., 1973,
J.Electron Spectrosc., 2, 267

48 Gardner, J.L., and Samson, J.A.R., 1974,
J.Chem.Phys., 61, 5472

49 Gardner, J.L., and Samson, J.A.R., 1975 a,
J.Chem.Phys., 62, 4460

50 Gardner, J.L., and Samson, J.A.R., 1975 b,
J.Electron Spectrosc., 6, 53

51 Gardner, J.L., and Samson, J.A.R., 1976 a,
J.Electron Spectrosc., 8, 123

52 Gardner, J.L., and Samson, J.A.R., 1976 b,
J.Electron Spectrosc., 8, 469

53 Gardner, J.L., and Samson, J.A.R., 1978,
J.Electron Spectrosc., 13, 7

54 Glangetas, A., 1980,
Rev.Sci.Instrum, 51, 390

55 Golden, D.E., and Bandel, H.W., 1965,
Phys.Rev., 138, A14

56 Golden, D.E., Bandle, H.W., and Salerno, J.A., 1966, Phys.Rev., 146, 40

57 Guyacq, D., Horani, M., Leach, S., and Rostas, J., 1975, Can.J.Phys., 53, 2040

58 Hafner, H., Arol Simpson, J., and Kuyatt, C.E., 1968, Rev.Sci.Instrum., 39, 33

59 Hasted, J.B., 1964, in Physics of Atomic Collissions (Butterworths, London) p.330

60 Heddle, D.W.O., 1971, J.Phys.E., Sci.Instrum., 4, 589

61 Johns, J.W.C., 1961, Can.J.Phys., 39, 1738

62 Johns, J.W.C., 1964, Can.J.Phys., 42, 1004

63 Jonathen, N., Morris, A., Smith, D.J., and Ross, K.J., 1970, Chem.Phys.Letters., 7, 497

64 Jonathen, N., Morris, A., Okuda, M., Ross, K.J., and Smith, D.J., 1974, J.Chem.Soc., Faraday Trans.II, 70, 1810

65 Judge, D.L., and Lee, L.C., 1973, J.Phys.B.Atom.Molec.Phys., 6, 2150

66 Judge, D.L., Morse, A.L., and Weissler, G.L., 1963, Sixth International Conference on Ionization Phenomena in Gases (Paris) Vol.3, p.373

67 Kinsinger, J.A., and Taylor, J.W., 1973, Int.J.Mass.Spectry.Ion Phys., 11, 464

68 Koryashkin, V.A., 1966, Dokl.Akad.Nauk.SSSR, 167, 1035

69 Kronig, Rde L., 1928, Z.Physik, 50, 347

70 Lee, L.C., and Judge, D.L., 1972,
J.Chem.Phys., 57, 4443

71 Lee, L.C., Carlson, R.W., and Judge, D.L., 1976,
J.Quant.Spectrosc.Radiative Transfer, 16, 873

72 Lowry, J.F., Tomboulian, D.H., and Ederer, D.L., 1965,
Phys.Rev. 137, A1054

73 Manson, S.T., 1971,
Phys.Rev.Letters, 26, 219

74 McCulloh, K.E., 1973,
J.Chem,Phys., 59, 4250

75 Morgenstern, R., Niehaus, A., and Ruf, M.W., 1971,
7th Int.Conf.on the Physics and Electronics of Atomic Collisions (North Holland, Armsterdam) p.167

76 Natalis, P., 1976
J. Phys.Chem., 80, 2829

77 Natalis, P., Delwiche, J., Collin, J.E., Caprace, G., and Praet, M.Th, 1977,
Phys.Scr. 16, 242

78 Niehaus, A., and Ruf, M.W., 1971,
Chem.Phys.Letters, 11, 55

79 Normand, C.E., 1930,
Phys, Rev., 35, 1217

80 Poole, R.T., Leckey, R.C.G., Liesegang, J., and Jenkin, J.G., 1973,
J.Phys.E.Sci.Instrum., 6, 226

81 Price, W.C., Potts, A.W., and Streets, D.G., 1972,
in Electron Spectroscopy, ed. Shirley, D.A., (North Holland, Armsterdam), p.187

82 Ramsauer, C., 1921 a,
Ann.d.Physik, 64, 513

83 Ramsauer, C., 1921 b,
Ann.d.Physik, 66, 546

84 Ramsauer, C., and Kollath, R., 1929,
Ann.d.Physik, 4, 91

85 Risley, J.S., 1972,
Rev.Sci.Instrum., 13, 95

86 Roy, D., Carette, J.D., 1977,
in Topics in Current Physics, Vol.4 ed.Ibach, H (Springer, Berlin) p.13

87 Samson, J.A.R., 1964,
J.Opt.Soc.Am., 54, 6

88 Samson, J.A.R., 1966,
in Advances in Atomic and Molecular Physics, ed.Bates, D.R., and Estermann, I.(Academic Press, New York), Vol.2

89 Samson, J.A.R., 1969 a,
J.Opt.Soc.Am., 59, 356

90 Samson J.A.R., 1969 b,
Rev.Sci.Instrum., 40, 1174

91 Samson, J.A.R., 1970,
Phil.Trans.Roy.Soc.(London), A268, 141

92 Samson, J,A.R., 1976,
Physics Reports, 28, 303

93 Samson, J.A.R., 1979,
in Handbuch der Physik, ed.W.Mehlhorn (Springer-Verlag, Berlin), Vol.31

94 Samson, J.A.R., and Gardner, J.L., 1973 a,
J.Geophys.Res., 78, 3663

95 Samson, J.A.R., and Gardner, J.L., 1973 b,
Phys.Rev.Letters, 31, 1327

96 Samson, J.A.R., and Gardner, J.L., 1975,
Can.J.Phys., 53, 1948

97 Samson, J.A.R., and Gardner, J.L., 1977a,
J.Chem.Phys., 67, 755

98 Samson, J.A.R., and Gardner, J.L., 1977 b,
J.Opt.Soc.Am., 62, 856

99 Samson, J.A.R., Gardner, J.L., and Haddad, G.N., 1977,
J.Electron Spectrosc., 12, 281

100 Sar-El, H.Z., 1967,
Rev.Sci.Instrum., 41, 351

101 Sharp, J.E., and Rosenstock, H.M., 1964,
J.Chem.Phys., 41, 3433

102 Siegbahn, K., Nordling, C., Fahlman, A., Nordberg, R.,
Hamrinn, K., Hedman, J., Kohansson, G., Bergmark, T.,
Karlsson, S.E., Lindgren, T., and Lindberg, B., 1967,
Nova Acta Regiae Soc.Sci. Upsal., Ser IV, 20

103 Smith, A.L., 1970,
Phil.Trans.Roy.Soc.(London), A268, 169

104 Sroka, W., and Zietz, R., 1973,
Phys.Letters, 43A, 493

105 Starace, A.F., 1979,
in Handbuch der Physik, ed.W.Mehlhorn(Springer-Verlag,
Berlin), Vol.31

106 Tanaka, Y., Jursa, A.S., and Le Blanc, F.J., 1960,
J.Chem.Phys., 32, 1199

107 Turner, D.W., 1968,
Proc.Roy.Soc.(London) A307, 15

108 Turner, D.W., Baker, A.C., Baker, A.D., and Brundle, C.R.,
1070,
in Molecular Photoelectron Spectroscopy (Wiley-Inter Science,
London).

109 Vijaykumar and Krishnakumar,E., 1979,
Rev.Sci.Instrum., 50, 776

110 Vilesov, F.I., Kurbatov, B.L., and Terenin, A.N., 1961, Sov.Phys.Dokl., 6, 490

111 Wannenberg, B., Gelius, U., and Siegbahn, K., 1974, J.Phys. E.Sci. Instrum, 7, 149

112 Yoshino, K., and Tanaka, Y., 1968, J.Chem.Phys., 48, 4859

113 Zashkvara, V.V., Korskunskii, M.I., and Kosmachev, O.S., 1966, Soviet Phys - Tech.Phys., 11, 96

Addendum

114 Huffman, R.E., Tanaka, Y., and Larrabee, J.C., 1963, J.Chem.Phys., 39, 902